

DESIGN, SYNTHESIS, AND CHARACTERIZATION OF IONICALLY
FUNCTIONALIZED CONJUGATED POLYMERS
WITH VARYING ION DENSITY
AND TYPE

by

DAVID PATRICK STAY

A DISSERTATION

Presented to the Department of Chemistry
and the Graduate School of the University of Oregon
in partial fulfillment of the requirements
for the degree of
Doctor of Philosophy

March 2012

DISSERTATION APPROVAL PAGE

Student: David Patrick Stay

Title: Design, Synthesis, and Characterization of Ionically Functionalized Conjugated Polymers with Varying Ion Density and Type

This dissertation has been accepted and approved in partial fulfillment of the requirements for the Doctor of Philosophy degree in the Department of Chemistry by:

Michael Haley	Chair
Mark C. Lonergan	Advisor
Darren Johnson	Inside Member
David Tyler	Inside Member
Hailin Wang	Outside Member

and

Kimberly Andrews Espy	Vice President for Research & Innovation/ Dean of the Graduate School
-----------------------	--

Original approval signatures are on file with the University of Oregon Graduate School.

Degree awarded March 2012

© 2012 David Patrick Stay

DISSERTATION ABSTRACT

David Patrick Stay

Doctor of Philosophy

Department of Chemistry

March 2012

Title: Design, Synthesis, and Characterization of Ionically Functionalized Conjugated Polymers with Varying Ion Density and Type

Phenylene-based conjugated polymers are of interest for their fascinating electronic and optical properties. The introduction of bound ions into these materials adds great versatility because it can affect solubility, aggregation properties, doping chemistry, luminescence, and response to electrical stimuli. Despite ionic density being a central materials parameter in ionically functionalized conjugated polymers (IFCPs), it has been explored only in limited ranges. The primary advance reported in this dissertation is the development of three complementary synthetic routes to anionic and cationic poly(fluorene)s where the density of ionic functional groups was systematically varied between 0.05 and 0.5 per phenylene unit. There have been very few reports of IFCPs in this range. The three routes all use the Suzuki polycondensation reaction (SPR) to form poly[(R-fluorene)-co-alt-(R'-fluorene)] (PFF) IFCPs, and they differ from one another in when ionic functionality is introduced to the polymer. The development of these approaches grew out of studies on the SPR as it applies to ionically functionalized monomers, specifically, complications created by the two-phase nature of typical Suzuki couplings. In the first route, ions are added to the monomer and directly polymerized into the polymer using a single-phase SPR made possible by using oligoether functionality

and a judiciously chosen solvent system. This route was used in the synthesis of a family of sulfonate and oligoether containing PFFs. In the second and third routes, ionic functionality is added after the polymer is formed either in solution or in solid films, respectively. The use of all nonionic monomers during the SPR avoided the complications encountered with two-phase reactions involving ionic monomers. The precursor polymers synthesized for these routes included a family of hexyl and bromohexyl containing PFFs and a family of oligoether and bromohexyl containing PFFs. The former were used to demonstrate post-polymerization quaternization to form cationic PFFs in solid films, and the later were quaternized in solution to yield soluble cationic PFFs. All of the polymers had very similar optical properties with the wavelengths of maximum absorption and emission in the range of 370-385 and 416-425 nm, respectively, and molecular weights greater than 10kDa and exhibited both positive and negative solvatochromism due to aggregation phenomena.

CURRICULUM VITAE

NAME OF AUTHOR: David Patrick Stay

GRADUATE AND UNDERGRADUATE SCHOOLS ATTENDED:

University of Oregon, Eugene, Oregon
Idaho State University, Pocatello, Idaho
Brigham Young University-Idaho, Rexburg, Idaho

DEGREES AWARDED:

Doctor of Philosophy in chemistry, 2012, University of Oregon
Master of Science in chemistry, 2004, Idaho State University
Bachelor of Science in chemistry, 2004, Idaho State University
Associate in Arts and Sciences in chemistry, 2001, Brigham Young University-
Idaho

AREAS OF SPECIAL INTEREST:

Explosives
Swing dance
Metal casting
Historical scientific apparatus

PROFESSIONAL EXPERIENCE:

Co-instructor of Teaching Science: Mix it up!, Department of Chemistry, 2010,
University of Oregon

Intern, Technology Entrepreneurship Program, 2009, Eugene, Oregon

Intern, University Venture Development Fund, 2008-2009, Eugene, Oregon

Researcher, Integrative Graduate Education and Research Traineeship Program,
2005-2007, Materials Science Institute, Eugene, Oregon

Adjunct Dance Faculty, Department of Theatre and Dance, 2004, Idaho State
University

GRANTS, AWARDS AND HONORS:

Harris Lectureship to Advance the Understanding of the Scientific Process

Transitional Research Grant, University Venture Development Fund

PUBLICATIONS:

Weber, C. D.; Robinson, S. G.; Stay, D. P.; Lonergan, M. C. *ACS Macro Letters* **2012**, Accepted

Stay, D. P.; Robinson, S. G.; Lonergan, M. C. Development and applications of ion-functionalized conjugated polymers. In *Iontronics: Ionic carriers in organic electronic materials and devices*; Leger, J., Berggren M., Carter S., Eds.; CRC Press, **2011**, 43–83.

Berryman, O. B.; Bryantsev, V.S.; Stay, D. P.; Johnson, D. W.; Hay, B. P. *Journal of the American Chemical Society* **2007**, *129*,48–58.

ACKNOWLEDGEMENTS

I would like to thank the many people who have helped me in earning my Ph.D and completing this document. I'll start with the members of the Lonergan Lab. First, Dr. Mark Lonergan has been an invaluable help in guiding my investigations, while at the same time allowing me to explore and lead my own research. Mark has been a great help in my family life as well. He is a marvelous mentor and I will cherish his friendship all my life. Next, I'd like to thank Dr. Calvin Cheng for recruiting me into the Lonergan Lab. When I came for the University of Oregon visitation weekend, I had no plans to work in a physical chemistry lab, and so had not considered the Lonergan Lab. Calvin was manning the Lonergan Lab poster and convinced me to talk to Mark, and the rest is history. I also thank Drs. Lei Gao, Yongjun Wang, and Fuding Lin for their expertise in ionically functionalized conjugated polymers and the many devices made from them. I appreciate Dr. Ian Moody for his encouragement in finishing my degree. Dr. Stephen Robinson was a great help in characterizing materials. Ethan Walker and Chris Weber have been most excellent colleagues. I thank them for their input and conversations during our time working together in the Lonergan Lab. Thanks to T.J. Mills and Lily Robertson who worked with me as undergraduate students, and helped me become a better mentor in my own right.

I'll next thank my family members for their help on the journey through my Ph.D. research. My parents, Randall and Rebecca Stay, have supported and encouraged me through many years of school, even when it did not seem likely that I would earn any degree, let alone a Ph.D. My children have been an inspiration. I have loved coming home to their hugs and kisses, while they motivate me to be better than I am.

Finally, I am overjoyed to thank and recognize my beautiful wife Marcelle E. H. Stay. We were married and moved to Oregon five days later, our entire married life so far has been here at the University of Oregon. She has loved and supported me through many long years of schooling, while sacrificing many of her own desires. It is through her encouragement and support that I have completed this project, thank you Marcelle.

For Marcelle, Jonas, and Magdalena. I love you.

TABLE OF CONTENTS

Chapter	Page
I. INTRODUCTION	1
1.1. Introduction to Polymers	2
1.2. Introduction to Ionically Functionalized Conjugated Polymers	15
1.3. Dissertation Overview	27
II. ANIONICALLY FUNCTIONALIZED CONJUGATED POLYMERS	28
2.1. Introduction	28
2.2. Results and Discussion	31
2.3. Summary	52
2.4. Experimental	53
III. CATIONICALLY FUNCTIONALIZED CONJUGATED POLYMERS	63
3.1. Introduction	63
3.2. Results and Discussion	67
3.3. Summary	89
3.4. Experimental	90

Chapter	Page
IV. SUMMARY	94
REFERENCES CITED	99

LIST OF FIGURES

Figure	Page
1.1. Line 1. A random copolymer of monomers A and B; Line 2. An alternating copolymer of monomers A and B; Line 3. A block copolymer of monomers A and B.	8
1.2. Examples of the initiation, propagation, and termination steps in a chain growth polymerization. A. Initiation of benzoyl peroxide. B. Propagation of polytetrafluoroethylene. C. Termination of polytetrafluoroethylene by phenyl radical.	11
1.3. A. The reaction between two monomers to form a dimer and in the process a molecule of HCl is expelled from the reaction. B. Two dimers joining together to form a tetramer.	12
1.4. Mechanism of the Suzuki cross coupling reaction. See text for detailed explanation.	14
1.5. Strength is engineered into Kevlar's® repeating unit (shown in red). Strength comes from interchain hydrogen bonding (dotted lines) between the amide H and carbonyl O and rigid aromatic rings between amide functional groups.	14
1.6. Structure of DNA with bases.	15
1.7. Teflon's® chemical resistance and nonstick properties are due to the strong C-F bond contained in the tetrafluoroethylene monomer. . .	15
1.8. Some common types of conjugated polymers: polyacetylene (PA), polyphenylene (PA), polythiophene (PT), poly(phenylene vinylene) (PPV), polypyrrole (PPy), and polyfluorene (PF).	16
1.9. A. A short segment of polyacetylene. B. The p_z orbitals of the same polyacetylene segment. C. Molecular π orbital extending across a polyacetylene oligomer.	17
1.10. As the extent of conjugation increases from the single double bond ethene to oligomeric polyacetylene, the energy between HOMO and LUMO decreases. Also, the number of molecular orbitals, each with a unique energy level, increases, leading to the band-like behavior of conjugated polymers.	18

Figure	Page
2.1. Synthetic conditions for PFP-SO₃ _{Alkyl[1:3]} : (i) Pd(PPh ₃) ₄ , 2M aqueous K ₂ CO ₃ , THF	33
2.2. Synthetic conditions for monomer 2 : (i) NBS and benzoyl peroxide; (ii) Na ₂ SO ₃	33
2.3. Synthetic conditions for 5 :(i) Na ₂ SO ₃ , CTAB, 5 , water, reflux, 36 hr	36
2.4. Synthetic conditions for original synthesis of 2 :(i) Na ₂ SO ₃ , CTAB; (ii) NaI in acetone; (iii) thiourea in EtOH, reflux, 16 hr; (iv) NaOH in H ₂ O, reflux, 3 hr; (v) H ₂ SO ₄ ; (vi) boiling HNO ₃ , (vii) 5% 9 , 6 , Na ₂ SO ₃ , cetyltrimethylammonium bromide in water.	37
2.5. Synthetic conditions for PFF-SO₃ _{Alkyl[1:2]} :(i) Pd(PPh ₃) ₄ , 2M aqueous K ₂ CO ₃ , THF	38
2.6. Synthetic conditions for PFF-SO₃ _{OE[1:x]} : (i) Pd(PPh ₃) ₄ , 2M aqueous Na ₂ CO ₃ , THF, methanol	39
2.7. Synthetic conditions for 11 and 12 : TEG=(CH ₂ CH ₂ O) ₃ CH ₃ ; (i) LDA, -78°C; (ii) Br(CH ₂ CH ₂ O) ₃ CH ₃ ; (iii) <i>n</i> -Butyllithium, -78°C; (iv) 2-isopropoxy-4,4,5,5-tetramethyl-1,3,2-dioxaborolane.	39
2.8. Correlation between $\chi_{monomer}$ and $\chi_{polymer}$ for PFF-SO₃ _{OE[1:x]} (■), PFP-SO₃ _{Alkyl[1:3]} (●), and PFF-SO₃ _{Alkyl[1:2]} (▲).	41
2.9. Synthetic conditions for PTPV-SO₃ _{H[1:3]} and PTPV-SO₃ _{Ph[1:3]} :(i) Pd(PPh ₃) ₄ , 2M aqueous K ₂ CO ₃ , THF	43
2.10. Synthetic conditions for monomers 15 and 16 :(i) PPh ₃ (ii) NaH; (iii) When R=H, then 4-bromobenzaldehyde, when R=Ph then 4-bromobenzophenone.	43
2.11. Synthetic conditions for 13 and 14 :(i) <i>n</i> -Butyllithium, -78°C; (ii) 2-isopropoxy-4,4,5,5-tetramethyl-1,3,2-dioxaborolane.	43
2.12. Three dimensional total luminescence plot for PFF-SO₃ _{OE[1:2]}	46
2.13. Two dimensional total luminescence plot for PFF-SO₃ _{OE[1:2]}	47
2.14. Normalized excitation (filled) and emission (open) spectra for the CP PFP _[1:1] (■)	47
2.15. Normalized excitation (filled) and emission (open) spectra for the PFF _{OE[1:2]} (■), PFF _{OE[2:5]} (●), PFF _{OE[1:3]} (▲), PFF _{OE[1:10]} (▼) and PFF _{Alkyl[1:1]} (◆) polymers	48

Figure	Page
2.16. Change in λ_{max} of the fluorescence emission spectra from a change in the polarity of the solvent in which the polymer is found. The value of pure methanol is indicated by the vertical red dashed line and has an $E_T(30)$ value of $55.4 \text{ kcal}\cdot\text{nm}\cdot\text{mol}^{-1}$	51
2.17. Normalized excitation (filled) and emission (open) spectra for PTPV-SO₃ H[1:3] (■), PTPV-SO₃ Ph[1:3] (●) polymers	52
3.1. Synthetic conditions for PFF-Br Alkyl[1:x]:(i) Pd(PPh ₃) ₄ , 2M K ₂ CO ₃ , THF and water.	68
3.2. Synthetic conditions for PFF-Br OE[1:x]:(i) Pd(PPh ₃) ₄ , 2M K ₂ CO ₃ , toluene and water.	69
3.3. Correlation between $\chi_{monomer}$ and $\chi_{polymer}$ for the polymer families PFF-Br OE[1:x] (black squares) and PFF-Br Alkyl[1:x] (blue triangles). . .	70
3.4. Excitation (left) and emission (right) spectra for PFF-Br Alkyl[1:2] (black), PFF-Br Alkyl[1:3] (red), PFF-Br Alkyl[1:5] (green), PFF-Br Alkyl[1:6] (blue), PFF-Br Alkyl[1:10] (cyan), and PFF-Br Alkyl[1:18], (magenta). Note that the trends in excitation spectra and relative intensity of the vibronic band at 440 nm follow the trends in molecular weight for the polymers.	73
3.5. Excitation (left) and emission (right) spectra for PFF-Br OE[1:2] (black), PFF-Br OE[1:4] (red), PFF-Br OE[1:5] (green), PFF-Br OE[1:6] (blue), PFF-Br OE[1:20] (cyan). Note that the trends in excitation spectra and relative intensity of the vibronic band at 440 nm follow the trends in molecular weight for the polymers.	73
3.6. Synthetic conditions for PFF-NMe₃ Alkyl[1:2]:(i) N(CH ₃) ₃ in THF . . .	74
3.7. Excitation and emission spectra of PFF AlkylBr[1:2] in chloroform (red) and PFF Alkyl[1:2] in methanol (black).	76
3.8. Excitation and emission spectra of the pre- (black, in chloroform) and post-polymerization (red, in methanol) functionalization of the PFF-Br Alkyl[1:2] family	77
3.9. XPS data for films of PFF-Br Alkyl[1:2] before (black line) and after (red line) exposure to triethylamine. PFF-NMe₃ Alkyl[1:2] (blue line) is given as a reference.	78
3.10. Synthetic conditions for PFF-NMe₃ Alkyl[1:2]:(i)Pd(PPh ₃) ₄ , 2 M K ₂ CO ₃ , methanol/water	79

Figure	Page
3.11. Synthetic conditions for 17 :(i) $\text{N}(\text{CH}_3)_3$	79
3.12. Excitation and emission spectra of directly synthesized PFF-NMe₃ Alkyl[1:2] (black) and PFF-NMe₃ Alkyl[1:2] synthesized through post-polymerization functionalization (red).	80
3.13. Plot of complex impedance magnitude as it varies with frequency and temperature for PFF-NMe₃ Alkyl[1:2] . Note the two separate experiments (red square and black circle) on the same sample showing that the device is not degraded during the measurements.	85
3.14. ϵ'_{app} for PFF-NMe₃ Alkyl[1:2] as a function of angular frequency and temperature.	85
3.15. σ'_{app} for PFF-NMe₃ Alkyl[1:2] as a function of angular frequency and temperature.	86
3.16. A representative set of impedance data collected from a 670 nm film of PFF-NMe₃ Alkyl[1:2] at 388K. Dielectric functions $\tan \delta$ (black square), ϵ'_{app} (red circle), and ϵ''_{app} (green triangle) are shown (left ordinate) along with σ'_{app} (solid blue line, right ordinate. ω_L is indicated on the $\tan \delta$ curve.	86
3.17. Changes in dielectric function $\tan \delta$ as a function of angular frequency and temperature in a sample of PFF-NMe₃ Alkyl[1:2]	87
3.18. Arrhenius plot of $\ln \sigma'_{\text{app}}(\omega_L)$ vs. $1000/T$ for two samples of PFF-NMe₃ Alkyl[1:2] (black squares and red circles) with different thicknesses (670 nm and 250 nm respectively). The green triangles are for PFF-NMe₃ OE[1:2] with a thickness of 1900 nm.	87
3.19. σ'_{app} at (ω_L) plotted against $1000/T$ for two samples of PFF-NMe₃ Alkyl[1:2] (black squares and red circles) with different thicknesses (670 nm and 250 nm respectively). The green triangles are for PFF-NMe₃ OE[1:2] with a thickness of 1900 nm.	88
4.1. Fluorescence emission spectra for PFF-NMe₃ OE[1:x] (red) and PFF-SO₃ OE[1:x] (black).	96

LIST OF TABLES

Table	Page
1.1. A table containing the major differences between step growth and chain growth polymerizations as discussed in the text.	13
1.2. Survey of IFCPs made by direct polymerization methods.	24
1.3. Survey of cationic IFCPs made by post-polymerization methods.	25
1.4. Survey of anionic IFCPs made by post-polymerization methods.	26
2.1. $\chi_{monomer}$ as determined by initial monomer concentration, $\chi_{polymer}$ found by ^1H NMR of purified polymer, apparent molecular weights of polymers as determined by GPC running against polystyrene sulfonate standards in 0.1 M LiNO_3 in 25% water/ 75% DMSO, λ_{max} of the excitation spectrum in nanometers, λ_{max} of the emission spectrum in nanometers	34
2.2. Table of emission λ_{max} of polyelectrolytes as a function of polymer type and solvent.	49
3.1. $\chi_{monomer}$, $\chi_{polymer}$ found by ^1H NMR, molecular weight of polymers as determined by GPC running against polystyrene standards in THF, λ_{max} of the excitation spectrum in nanometers, λ_{max} of the emission spectrum in nanometers	71

CHAPTER I

INTRODUCTION

Throughout time, all of civilization has been built upon the backbones of natural polymers. Wood, wool, hide, horns, fur, flax, resins, and rubbers, along with stone and a few metals have been instrumental in the development of the world's great civilizations. Without protein-based parchment, cellulose-based paper and papyrus, we would have no record of Euclid's mathematical masterpiece *Στοιχεῖα*¹, *Metamorphoses* by the Roman poet Ovid, or the collected writings that are now the Bible. The great Viking ships that sailed across the Atlantic were made of wood with sails and rope made from cellulose. The paintings of van Gogh and Vermeer would not have existed without cellulose-based canvas and naturally polymerizing drying oils. The stringed instruments of Antonio Stradivari, used to play the music of the world's greatest composers, are made of wood, natural resins, and lacquers then strung by stretched, dried, and twisted proteins of sheep's gut. Only music written by the world's greatest composers can do justice to these instruments. But that music has survived because Vivaldi, Bach, Mozart, and Beethoven had protein-based parchment and cellulosic paper on which to record their genius, using inks made with water-soluble gums.

We take natural polymers for granted in day to day life. Still, as useful as natural proteins, carbohydrates, and resinous products are, they are not sufficient in quality or quantity for all the practical or technological applications we demand. These natural products have been used for millennia and will never become completely obsolete, but

¹Stoicheia or Elements

the future lies in different directions. Synthetic polymers, a relatively new endeavor, are one of these directions.

1.1. Introduction to Polymers

1.1.1. Short History of Polymers

The word “polymer” comes from the Greek word *πολυμερής* *polyméros* itself a compound of *πολυ* *poly-* (many) and *μέρης* *-méros* (parts). The Oxford English Dictionary defines polymer as:

polymer, *n.* *Chem.* a compound with a molecular structure in which a (usually large) number of similar polyatomic units are bonded together...

The “similar polyatomic units” are called monomers. The reactions that turn monomers into polymers are called polymerizations.

To guide this history of polymers we will look at several Nobel Prize winners. The first completely synthetic polymer was developed by Leo H. Baekeland between 1907 and 1909. Bakelite, as he dubbed it, was a polymer made from formaldehyde and phenol. It was used to make everything from billiard balls to radios. About a decade later, in his 1920 paper *Über Polymerisation*, Hermann Staudinger put forward the theory that, contrary to popular belief, polymers were long chains of small repeating units bound together by covalent bonds.¹ In this paper, he called the polymers *hochmolekulare Verbindungen* or high molecular weight compounds, and correctly drew the structures of polystyrene, rubber, and polyoxymethylene. Many of Staudinger’s contemporaries believed that the *Makromoleküle*, or macromolecules as Staudinger would come to call them, were actually just small organic molecules

held together by peculiarly strong intermolecular forces. The vast majority of known polymers at that time (carbohydrates, proteins, and rubber) were biological in origin, and chemists, not having a good understanding of what caused aggregation or agglomeration, proposed that some heretofore unknown force only found in natural products could be holding them together. Over decades, Staudinger's theory was supported by the experimental data, and the chain understanding was accepted. Then in 1953, Hermann Staudinger was awarded the Nobel Prize in Chemistry "for his discoveries in the field of macromolecular chemistry."²

A contemporary of Staudinger named Wallace Carothers went to work for DuPont in 1927 where he pursued basic research in polymers. It was while at DuPont that Carothers did his ground-breaking work on what he termed "A-polymers" (addition polymers) and "C-polymers" (condensation polymers). Carothers worked on the polycondensation of diacids and diamines which lead to the development of one of DuPont's best selling materials: Nylon®.^{3;4} His division of synthetic strategies paved the way for future synthetic developments by other chemists.

Two of these chemists were Karl Ziegler and Giulio Natta. In 1953, the same year that Staudinger received his Nobel Prize, Ziegler found that ethylene gas will polymerize at normal pressure to form high molecular weight polymers when in the presence of organometallic mixed catalysts. The previous method for forming polyethylene was to place it under high pressure (1000-2000 atm) and temperature (>200°C).⁵ The new low pressure polyethylene was more temperature stable, had a higher density, and was also more rigid. As news of this new method of polymerization spread, a middle-aged Italian professor, Giulio Natta heard about the reaction and started developing this catalyst to polymerize other monomers.

Natta was not new to the polymer field. He began using X-rays to study the structure of small molecule crystals in 1924, but after meeting Staudinger in Freiburg in 1932, he began looking at polymers to try to determine their molecular structure. Unlike polyethylene, these new polypropylene chains had methyl groups pointing off the main chain of the polymer. These side chains were not neatly arranged along the polymer backbone, which made it difficult for the polymer's chains to pack together tightly. Natta designed a catalyst to overcome this problem. The new catalyst was shaped so that it could only accept new monomers when they were aligned in a specific manner, giving regio- and stereoregularity to the polymers. For their work in "polymer synthesis techniques" Nobel Prizes were awarded to Giulio Natta and Karl Ziegler in 1963.⁶

So far this discussion has been mainly about the work of synthetic chemists. Concurrent with the advances made by synthetic chemists, physical chemists were trying to understand how these macromolecules behaved both in and out of solution. With the falling away of the small molecule aggregation and agglomeration theories, chemists came to understand that the chemical bonds in polymers do not differ from those in their monomer in any detectable way. Number, strength, type, and length of bonds formed by atoms are the same, whether the bonds are formed in a molecule with a molecular weight of 1000 or 100,000. This simple observation has two very important implications. The first is that the chemistry of macromolecules coexists with that of small molecules and follows the same rules. The second implication is that the special properties of both biological and synthetic polymers must come from their extended chain structure and not from some special type of polymer bond.

One physical chemist, Paul Flory, worked at DuPont with Carothers until Carothers's untimely death in 1938. At DuPont, Flory worked on the kinetics of both

condensation and addition polymerization reactions making significant contributions to both fields. Flory was the first to apply the excluded volume rule to the field of polymer physics.^{7;8} This rule states that as a polymer randomly coils, one part of the polymer cannot occupy the same space as another part of the polymer. The result of applying excluded volume is that the two ends of the polymer are farther away from each other than would be predicted without excluded volume. Excluded volume accounts for the steric effects of chain coiling. The implications of excluded volume led to another breakthrough for Flory, that of the theta point. When a polymer is in solution, the polymer chain has interactions with the solvent and with other parts of the polymer chain. When interactions between the polymer and solvent are favorable, the polymer coil will expand to make the most polymer solvent interactions possible. However, when the polymer solvent interactions are unfavorable, the polymer coils more tightly. The theta point is when the polymer-solvent interactions are just poor enough to cancel out the effect of excluded volume. Characteristics of two polymers at their theta points can be compared to one another without needing corrections for excluded volume. At the theta point a polymer chain behaves as if it were an ideal chain following an ideal random walk coiling. For his “theoretical and experimental work in polymer chemistry,” Paul Flory received the Nobel Prize in Chemistry in 1974.⁹

As we uncoil this historical chain, the story picks up again with Giulio Natta in 1958. Using a $\text{Et}_3\text{Al}/\text{Ti}(\text{OPr})_4$ catalyst, Natta and coworkers polymerized acetylene to make polyacetylene.¹⁰ The polyacetylene was a highly crystalline, air-sensitive, and insoluble powder. A little over a decade later, Hideki Shirakawa and his graduate student Sakuji Ikeda developed a way to make films of polyacetylene.¹¹ This was done by coating the inside of a vessel with a slightly altered catalyst $\text{Et}_3\text{Al}/\text{Ti}(\text{OBu})_4$ and

then exposing the catalyst to acetylene gas at reduced temperature. This produced a silvery film of polyacetylene.

While Shirakawa was working on polyacetylene, Alan MacDiarmid and Alan Heeger were studying the metallic properties of a silvery inorganic polymer $(\text{SN})_x$. In 1976 MacDiarmid visited Tokyo, saw the silvery films of polyacetylene, and offered to collaborate with Shirakawa on exploring the conductive properties of polyacetylene. MacDiarmid and Heeger knew that when $(\text{SN})_x$ was exposed to I_2 , its conductivity increased dramatically and so they decided to do a similar experiment with the polyacetylene. They reported their findings in 1977 in a paper entitled *Synthesis of Electrically Conducting Organic Polymers: Halogen Derivatives of Polyacetylene, $(\text{CH})_x$* ¹² where they reported a conductivity 10^7 times greater than the undoped film. This report, and two more the same year, kicked off a new field of polymer science: conducting polymers. For their work on “electrically conductive polymers” Alan MacDiarmid, Alan Heeger, and Hideki Shirakawa received the Nobel Prize in Chemistry in the year 2000.¹³

While unfunctionalized polyacetylene is a fascinating polymer, new synthetic strategies were needed to develop functionalized polyacetylenes and other electronically conductive polymers. Six more men were also awarded Nobel prizes in Chemistry for work that was later applied to the synthesis of conjugated polymers: Yves Chauvin, Robert Grubbs, and Richard Schrock “for the development of the metathesis method in organic synthesis”¹⁴ in 2005 and Richard Heck, Ei-ichi Negishi, and Akira Suzuki “for palladium-catalyzed cross couplings in organic synthesis”¹⁵ in 2010.

In this short introduction we have looked at six different Nobel Prizes and how the field of polymer chemistry has evolved over the last century. We have looked at

the beginnings of our understanding of how atoms are bonded together to ways of manipulating those bonds to induce conductivity in polymers. In the next section of this work different methods of categorizing polymers will be presented.

1.1.2. Types of Polymers

The types of polymers discussed in this work are linear alternating copolymers, synthesized using a condensation polymerization mechanism.

Polymers can either be a long chain with just two ends or they can be branched with multiple ends. A branched polymer has extra polymeric chains coming off the main linear backbone. If the polymer branches connect two long chains together, the molecule is called cross-linked. The polymers herein are linear and not branched.

As indicated by the name, a polymer is made up of many repeating subunits or monomers. A polymer with just one type of monomer is called a homopolymer, however, not all polymers are made from just one monomer. When two or more different subunits are present, the polymer they form is called a heteropolymer, or a copolymer. The chemical structure of the monomer is important and the order in which the subunits are incorporated into the polymer is also important. The three main types of polymers are random, alternating, and block. Consider Figure 1.1 which contains some hypothetical copolymers made from just two monomers, A and B.

Line 1 in Figure 1.1 shows a random distribution of A and B. In this copolymer, the probability of finding a given monomer at any given site on the chain is independent of the neighboring monomers.¹⁶ Figure 1.1 line 2 has an alternating copolymer of A and B. In this polymer, the monomers are incorporated into the chain in an alternating sequence. An alternating copolymer could be considered a

1. A-A-B-A-A-A-B-B-A-A-A-B-A-A-A-A-B-A-B-B-B-B-B-B-A-A-B-A-B-A-A-A-B-B-
2. A-B-A-B-A-B-A-B-A-B-A-B-A-B-A-B-A-B-A-B-A-B-A-B-A-B-A-B-A-B-A-B-
3. A-A-A-A-A-A-A-A-A-A-A-A-A-A-A-A-B-B-B-B-B-B-B-B-B-B-B-B-B-B-B-B-B-

FIGURE 1.1. Line 1. A random copolymer of monomers A and B; Line 2. An alternating copolymer of monomers A and B; Line 3. A block copolymer of monomers A and B.

homopolymer of the hypothetical monomer AB. The polymers synthesized in this work are alternating copolymers; it will at times be useful to think of them as random copolymers of hypothetical monomers AB and AC.¹⁶ Line 3 of Figure 1.1 illustrates a block copolymer. In a block copolymer, the polymer is made up of two or more segments or blocks, covalently bound to each other where each block is a homopolymer. If the block polymer has two or three blocks, it is referred to as a di- or triblock copolymer, respectively. This work will explore homopolymers, and both random and alternating copolymers.

1.1.3. Polymerization

The previous classifications have been based on the structure of the polymer but polymers can also be classified according to the chemical reactions used to create them. As indicated on page 3 in the brief history of Carothers's work, the two major categories of polymers are addition and condensation polymers.

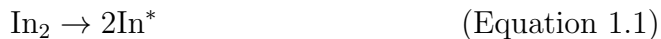
The easiest way to determine whether a polymer is an addition or condensation polymer is to look and see if all of the atoms that were in the monomer are in the polymer. Addition polymers contain all of the original elements, while in condensation polymers some of the monomers' atoms are lost during the polymerization.

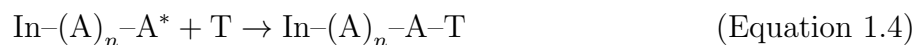
Addition polymers usually have all-carbon backbones with pendant side groups coming off the main chain. The mechanism behind the growth of these polymers is generally chain growth, usually using free radicals or ionic groups.

In contrast, condensation polymers often have functional groups spaced periodically along the polymer backbone. These functional groups are generally formed during the condensation reaction of two different monomers, thus condensation polymers are commonly alternating copolymers. Polymer growth in condensation polymers often happens in a stepwise fashion.

In the previous section, the concepts of chain and step polymerizations were mentioned and will now be more explicitly described.

A polymer formed by chain growth has three separate steps: initiation, propagation, and termination. For a chain to start growing it needs to initiate. This is usually done by adding a more reactive molecule called an initiator into the reaction mixture. Initiation mechanisms vary by initiator, but they produce either cationic, anionic, or free radical sites and must be chosen for specific polymerization mechanism as shown in Equation 1.1. The activated initiator then reacts with a monomer adding the first monomer to the chain and forming a new active cationic, anionic, or free radical site at the end of the chain, illustrated in Equation 1.2. This propagation continues until the monomer is used up (Equation 1.3) or the chain terminates. Chain termination can occur in a variety of ways but once a polymer terminates, it can no longer grow (Equation 1.4). In chain growth polymerization, the only way for a monomer to be consumed is by reacting it with the active end of a polymer chain. Because of this, some of the monomer remains in the reaction even after long reaction times. The molar mass of the backbone chain increases rapidly during polymerization until it terminates and then the molar mass stays constant.





Unlike chain growth, step growth polymerizations have the same mechanism throughout the polymerization. True to its name, growth in step polymerizations happens in steps, with monomers quickly reacting to form dimers and trimers. These dimers and trimers then couple to form short oligomers. This joining of short chains continues even while longer chains are formed. Equation 1.5 shows the general formula for step growth. Step growth leads to a mixture of monomer, oligomers, and polymers all present at the same time.



I will now show examples of both chain and step polymerizations using well-known commercial compounds. Figure 1.2 illustrates a specific example of the steps outlined above for chain growth with polytetrafluoroethylene, or as it is better known: Teflon®. Figure 1.2A. shows the radical initiator benzoyl peroxide as it homolytically cleaves across the O–O bond to form two benzoyloxyl radical fragments. The daughter radical fragments (only one is shown for clarity) also dissociate to form a phenyl radical and carbon dioxide. It is the phenyl radical that acts as the initiator in the polymerization. Free radicals are extremely reactive and so the phenyl

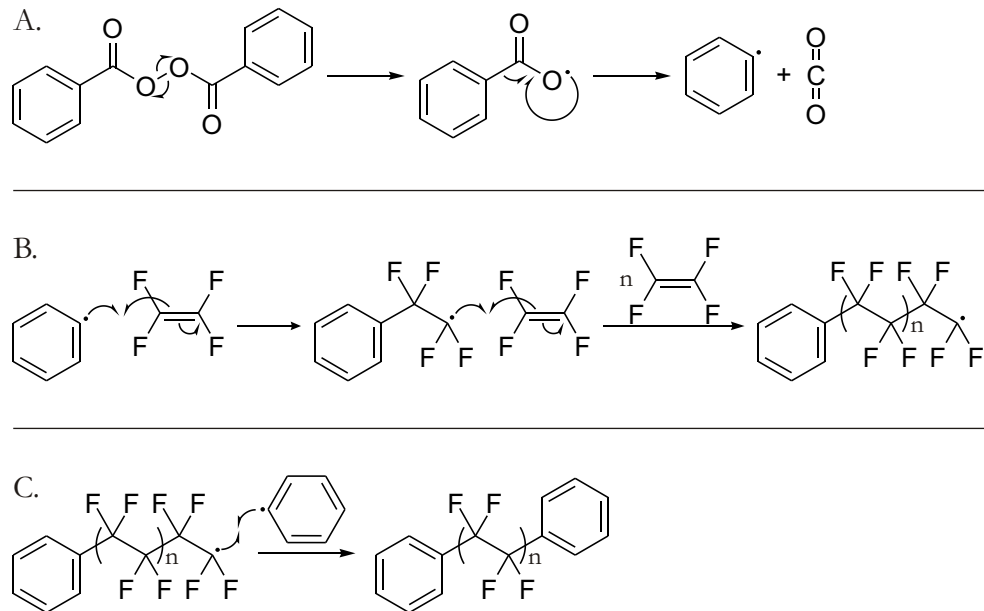


FIGURE 1.2. Examples of the initiation, propagation, and termination steps in a chain growth polymerization. A. Initiation of benzoyl peroxide. B. Propagation of polytetrafluoroethylene. C. Termination of polytetrafluoroethylene by phenyl radical.

radical attacks a tetrafluoroethylene monomer (Figure 1.2B.) The newly formed radical then quickly reacts with n tetrafluoroethylene units to form the polymer. For polytetrafluoroethylene this can be as high as 10^6 or 10^7 monomers in just seconds. One possible termination step is shown in Figure 1.2C, where a phenyl radical reacts with the radical at the end of the polymer chain, removing both radicals and ending growth on the chain.

Kevlar® is a good example of a step growth polymer. Figure 1.3A shows the reaction between two monomers to form a dimer and in the process a molecule of HCl is expelled from the reaction. Figure 1.3B illustrates two dimers joining together to form a tetramer. Notice that the reaction to form the dimer and the tetramer are the same: an amine reacts with an acyl chloride to form an amide while losing HCl.

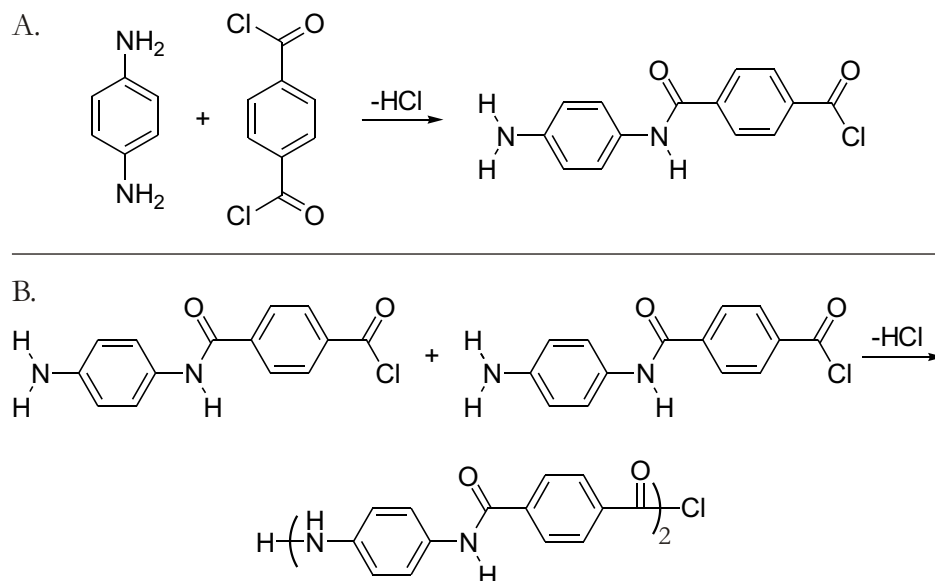


FIGURE 1.3. A. The reaction between two monomers to form a dimer and in the process a molecule of HCl is expelled from the reaction. B. Two dimers joining together to form a tetramer.

To summarize, Table 1.1 lists the major differences between step growth and chain growth polymerizations. All polymers discussed in this work are step growth polymers.

1.1.3.1. Suzuki Polycondensation

As mentioned in 1.1.1., Akira Suzuki did ground-breaking work with palladium catalysts. I have relied heavily on one implementation of his catalysts to make conjugated polymers.

The Suzuki reaction is an organometallic cross-coupling of the general form shown in Equation 1.6,¹⁷ where the connecting carbon in R is either sp^2 or sp^3 and the connecting carbon in R' is sp^2 . For the purposes of this paper, we will be focusing on reactions where the sp^2 based carbons in R and R' come from aromatic rings.

Chain Polymerization	Step Polymerization
Growth only occurs with addition of monomer to the end of the chain.	All monomers, dimers, trimers, etc. in the reaction can react to increase polymer chain length.
Chains are no longer active after termination	Ends always remain active
Monomer is present throughout the polymerization	Monomer is quickly consumed
Polymers usually contain all of the atoms in the monomer	Polymers often have fewer atoms per repeat unit than the monomer
Chain growth happens rapidly	Growth of chain is usually slow
High molecular weight polymers can occur rapidly	High molecular weight polymers are present after long reaction times

TABLE 1.1. A table containing the major differences between step growth and chain growth polymerizations as discussed in the text.



The mechanism of the Suzuki reaction is shown in Figure 1.4 and has 5 steps. Step I starts with the Pd(0) ligand oxidatively inserting into the aryl halide bond to give the Ar-Pd(II)-X compound. Step II is the activation of the aryl boronic acid by the base. Step III is a metathesis reaction between Ar-Pd(II)-X and Ar'B(OH)₃ to give Ar-Pd(II)-Ar' and BX(OH)₃⁻. Step IV is a *cis/trans* isomerization. Step V is the reductive elimination of Ar-Ar' from the Pd catalyst regenerating Pd(0) and forming a new C-C bond. The Suzuki polycondensation reaction is a variation on the Suzuki reaction, in which the aryl halide and the aryl boronic acid or esters are both difunctionalized.¹⁸

Polymers can be designed to exhibit specific characteristics by selecting monomers that imbue the polymer with desired traits. Polymers such as Kevlar®[®], DNA, and Teflon®[®] are all known for their unique properties and each property is

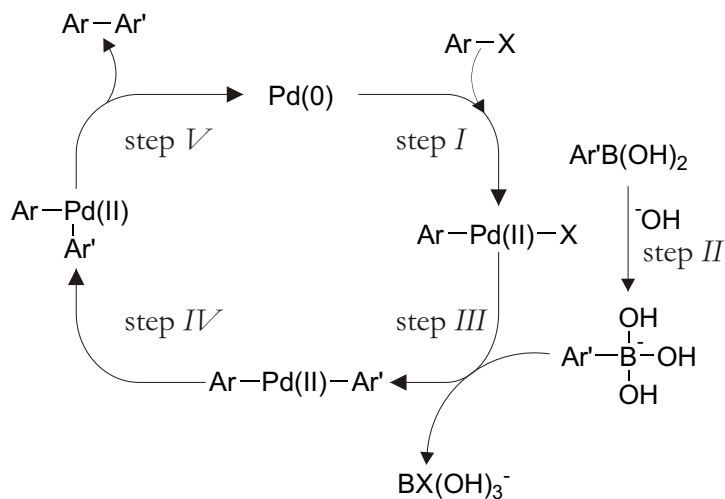


FIGURE 1.4. Mechanism of the Suzuki cross coupling reaction. See text for detailed explanation.

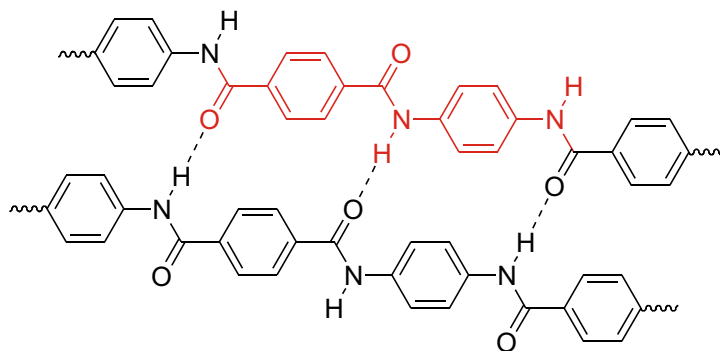


FIGURE 1.5. Strength is engineered into Kevlar's® repeating unit (shown in red). Strength comes from interchain hydrogen bonding (dotted lines) between the amide H and carbonyl O and rigid aromatic rings between amide functional groups.

specifically designed into the monomer. Figure 1.5, Figure 1.6, and Figure 1.7 contain the structures of these three polymers. Kevlar® gets its strength from interchain hydrogen bonding and rigid aromatic groups between the amide functional group linkages. The DNA monomer groups store genetic coding information. The strong C-F bonds in Teflon® endow it with its nonstick properties. Just as strength, genetic information, and nonstick properties can all be designed into a polymer, so also can electrical conductivity.

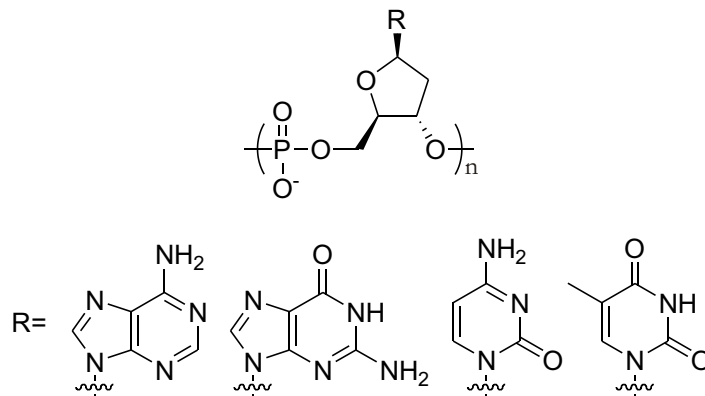


FIGURE 1.6. Structure of DNA with bases.

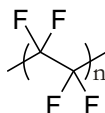


FIGURE 1.7. Teflon's® chemical resistance and nonstick properties are due to the strong C-F bond contained in the tetrafluoroethylene monomer.

1.2. Introduction to Ionically Functionalized Conjugated Polymers

Work on ionically functionalized conjugated polymers (IFCP) can be seen as growing out of the work done on two broader classes of polymers, namely, conjugated polymers and ionically functionalized polymers. Consequently, it is useful to discuss these latter two classes of polymers first before introducing IFCPs.

1.2.1. Conjugated Polymers

As described on page 6, MacDiarmid, Heeger, and Shirakawa found that when films of prototype conjugated polymer polyacetylene are exposed to halogen vapors, electronic conductivity increases dramatically.¹² This discovery led to an explosion of research into conjugated polymers and also to the term “conducting polymers” to describe them. Burroughes cemented the role of conducting polymers in the scientific fields, when he synthesized poly(phenylene vinylene) (PPV).¹⁹ Unlike

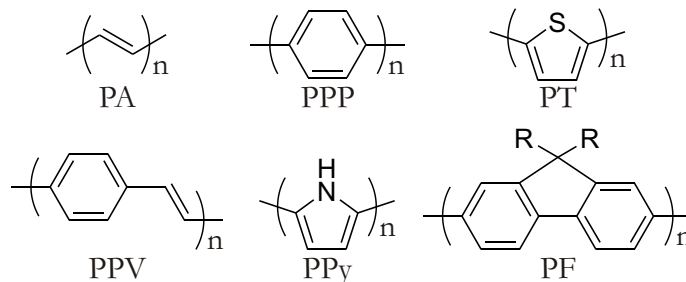


FIGURE 1.8. Some common types of conjugated polymers: polyacetylene (**PA**), polyphenylene (**PA**), polythiophene (**PT**), poly(phenylene vinylene) (**PPV**), polypyrrole (**PPy**), and polyfluorene (**PF**).

polyacetylene, PPV exhibits strong visible luminescence, and this ultimately led to the development of polymer-based electroluminescent devices. Such devices remain one of the most important application areas for conjugated polymers. They are also a prime example of the types of applications made possible by the unique combination of optical and electronic properties found in conjugated polymers along with their solution processability. A brief survey of the literature finds many other application areas including photovoltaics, field effect transistors, electromagnetic shielding, and nonlinear optical devices. Figure 1.8 shows some of the conducting polymers used in these applications. While the structures for these materials are varied, they all have common features. The most prominent and important feature is the presence of conjugated π -bonds throughout the backbone of the polymer. The term “conjugate” comes from the Latin *conjugare* meaning “to join together” or “to unite.” The collective name for macromolecules with extended conjugation are called conjugated polymers.

In an atom, an electron is found in an atomic orbital, an area where the probability of finding the electron is high. When two atoms are brought together in a molecule, the atomic orbitals interact with one another to form two molecular orbitals, one bonding and one antibonding, which describe the wave-like nature of

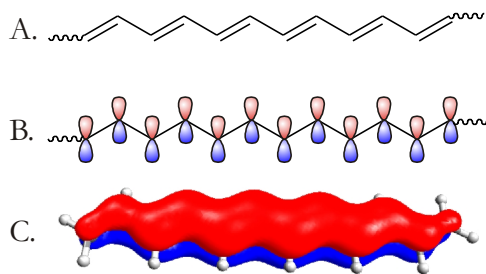


FIGURE 1.9. A. A short segment of polyacetylene. B. The p_z orbitals of the same polyacetylene segment. C. Molecular π orbital extending across a polyacetylene oligomer.

an electron in that orbital. The more atoms that are brought into interaction with one another, the more molecular orbitals are formed, each with their own discrete energy level. The simplest conjugated system is 1,3-butadiene ($\text{H}_2\text{C}=\text{CH}-\text{CH}=\text{CH}_2$), in which two pairs of doubly bonded carbons are joined together with a single bond.²⁰ In this system the π -electrons are delocalized over all four sp^2 -hybridized carbons in what is known as a π -molecular orbital. This delocalization of the four π -electrons leads to a lower overall energy for the molecule compared to when there are two localized ethene type double bonds. Polyacetylene is the simplest of all the conjugated polymers with a repeat unit of just CH where each carbon is sp^2 hybridized allowing all of the p_z electrons in the chain to delocalize over the entire polymer backbone. Figure 1.9 shows the structure of a short segment of polyacetylene (A), the p_z orbitals of the same polyacetylene segment (B), and molecular π orbital extending across a polyacetylene oligomer (C).

As the number of conjugated double bonds increases, like in a polymer, the number of molecular orbitals, each with a unique energy level, also increases. The effect of many discrete but closely spaced energy levels is that of a band type behavior. This effect can be seen in Figure 1.10. The HOMO (Highest Occupied Molecular Orbital) lies at the top of a “band” of closely spaced orbitals. This so-called valence

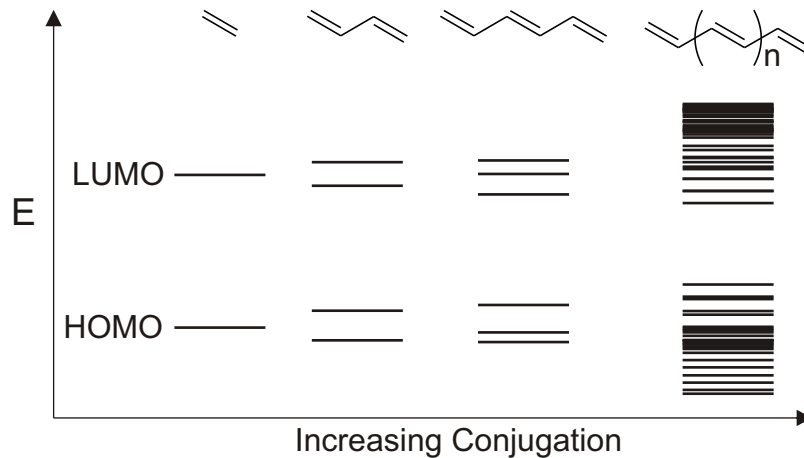


FIGURE 1.10. As the extent of conjugation increases from the single double bond ethene to oligomeric polyacetylene, the energy between HOMO and LUMO decreases. Also, the number of molecular orbitals, each with a unique energy level, increases, leading to the band-like behavior of conjugated polymers.

band is filled with one electron from each carbon in the chain. The empty LUMO (Lowest Unoccupied Molecular Orbital) lies at the bottom of a collection of empty orbitals in the so-called conduction band. The difference in energy between the top of the valence band and the bottom of the conduction band is called the band gap. This structure, a filled conduction band, band gap, and empty valence band, is the exact same structure as more traditional inorganic semiconductors.

When an isolated double bond (say in a small molecule) absorbs a photon with energy greater than the difference between the HOMO and LUMO a π -electron from the HOMO is excited into the LUMO resulting in a peak in the UV-Vis spectrum. The excited electron can then fall back to its ground state emitting either through radiative or non-radiative pathways. A similar event can be seen in π -conjugated polymers. When a photon with an energy greater than the band gap of the polymer is absorbed, an electron is promoted from the valence band to the conduction band, producing an exciton. An exciton is an excited state quasiparticle consisting of an electrostatically bound electron and hole pair. This exciton can then move along the

polymer for some period of time at which point it relaxes back to the ground state. One way in which it can relax is through fluorescence (light-emission). As can be seen in Figure 1.10 for polyacetylene, and it holds true for other conjugated polymers, as the extent of conjugation increases the band gap narrows. For light emission to occur there needs to be an electron in the conduction band and a place for it to go (often called a hole) in the valence band. In fluorescence spectroscopy, the electron is promoted from the valence band to the conduction band through the absorption of light. Another way to populate the conduction band is to inject electrons into the conduction band and remove them from the valence band using an electric field. After the electrons are injected into the polymer they can move through the polymer until they become bound to a hole and become an exciton electron-hole pair. The electron can then fall to the valence band emitting a photon with an equal energy to that of the band gap. It is these unique properties that make conjugated polymers of such important scientific and technical importance.

1.2.2. Ionically Functionalized Polymers

Well before the study of conjugated polymers, a substantial literature on ionically functionalized polymers had already developed. In general, the addition of ionic functional groups to polymers can have a dramatic influence on properties. In particular, the effect of ion density and location of ion functionalization has been studied in great detail. Ion concentration has been shown to affect the glass transition temperature, modulus, melt strength, viscosity, and ion transport.²¹ Several key phenomena related to ionically functionalized polymers – such as hydrophilicity, rheology modification, colloid stability, and complexation/network formation – have led to many industrial applications. The hydrophilicity of these polymers has been

exploited by the diaper and agriculture industries. Rheological modification, such as drag reduction, has been used in fluid transfer applications such as those found in the oil, firefighting, and irrigation industries. Ionically functionalized polymers are also used as thickeners in the textiles, paints, adhesives and coatings industries. Their effects on colloid stability are exploited by the oil industry to inhibit growth of gas hydrates during oil extraction, while the ability to form networks is used by the water treatment industry to sequester and complex metal ions.^{22;23}

The most common backbones for ionically functionalized non-conjugated polymers are based on rubbers, ethylene, styrene, acrylates or methacrylates, and tetrafluoroethylene, largely due to their ease of synthesis or commercial availability. The most common anions in these polymers are carbonates and sulfates, while used less often are phosphonates. Common cations include pyridiniums and alkyl or aryl ammoniums. The introduction of ionic functionality into these polymers is accomplished in one of two ways, either into the monomers before polymerization or into the polymer post-polymerization. The introduction of ions into the monomers sometimes leads to difficulty finding solvents in which both monomers are soluble.²¹ Post-polymerization functionalization maintains the solubility of the polymers, but often runs into problems when trying to completely functionalize the polymer.

1.2.3. Ionically Functionalized Conjugated Polymers

Ionically functionalized conjugated polymers are polymers that have ions covalently bonded to a conjugated polymer backbone. They bring together many of the important physical properties of ionically functionalized polymers with the unique optical and electronic properties of conjugated polymers. Ionic functionalization of conjugated polymers has been studied in great depth in the past decade.²⁴⁻³⁰ Ionic

functional groups have been shown to impart new properties when compared to those of nonionically-functionalized, conjugated polymers. The presence of tethered ions in IFCPs affects intermolecular interactions, photophysics and quenching in solid films, ionic transport in films, mixed ionic electronic conduction, and doping chemistry of IFCP films.³¹ There has been a significant effort to understand the effect of tethered ion and counter ion type on the properties listed above. Despite this, there have been relatively few reports on methods to control ionic functional group density in IFCPs, which is surprising, given that this is a central compositional parameter. The main body of this dissertation will look at methods for varying the type and ionic density of ions on conjugated polymers.

The most common backbones for IFCPs are variations on **PPV**, **PF**, **PT**, and **PPP**. Some of the more uncommon backbones include **PPy**, poly(carbazole), **PA**, and poly(arylene-ethynylene) (**PPE**). As with more classic ionically functionalized polymers, the most common ionic functional groups in IFCPs are sulfonate ($-\text{SO}_3^-$),^{32;33} carboxylate ($-\text{CO}_2^-$),^{34;35} and alkylammonium ($-\text{NR}_3^+$),³⁶ although other functional groups such as phosphonates ($-\text{PO}_3^{2-}$),³⁷ alkyipyridines ($-\text{C}_5\text{H}_4\text{N}^+-\text{Alkyl}$),^{38;39} and cationic phospholiums ($-\text{PR}_3^+$)⁴⁰ are also occasionally found.

In an effort to make solvent processable IFCPs, paths toward solubility in both organic solvents and water have been explored. It was hypothesized that adding ionic functionality to the backbone of the polymer would increase the solubility in water and other polar solvents. The ions along the backbone can also be used to form nanostructured assemblies. Additionally, chain conformation, complex formation, long range assemblies and strong interaction with other ionic compounds are now programmable properties.

In 1987 Patil, working in Wudl's lab, synthesized some polythiophenes functionalized with either ethylsulfonate or butylsulfonate, via electropolymerization. The ionic functionalization allowed the polymers to be water soluble in both the doped and undoped states.³³ The solubility of IFCPs is one of the main differences when compared to traditional inorganic semiconductors. Solubility continues to be a focus of IFCP research due to the desire for solution processable (and therefore lower cost) semiconductors.^{41;42} Increasing the number of ionic functional groups attached to the polymer is one way in which chemists have tried to increase solubility. The strong ion-dipole interactions and the potential for ion dissociation drive solubility in polar solvents. The presence of ions has even overcome the hydrophobic character of the polymer backbone making many IFCPs water soluble.

The vast majority of undoped IFCPs are soluble in either polar protic or polar aprotic solvents. As mentioned above, there are even examples of some IFCPs which are soluble in their doped forms.^{33;43-46} The density and type of ion have a significant effect on the solubility of IFCP and provide a good handle for tuning the solubility and solution properties of IFCPs. Previous work in the Lonergan group has shown that the solubility of sulfonate functionalized PAs can be tuned from dichloromethane, to dimethylformamide, to methanol, to water by varying the density of ionic functional groups and tuning the counter cation.⁴⁷⁻⁴⁹

As with their non-conjugated counterparts, the syntheses of IFCPs can be broken into two categories based on when the ions are introduced to the polymer. The first category is direct polymerization. In this route, the ion is present in the monomer before polymerization. The second category is post-polymerization functionalization, in which the ions are added after the polymerization takes place. Tables 1.2, 1.3,

and 1.4 show examples of IFCPs synthesized through direct polymerization and post-polymerization functionalization.

An advantage of post-polymerization functionalization is that the extensively studied polymerization conditions and characterization techniques for neutral CPs can still be applied. For instance, Patil *et al.* found in their original syntheses of the family of anionic PTs that not all of their ionic monomers could be directly polymerized with standard polythiophene oxidative polymerization protocols.³³ This complication led them to use a post-polymerization functionalization strategy. Post-polymerization functionalization can also be advantageous in molecular weight determination, as ionic functionality often leads to aggregation or specific interactions with the size-exclusion columns commonly employed for molecular weight determination.^{47;50;51} The post-polymerization approach, however, requires the use of a monomer with a functional group that can be easily converted to an ionic functional group. Popular choices include esters⁵² and phosphonate esters,³⁷ which can be converted to carboxylates and phosphonates (often via their silyl esters) by hydrolysis; alkyl halides, which can be converted to, for instance, alkylammoniums by nucleophilic substitution;³⁸ or amines, which can be quaternized to their ammonium derivatives.⁵³

In contrast to post-polymerization functionalization, direct polymerization removes the ambiguity of complete conversion of the precursor polymer to IFCP. While complete functionalization is not one of them, direct polymerization presents its own set of difficulties such as differential solubility between the ionically functionalized monomer and the nonionically functionalized monomer, insolubility of growing polymer chain, and longer reaction times.¹⁸

Backbone	Ionic Group	Poly. Method	Catalyst	Ref
PPP	-CO ₂ ⁻	Suzuki	Pd with Sulfonated phosphine	35
PPP	-SO ₃ ⁻	Suzuki	Pd with Sulfonated phosphine	54
PA	-SO ₃ ⁻	ROMP	W=CH(<i>o</i> -C ₆ H ₄ OMe)(NC ₆ H ₅)[OCCH ₃ (CF ₃) ₂] ₂ (THF)	47
PA	-N(CH ₃) ₃ ⁺	ROMP	W=CH(<i>o</i> -C ₆ H ₄ OMe)(NC ₆ H ₅)[OCCH ₃ (CF ₃) ₂] ₂ (THF)	47
PFP	-PO ₃ ²⁻	Suzuki	Pd(OAc) ₂	55;56
PFP	-CO ₂ Na	Suzuki	Pd(OAc) ₂	57
PPE	-SO ₃ ⁻	Sonagashira	Pd with Sulfonated phosphine	58
PPE	-NR ₃ ⁺	Sonagashira	Pd(PPh ₃) ₄	59
PT	-CO ₂ H	FeCl ₃ oxidation	-	60
PPE	-SO ₃ ⁻	Sonagashira	Pd(PPh ₃) ₄	61
PPE	-SO ₃ ⁻	Sonagashira	Pd(PPh ₃) ₄	62
PPP-co-NPh ₃	-SO ₃ ⁻	Suzuki	Pd(OAc) ₂	63

TABLE 1.2. Survey of IFCPs made by direct polymerization methods.

Backbone	Ionic Group	Poly. Method	Catalyst	Ref
PPP	$-\text{NR}_2 \rightarrow -\text{NR}_3^+$	Suzuki	$\text{Pd}(\text{OAc})_2$	64
PPP	$-\text{I} \rightarrow -\text{N}(\text{CH}_2\text{CH}_3)_3^+$	Suzuki	$\text{Pd}(\text{PPh}_3)_4$	38;65
PPP	$-\text{I} \rightarrow -(\text{NC}_5\text{H}_5)^+$	Suzuki	$\text{Pd}(\text{PPh}_3)_4$	38;65
PPP	$-\text{NR}_2 \rightarrow -\text{NR}_3^+$	Suzuki	$\text{Pd}(\text{OAc})_2$	66
PPP-co-PT	$-\text{NR}_2 \rightarrow -\text{NR}_3^+$	Stille	$\text{PdCl}_2(\text{PPh}_3)_2$	64
PT	$-\text{Br} \rightarrow -\text{NH}_3^+$	-	ZnCl_2 and $\text{Ni}(\text{dppp})\text{Cl}_2$	67
PT	$-\text{Br} \rightarrow -\text{NHR}_2^+$	-	ZnCl_2 and $\text{Ni}(\text{dppp})\text{Cl}_2$	67
PT	$-\text{N}-^t\text{Boc} \rightarrow -\text{NH}_3^+$	FeCl_3 oxidation	-	68
PFF	$-\text{NR}_2 \rightarrow -\text{NR}_3^+$	Suzuki	$\text{Pd}(\text{PPh}_3)_4$	69
PFP	$-\text{NR}_2 \rightarrow -\text{NR}_3^+$	Suzuki	$\text{Pd}(\text{dppf})\text{Cl}_2$	69
PFF	$-\text{Br} \rightarrow -\text{NR}_3^+$	Suzuki	$\text{Pd}(\text{PPh}_3)_4$	70
PFP	$-\text{NR}_2 \rightarrow -\text{NR}_3^+$	Suzuki	$\text{Pd}(\text{PPh}_3)_4$	50
PF-co-BTDZ	$-\text{NR}_2 \rightarrow -\text{NR}_3^+$	Suzuki	$\text{Pd}(\text{PPh}_3)_4$	36
PFE	$-\text{N}(\text{C}_2\text{H}_5)_2 \rightarrow -\text{N}(\text{C}_2\text{H}_5)_2\text{CH}_3^+$	Sonagashira	$\text{Pd}(\text{PPh}_3)_4/\text{CuI}$	71
PPV	$-\text{N}(\text{C}_2\text{H}_5)_2 \rightarrow -\text{N}(\text{C}_2\text{H}_5)_3^+$	Gilch	-	72
PPV	$-\text{N}(\text{C}_2\text{H}_5)_2 \rightarrow -\text{N}(\text{C}_2\text{H}_5)_3^+$	Heck	$\text{Pd}(\text{OAc})_2$, $\text{P}(o\text{-Tol})_3$	73
PPV	$-\text{N}(\text{CH}(\text{CH}_3)_2) \rightarrow -\text{N}(\text{CH}(\text{CH}_3)_2)(\text{C}_2\text{H}_5)^+$	Heck	$\text{Pd}(\text{OAc})_2$, $\text{P}(o\text{-Tol})_3$	74

TABLE 1.3. Survey of cationic IFCPs made by post-polymerization methods.

Backbone	Ionic Group	Poly. Method	Catalyst	Ref
PFP	$-\text{OPh} \rightarrow -\text{O} - \text{SO}_3^-$	Suzuki	$\text{Pd}(\text{PPh}_3)_4$	75
PFP	$-\text{CO}_2\text{CH}_3 \rightarrow -\text{CO}_2^-$	Suzuki	$\text{Pd}(\text{PPh}_3)_4$	76
PFP	$-\text{CO}_2^t\text{Bu} \rightarrow -\text{CO}_2^-$	Suzuki	$\text{Pd}(\text{PPh}_3)_4$	77
PPP	$-\text{Br} \rightarrow -\text{CO}_2^-$	Suzuki	$\text{Pd}(\text{PPh}_3)_4$	78
PPP	$-\text{CO}_2\text{CH}_3 \rightarrow -\text{CO}_2^-$	Colon	NiBr_2	79
PPP	$-\text{SO}_3(\text{Ph})\text{CH}_3 \rightarrow -\text{SO}_3^-$	Suzuki	$\text{Pd}(\text{PPh}_3)_4$	80
PT	$-\text{Br} \rightarrow -\text{CO}_2^-$	-	ZnCl_2 and $\text{Ni}(\text{dppp})\text{Cl}_2$	67
PFP	$-\text{N}((\text{CH}_2)_2\text{CO}_2\text{CH}_3)_2 \rightarrow -\text{N}((\text{CH}_2)_2\text{CO}_2^-)_2$	Suzuki	$\text{Pd}(\text{dppf})\text{Cl}_2$	81
PFP-co-BTDZ	$-\text{CO}_2^t\text{Bu} \rightarrow -\text{CO}_2^-$	Suzuki	$\text{Pd}(\text{PPh}_3)_4$	82
PPE	$-\text{CO}_2\text{CH}_2\text{CH}(\text{CH}_2\text{CH}_3)\text{C}_4\text{H}_9 \rightarrow -\text{CO}_2^-$	Sonagashira	$\text{Pd}(\text{PPh}_3)_4$	83
PPE	$-\text{CO}_2\text{C}_{12}\text{H}_{25} \rightarrow -\text{CO}_2^-$	Sonagashira	$\text{Pd}(\text{PPh}_3)_4/\text{CuI}$	84
PPE	$-\text{P}(\text{O})(\text{OC}_4\text{H}_9)_2 \rightarrow -\text{PO}_3^{2-}$	Sonagashira	$\text{Pd}(\text{PPh}_3)_4/\text{CuI}$	37
PFF-co-BTDZ	$-\text{CO}_2^t\text{Bu} \rightarrow -\text{CO}_2^-$	Suzuki	$\text{Pd}(\text{PPh}_3)_4$	85
PPV	$-\text{SO}_2\text{Cl} \rightarrow -\text{SO}_3^-$	Wessling	-	32
PPV	$-\text{CO}_2\text{C}_2\text{H}_5 \rightarrow -\text{CO}_2^-$	Heck	$\text{Pd}(\text{OAc})_2, \text{P}(o\text{-Tol})_3$	52
PPV	$-\text{CO}_2\text{C}_2\text{H}_5 \rightarrow -\text{CO}_2^-$	Gilch	-	86

TABLE 1.4. Survey of anionic IFCPs made by post-polymerization methods.

1.3. Dissertation Overview

In this chapter I have presented a brief introduction to polymer chemistry, while also introducing IFCPs as a scientifically interesting class of polymers. In Chapter II, I will present the design and synthesis of several types of IFCPs including one family of anionic polyfluorene IFCPs with ionic densities varying between $\chi = 0.05$ and $\chi = 0.5$. I will then show the effect of ion-density on the solubility and optical properties of the IFCPs. The anionic polyfluorene IFCPs are synthesized in a one phase reaction made possible through careful choice of solvent and monomer. Chapter III describes the synthesis and characterization of two families of cationically functionalized conjugated polymers, and several methods for making them. These families of cationic PFF IFCPs are synthesized via the post-polymerization functionalization route, and so comparisons between the non-ionically functionalized polymer and the ionically functionalized polymer are reported. Impedance spectroscopy is used to measure the ionic conductivity of thin films of these polymers. Chapter IV will include a summary of this work and my final thoughts.

CHAPTER II

ANIONICALLY FUNCTIONALIZED CONJUGATED POLYMERS

2.1. Introduction

Phenylene-based conjugated polymers are important to the scientific community for their fascinating physical, optical, and electronic properties as shown by their use in light-emitting devices, sensors, and biological applications. Ionic functionalization of these polymers is of interest because it affects solubility, conductivity, interactions with other molecules, photophysics, doping chemistry, and electronic, ionic, and mixed ionic/electronic conductivity.²⁴⁻³¹ A central compositional parameter of ionically functionalized conjugated polymers (IFCPs) is the density of ionic functional groups. Despite this, there have been relatively few reports on methods to control this density in phenylene-based conjugated polymers. This chapter presents the synthesis and characterization of a family of soluble, phenylene-based, anionically functionalized, conjugated polymers with variable ionic density. The synthesis developed utilizes the direct polymerization of ionic monomers, permits for the facile control over the ionic density in the polymers, and through judicious selection of monomer and solvent pairs avoids complications introduced by the two phase nature of typical Suzuki cross-coupling reactions.¹⁸

Metal-catalyzed cross coupling reactions are the most commonly employed reactions for synthesizing phenylene-based conjugated polymers.^{18;25} Typically, the Suzuki coupling of an aryl dihalide with an aryl diboronic acid or acid ester is used in the synthesis of ionically functionalized derivatives.^{25;30} Other approaches include Ni catalyzed Colom coupling,^{25;79} and Pd catalyzed Sonagashira coupling to form

poly(phenylene ethylenes).^{25;53;58;83;87} Ionic functionality is introduced by coupling a monomer A containing one or more ionic functional groups (or a precursor to it) with a nonionic monomer B, which results in an alternating AB copolymer. All reports to further dilute the ionic monomer A have relied on an indirect, post-polymerization conversion approach, and nearly all have involved the synthesis of cationic materials.

There have been two primary approaches to post polymerization conversion. In the first, a nonionic AB copolymer is made by metal-catalyzed cross coupling with one of the monomers containing a functional group that can be converted to an ionic group.⁵⁰ The density of ionic functionality is then controlled by the extent of conversion post-polymerization. In the second approach, a diluent monomer C is introduced with the same functionality (boronic ester or arylhalide) as the monomer to be later converted to an ionic group.^{79;88;89} If complete conversion of the precursor monomer can be achieved, the ionic functional group density is controlled by the polymerization step rather than the conversion step. Complete conversion is rare post-polymerization, as conversions of 80-90% are commonly cited, and it has been reported that it is not necessarily reproducible.⁷⁴ To date, post-polymerization conversion approaches to controlling ionic density have nearly all involved the quaternization of an amine to form a cationic polymer. There are far fewer examples of an anionic polymer formation, formed from the hydrolysis of an ester. It is noted that the control of ionic functional group density was not the focus of many of these studies. As a result, some report only two different ionic functional group densities (including the parent AB polymer) or use a third monomer not really intended to dilute ionic functionality, but to serve a different purpose such as being an electron acceptor.

Although less explored, the direct polymerization of ionic monomers is of interest because the polymer is synthesized in a single step, it eliminates possible issues with the intentional or unintentional incorporation of unconverted precursor groups, and it is potentially applicable to a wider range of ionic functional groups. Kim et al. demonstrate the direct polymerization of an anionic monomer with phenylbiboronic ester and a different reaction with biphenyl diborinic ester to give two densities of anionic monomer along the backbone of the polymer.⁹⁰ This approach of changing the length of one of the monomers to change ionic density requires the synthesis of a new monomer each time a new density is wanted. There is no reason both cationic and anionic direct polymerization are not possible.²⁵

One possible reason that control of ionic functional group density of phenylene-based polyelectrolytes has not been reported using the direct polymerization of ionic monomers is the two-phase nature of many Suzuki cross-couplings.¹⁸ In the synthesis of non-ionic polymers, the two monomers A and B are typically dissolved in an organic phase with the base catalyst in an aqueous layer. With ionic monomers, the situation is somewhat different because the ionic monomer, say A, will partition into the aqueous layer while the nonionic monomer B stays in the organic layer. The addition of a nonionic monomer C to compete with A in the coupling reaction will, in many cases, partition into the nonaqueous layer. As demonstrated more fully herein, this will favor the formation of a poly(BC) because both of these monomers are in the same phase rather than the desired poly[(AB)(CB)]. Several methods were employed to overcome the challenges faced in developing the new synthesis reported here. By choosing amphiphilic monomers and carefully selected solvent systems, we were able to take advantage of the control afforded by direct polymerization and synthesize a

family of soluble, phenylene-based, anionically functionalized, conjugated polymers with variable ionic density.

The abbreviations used in this dissertation to describe the polymers synthesized are broken into four parts. The first part is a bold abbreviation of the backbone of the polymer; in this chapter the three polymers are poly(flourene-co-alt-phenylene) (**PFP**), poly(flourene-co-alt-flourene) (**PFF**), and poly(terphenylene vinylene) (**PTPV**). The second part of the label indicates the attached functionality along the backbone of the polymer, in this chapter all of them will be $-\text{SO}_3^-$, also in bold. The third part is a subscript indicating the type of nonionic functionality on the polymer, examples in this chapter are “OE” for oligoether, “Alkyl” for hexyl chains, “Ph” for phenyl substitution, or “H” for simple hydrogen substitution. The last part is subscripted in brackets and indicates the idealized density of functional groups from the second part of the abbreviation in units of functional group per aromatic ring shown in the $[y : z]$ where y is the number of functional groups and z is the number of aromatic rings. An example of this is the polymer **PFF-SO₃⁻ Alkyl_[1:2]**. In this example, we see that it has a poly(flourene-co-alt-flourene) backbone. Sulfonate ($-\text{SO}_3^-$) is the attached ionic group, while the nonionic functionality is a hexyl chain. The density of functionality is one $-\text{SO}_3^-$ per two aromatic rings.

2.2. Results and Discussion

2.2.1. Synthesis

The coupling of a dialkyfluorene bisboronic acid ester monomer with either a phenylene or fluorene dihalide monomer was explored in the synthesis of PFP and PFFs, respectively. Initial studies involved the direct polymerization of ionic and nonionic dihalide monomers with 9,9-Dihexylfluorene-2,7-diboronic acid bis(1,3-

propanediol) ester (**1**) in a Suzuki polycondensation. The dihexylfluorene monomer is commercially available and has been widely used in the synthesis of non-ionic polymers because the flexible alkyl side chains promote solubility.

Figure 2.1 shows the direct coupling of sodium 2,5-dibromobenzylosulfonate (**2**) with **1** to yield a poly(fluorene-co-alt-phenylene) (PFP). The synthesis of **2**, shown in Figure 2.2, was completed in two steps from commercially available 2,5-dibromotoluene (**3**). In the first step, **3** was brominated in the α position with NBS to form $\alpha,2,5$ -tribromotoluene (**4**). In the second step, **4** was sulfonated with sodium sulfite in water to form the monohydrate of **2**. The monohydrate was then dehydrated by heating to 100°C while under vacuum for 48 hours. The monomers **2** and **1** were coupled using Pd(PPh₃)₄ in a mixture of THF, methanol, and 2M K₂CO₃, see Figure 2.1. Precipitation of polymer from the two-phase mixture was observed after 48 hours and continued over the full course of the reaction (5 days). The needed reaction times were longer than typically required for the Suzuki polycondensation of nonionic monomers, but were consistent with other polymerizations involving ionic monomers.^{18;25}

The isolated polymer **PFP-SO₃ Alkyl[1:3]** was characterized by ¹H NMR. The ionic density of the purified **PFP** was confirmed using the integrals of two sets of resonances. The first set is from two equivalent benzylic protons between the sulfonate and the phenyl ring. The second integral is the total number of aromatic protons. As the polymerization was carried out in 2 M K₂CO₃, it is presumed that the isolated polymer was the potassium salt of **PFP-SO₃ Alkyl[1:3]**. The polymer was soluble in methanol at concentrations greater than 25 mg / mL. Its apparent molecular weight was 18 kDa, as seen in Table 2.1. Molecular weights of IFCPs were obtained using gel permeation chromatography using a Waters Styragel HR4 column with a nominal

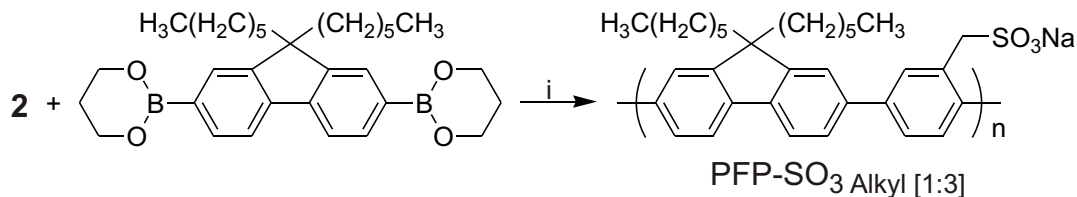


FIGURE 2.1. Synthetic conditions for **PFP-SO₃ Alkyl[1:3]**: (i) Pd(PPh₃)₄, 2M aqueous K₂CO₃, THF

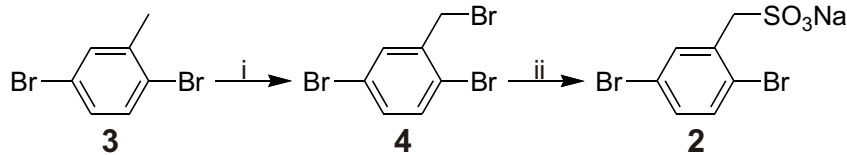


FIGURE 2.2. Synthetic conditions for monomer **2**: (i) NBS and benzoyl peroxide; (ii) Na₂SO₃

molecular weight range of $5 \times 10^3 - 6 \times 10^5$ Da with 0.1 M LiNO₃ in H₂O/DMSO 25/75 (v/v%) as an eluent. The sodium salts of polystyrene sulfonate standards were used to calibrate the column and solvent system. The 0.1 M LiNO₃ was used to screen the charge of the polymers from the charge on the column. This allowed for determination of apparent molecular weight. While standards were used in the calibration, there are vast differences in the structure of the standards and the polymers used. Due to the differences in polymer structure, the reported molecular weights should be thought of as apparent molecular weights instead of absolute molecular weights.

In an effort to control the functional group density of the **PFP-SO₃ Alkyl[1:x]** family, **1** was reacted with both **2** and a diluent monomer dibromo-p-xylylene under the same conditions used for the parent PFP with no success. As with **PFP-SO₃ Alkyl[1:3]**, the polymerizations incorporating dibromo-p-xylylene resulted in the precipitation of a yellow solid from the reaction mixture. This solid, however, was found to be a mixture of polymers, specifically, **PFP-SO₃ Alkyl[1:3]**, and the polymer of **1** and dibromo-p-xylylene. Although attempts at diluting the ionic functional group density were

IFCP	$\chi_{monomer}$	$\chi_{polymer}$	M.W. (kDa)	Ex. λ_{max}	Em. λ_{max}
PFP-SO₃ Alkyl[1:3]	0.33	0.29	18	344	390
PFF-SO₃ Alkyl[1:2]	0.5	0.55	17	380	425
PFF-SO₃ OE[1:2]	0.50	0.51	14	380	425
PFF-SO₃ OE[1:4]	0.25	0.21	19	380	425
PFF-SO₃ OE[1:5]	0.20	0.18	15	380	425
PFF-SO₃ OE[1:6]	0.17	0.17	23	380	425
PFF-SO₃ OE[1:20]	0.050	0.048	12	380	425
PTPV-SO₃ H[1:3]	0.33	0.35	13	380	425
PTPV-SO₃ Ph[1:3]	0.33	0.31	16	380	425

TABLE 2.1. $\chi_{monomer}$ as determined by initial monomer concentration, $\chi_{polymer}$ found by ¹H NMR of purified polymer, apparent molecular weights of polymers as determined by GPC running against polystyrene sulfonate standards in 0.1 M LiNO₃ in 25% water/ 75% DMSO, λ_{max} of the excitation spectrum in nanometers, λ_{max} of the emission spectrum in nanometers

not successful, the **PFP-SO₃** Alkyl[1:3] polymer is a new IFCP with a relatively low $\chi = 1/3$. The other known anionic examples of **PFPs** are a sulfate,⁷⁵ sulfonate,⁹¹ and phosphonate⁵⁵ with $\chi = 2/3$.

It is believed that a mixture of polymers was obtained in an attempt to dilute ionic functionality because of the two-phase nature of the polymerization. Nearly all Suzuki polycondensations are two phase systems. In the synthesis of nonionic polymers, both the aryl halide and boronic ester partition into the organic layer, thereby providing optimal contact between monomers. In the synthesis of ionic polymers, as with **PFP-SO₃** Alkyl[1:3], the aryl halide and boronic ester are in separate phases leading to poorer contact, which requires longer polymerization times. In the copolymerization of **1**, **2** and dibromo-p-xylene, it is possible for polymerization to occur both within the organic layer and across the organic/aqueous interface. It is hypothesized that the **1** preferentially reacts with the dibromo-p-xylene over the **2**, which is within a separate phase, leading to the rapid formation of **1**/dibromo-p-xylene, with the slower formation of **PFP-SO₃** Alkyl[1:3] at the organic/aqueous

interface. Polymerizations in acetonitrile further support this hypothesis. In this solvent, the **1**/dibromo-p-xylene polymer is observed to precipitate immediately upon addition of catalyst. No **PFP-SO₃ Alkyl[1:3]** is observed at these early stages of the reaction, and the **2** can be nearly quantitatively recovered by simple separation of the aqueous layer. At later stages, whether or not the **1**/dibromo-p-xylene was separated out, **PFP-SO₃ Alkyl[1:3]** was observed.

A multitude of approaches were pursued in an effort to better balance the activity of **2** and dibromo-p-xylene. As alluded to above, several different solvent combinations, such as CH₃CN/H₂O, MeOH/THF/H₂O, were tried, but each of them still resulted in a mixture of polymers. An attempt to emulsify the polymerization through the addition of phase transfer agents including CTAB and TBABr was also unsuccessful even in combination with the range of solvent systems explored. This is perhaps not surprising given the large concentration of K₂CO₃ used as the base in these polymerizations. In a number of ionic polymerizations, Pd(OAc)₂ is used because of greater solubility in polar solvents than Pd(PPh₃)₄, but when we attempted three-component polymerizations using Pd(OAc)₂, they still resulted in a mixture of polymers.

As reaction conditions leading to the target family of polymers could not be identified, two different monomer combinations were explored. In the first, the **2** was replaced with a sulfonated fluorene derivative, 2,7-dibromo-9,9-di-(6-sodium sulfonate-hexyl)fluorene (**5**), which is similar to that used in syntheses of ionic polyfluorenes in the absence of a diluent monomer. The monomer **5** was synthesized by the sulfonation of 2,7-dibromo-9,9-di-(6-bromohexyl)fluorene (**6**) in water using sodium sulfite with cetyltrimethylammonium bromide and **5** as phase transfer agents, see Figure 2.3. The **6** was synthesized according to previously published procedure.⁸⁹

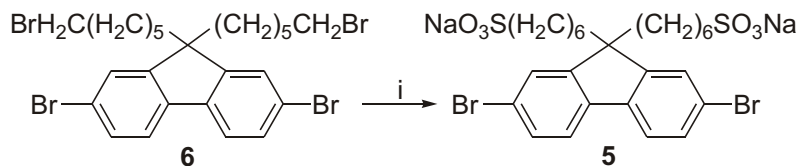


FIGURE 2.3. Synthetic conditions for **5**:(i) Na_2SO_3 , cetyltrimethylammonium bromide, **5**, water, reflux, 36 hr

Several approaches were attempted in the synthesis of **5** before it was recognized that it could be used as a phase transfer agent in its own synthesis. These approaches are shown in Figure 2.3. Sulfonation of the **6** alkyl halide chains using sodium sulfite and cetyltrimethylammonium bromide in water, water/methanol mixtures, and dimethylsulfoxide/water mixtures did not yield sulfonated monomer. Exchanging the $-\text{Br}$ for $-\text{I}$ was successful, but sulfonation of the iodo- functionalized 2,7-dibromo-9,9-di-(6-iodohexyl)fluorene (**7**) with sodium sulfite and cetyltrimethylammonium bromide in water, water/methanol mixtures, and dimethylsulfoxide/water mixtures did not yield sulfonated monomer.

An alternative approach to introducing the sulfonate group functionality is through the oxidation of a precursor such as thiol or dithiol. The thiol functionalized, 2,7-dibromo-9,9-di-(6-thiolhexyl)fluorene (**8**), was synthesized via the diisothiuronium salt, the sulfur was introduced through nucleophilic attack by thiourea in refluxing ethanol, which was then hydrolyzed with sodium hydroxide and neutralized with sulfuric acid. The thiol **8** was then oxidized using refluxing nitric acid to give the sulfonated monomer 2,7-dibromo-9,9-di-(6-sulfonic acid-hexyl)fluorene (**9**). Unfortunately, the fluorene monomer was also nitrated. More gentle oxidation conditions (30% hydrogen peroxide in acetic acid) only oxidized to the dithiol. We suspected that this monomer would be a good phase transfer agent and so it was added to the sodium sulfite reaction shown above, allowing the reaction to go to

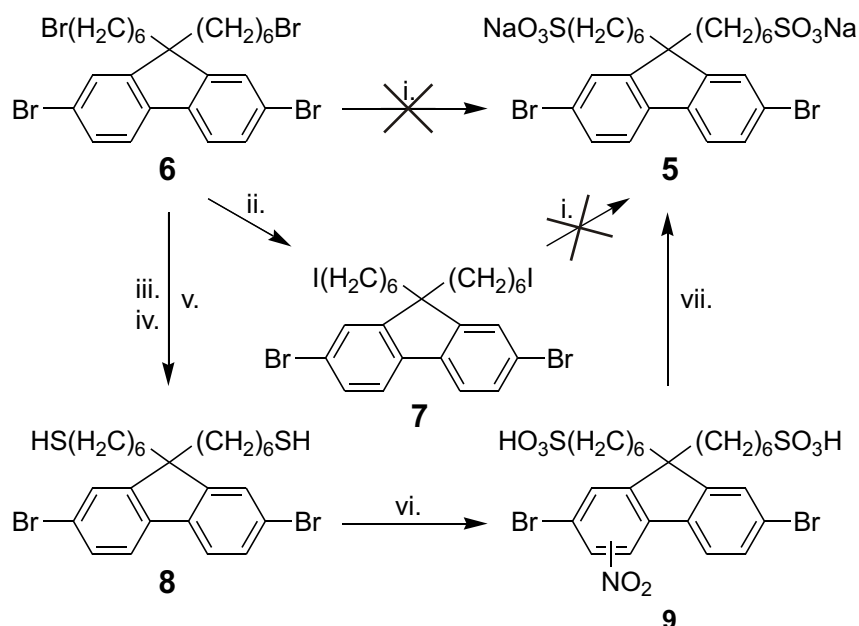


FIGURE 2.4. Synthetic conditions for original synthesis of **2**: (i) Na_2SO_3 , CTAB; (ii) NaI in acetone; (iii) thiourea in EtOH, reflux, 16 hr; (iv) NaOH in H_2O , reflux, 3 hr; (v) H_2SO_4 ; (vi) boiling HNO_3 , (vii) 5% **9**, **6**, Na_2SO_3 , cetyltrimethylammonium bromide in water.

completion. Some of the newly synthesized **5** was used as a phase transfer reagent, and it was also shown to work well. The inclusion of approximately five percent **5** is vital for the success of the reaction, for when it is left out, the reaction does not proceed even when refluxed for several days.

Sulfonated fluorene monomer **5** was used in the synthesis of **PFF**. Monomer **5** was reacted with **1** and its commercially available dihalide analogue 2,7-dibromo-9,9-dihexylfluorene (**10**). It was hoped that the **5** would act as a better surfactant than **2**. Polymerization of **1** with **5** alone led to polymer **PFF-SO₃ Alkyl[1:2]** as shown in Figure 2.5. The integrals of two sets of protons in the ^1H NMR in DMSO confirmed polymer composition. The resulting polymer was soluble in DMSO to a level of > 5 mg/mL. The molecular weight of the polymer by GPC was found to be 17 kDa for a polymerization carried out under identical conditions as that of **PFF-SO₃ Alkyl[1:3]**.

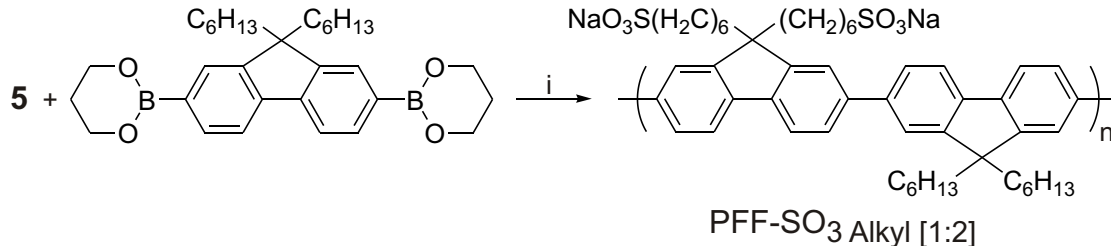


FIGURE 2.5. Synthetic conditions for **PFF-SO₃ Alkyl[1:2]**: (i) Pd(PPh₃)₄, 2M aqueous K₂CO₃, THF

However, the addition of the **10** diluent was not successful in that it resulted in a mixture of polymers. As in the **PFP-SO₃ Alkyl[1:x]** system, this result was unaffected by changes in solvent system and the addition of phase transfer agents.

In the second approach, **5** was copolymerized with an oligoether-functionalized dibromofluorene 2,7-Dibromo-9,9-di(1-(2-(2-methoxy ethoxy)ethoxy)ethyl)fluorene (**11**) and its boronic ester derivative 2,7-Bis(4,4,5,5-tetramethyl-1,3,2-dioxaborolan-2-yl)-9,9-di(1-(2-(2-methoxy ethoxy)ethoxy)ethyl)fluorene (**12**) as shown in Figure 2.6 to yield a group of oligoether functionalized polyfluorenes **PFF-SO₃ OE[1:x]** where x varies between 2 and 20 ($\chi = 0.5 - 0.05$). The oligoether functionality was introduced to improve the solubility of both the monomers and growing polymer in polar solvents. It was also found that these oligoether functionalized monomers did not break the THF/CH₃OH/H₂O solution into two phases, as seen in the systems above. The monomer **11** is an oligoether derivative of commercially available 2,7-dibromofluorene. Functionalization was accomplished using LDA to deprotonate the 9 position of fl followed by the addition of excess Br(CH₂CH₂O)₃CH₃. The monomer **12** is the boronic acid ester of **11**, functionalized by lithium halide exchange of **11** using *n*-Butyllithium at -78°C followed by quenching with 2-isopropoxy-4,4,5,5-tetramethyl-1,3,2-dioxaborolane, as can be seen in Figure 2.7.

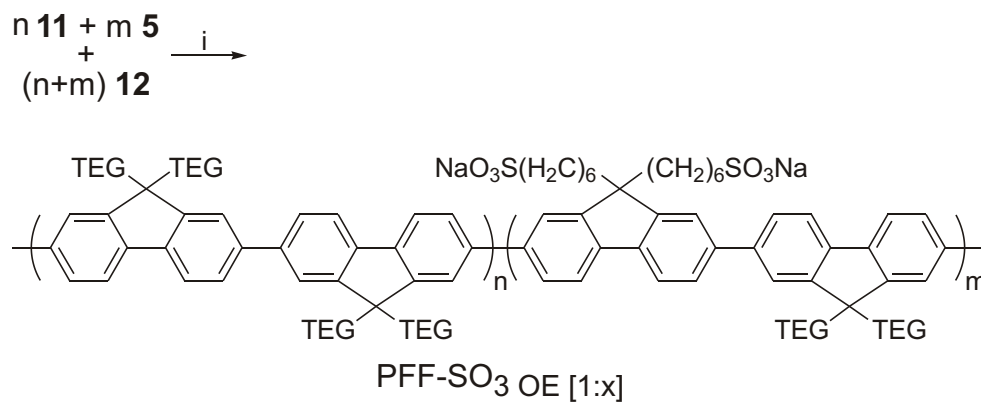


FIGURE 2.6. Synthetic conditions for **PFF-SO₃ OE [1:x]**: (i) Pd(PPh₃)₄, 2M aqueous Na₂CO₃, THF, methanol

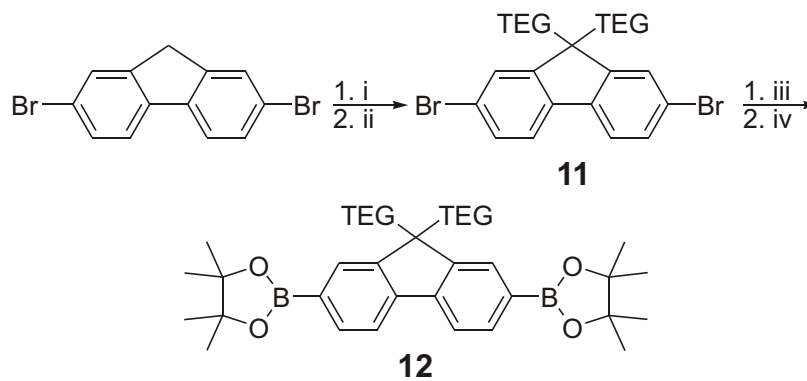


FIGURE 2.7. Synthetic conditions for **11** and **12**: TEG=(CH₂CH₂O)₃CH₃; (i) LDA, -78°C; (ii) Br(CH₂CH₂O)₃CH₃; (iii) *n*-Butyllithium, -78°C; (iv) 2-isopropoxy-4,4,5,5-tetramethyl-1,3,2-dioxaborolane.

The polymerization of **5**, **11**, and **12** using the Suzuki polycondensation reaction was carried out with monomer compositions targeting the following polymers **PFF-SO₃ OE[1:2]**, **PFF-SO₃ OE[1:4]**, **PFF-SO₃ OE[1:5]**, **PFF-SO₃ OE[1:6]**, and **PFF-SO₃ OE[1:20]**. All of these polymerizations used an 8:1 organic solvent to aqueous base ratio, instead of the more common 3:2. With the organic solvent being a mixture of equal volumes of THF and methanol, the reaction was single phase over the full range of monomer compositions. The reactions all proceeded with the formation of a yellow-orange precipitate that began forming around 18 hours. The resulting polymer was washed with CHCl₃, THF and water. The organic washes were found to contain unreacted monomer and reaction byproducts but no polymer. It is noted that the polymer of **11** and **12** is known to be soluble in both CHCl₃ and THF. The water wash was found to contain a small amount of unreacted ionic monomer but again no polymer. The isolated polymers were all found to be soluble in DMSO to a level of at least 5 mg / mL, and **PFF-SO₃ OE[1:2]**, **PFF-SO₃ OE[1:4]** were soluble in methanol. These solubility characteristics strongly argue against the formation of a mixture of polymers. In particular, no component of the polymers with lower ionic concentration was soluble in either methanol or THF, whereas the endpoint polymers from the reaction of **12** with either **5** or **11** are soluble in methanol or THF, respectively. Gel permeation chromatography on all of the polymers in a 0.1 M LiNO₃ DMSO/H₂O 75/25 (v/v) eluent revealed a single broad peak. The apparent molecular weights are reported in Table 2.1

The ionic density in the **PFF-SO₃ OE[1:x]** series was determined by ¹H NMR of the purified polymers in DMSO-*d*₆ using the integral of two sets of resonances. The first set is from four equivalent methylene protons on the sulfonate side chains (the fifth carbon from the sulfonate). The second integral is the total number of

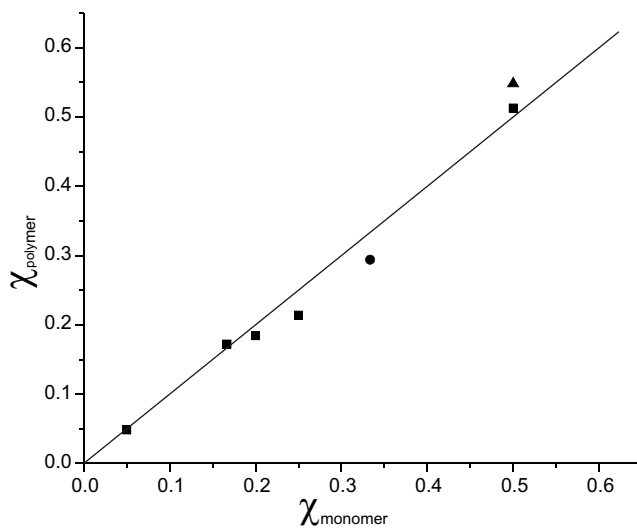


FIGURE 2.8. Correlation between $\chi_{monomer}$ and $\chi_{polymer}$ for **PFF-SO₃ OE[1:x]** (■), **PFF-SO₃ Alkyl[1:3]** (●), and **PFF-SO₃ Alkyl[1:2]** (▲).

aromatic protons. Table 2.1 and Figure 2.8 compare the polymer compositions from ¹H NMR to the idealized compositions based on the monomer feedstock. The polymer composition was successfully varied between $\chi = 0.05$ and $\chi = 0.5$. As can be seen, there is a good correlation between input monomer ratio and the ratio of monomers incorporated into the IFCPs.

There comes a point where the ionic density is so low that it is statistically improbable, or impossible, for each polymer chain to contain an ionic monomer. A molecular weight of 9.2 kDa is needed for the lowest concentration of **PFF-SO₃ OE[1:20]** to have one ionic functional group. With an apparent molecular weight of 12 kDa, **PFF-SO₃ OE[1:20]** is probably above this minimum range.

The tuning of ionic functional group density over the range achieved in the **PFF-SO₃ OE[1:x]** system has not been demonstrated in other luminescent ionically functionalized conjugated polymers. Most typically, an ionic monomer (or its precursor) is coupled with either another ionic monomer or a nonionic monomer in a one-to-one ratio leading to relatively high ionic functional group densities. This

is the case with anionic poly(fluorene) IFCPs where carboxylate⁸², sulfonate⁹¹ and phosphonate⁵⁵ examples are known, with $\chi = 0.5, 0.5$, or 1, respectively. More broadly speaking, there are very few examples of IFCPs with ionic functional group densities much lower than this or where deliberate variation has been demonstrated. The most notable examples come from the nonexhaustive quaternization of amine derivatized conjugated polymers to yield cationic IFCPs. For instance, Liu *et al.* have demonstrated using this approach the synthesis of **PFP**s with $\chi = 0.2, 0.4$, and 0.53 using this approach. In their work, the varying level of quaternization was achieved by control over reaction conditions, including solvent, temperature, and time.⁵⁰ Quaternization yields in similar reactions have also been reported by Mikroyannidis *et al.* to be very sensitive to such conditions.⁷⁴

In the course of these studies, the synthesis of anionic IFCPs based on the poly(terphenylene vinylene) (**PTPV**) backbone were also explored. Specifically, the synthesis of two sulfonate derivatized PTPVs from the coupling of **2** with either 1,2-di-(4,4'-bis-(4,4,5,5-tetramethyl-1,3,2-dioxaborolan-2-yl))-1-ethene (**13**) or 1,2-di-(4,4'-bis-(4,4,5,5-tetramethyl-1,3,2-dioxaborolan-2-yl))1-phenyl-1-ethene (**14**) was pursued, as shown in Figure 2.9. The synthesis of **13** and **14** starts with a Wittig reaction between 4-bromobenzyltriphenylphosphonium bromide and either 4-bromobenzaldehyde or 4-bromobenzophenone to form stilbenes *E*-4,4-dibromostilbene (**15**) or 1,2-di-(4-bromophenyl)-1-phenylethene (**16**) as seen in Figure 2.10. Figure 2.11 shows the synthesis of **13** and **14** which were formed by the reaction of **15** or **16** with *n*-BuLi and 2-isopropoxy-4,4,5,5-tetramethyl-1,3,2-dioxaborolane.

PTPV-SO₃ H[1:3] was synthesized using Pd(PPh₃)₄ as a catalyst in a Suzuki polycondensation in a biphasic mixture of THF and water to give **PTPV-SO₃ H[1:3]**

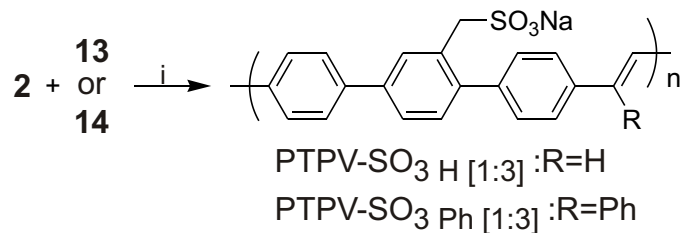


FIGURE 2.9. Synthetic conditions for **PTPV-SO₃ H** [1:3] and **PTPV-SO₃ Ph** [1:3]:(i) Pd(PPh₃)₄, 2M aqueous K₂CO₃, THF

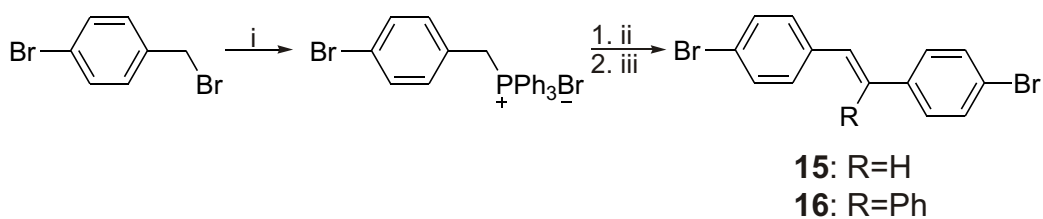


FIGURE 2.10. Synthetic conditions for monomers **15** and **16**:(i) PPh₃ (ii) NaH; (iii) When R=H, then 4-bromobenzaldehyde, when R=Ph then 4-bromobenzophenone.

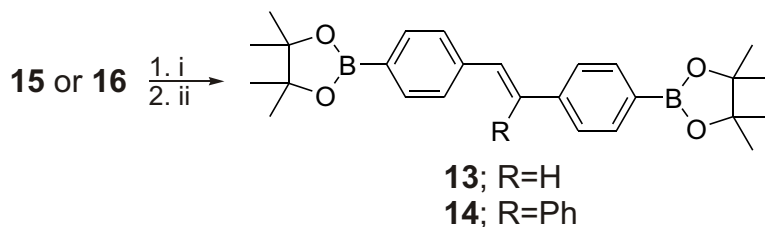


FIGURE 2.11. Synthetic conditions for **13** and **14**:(i) *n*-Butyllithium, -78°C; (ii) 2-isopropoxy-4,4,5,5-tetramethyl-1,3,2-dioxaborolane.

as shown in Figure 2.9 where R=H. The resulting polymer had an apparent molecular weight of 13 kDa, and it was soluble in DMSO to greater than 5 mg / mL. Efforts to dilute the ionic functionality with either **3** or 1,4-dibromo-2,5-dihexylbenzene to give either **PTPV-SO₃ H[1:6]** or **PTPV-SO₃ H[1:30]** gave only insoluble products.

In an effort to improve the solubility of the lower ionic functional group density polymers, the addition of a phenyl group to the vinyl portion of the polymer with **14** was pursued, as seen in Figure 2.9 where R=Ph. **PTPV-SO₃ Ph[1:3]** was successfully synthesized and yielded a polymer soluble in DMF or DMSO to a concentration of greater than 5 mg / mL and with an apparent molecular weight of 16 kDa. As in the case of **PTPV-SO₃ H[1:3]**, attempts to dilute the ionic functional group density by copolymerization with **3** or 1,4-dibromo-2,5-dihexylbenzene in the formation of **PTPV-SO₃ Ph[1:6]** or **PTPV-SO₃ Ph[1:30]** yielded only insoluble products. Polymerizations in different solvents (THF, toluene, chloroform, and acetonitrile) or with varying reaction times did not yield processable polymers. Washing the polymer with salt solutions to exchange the polymer counter ions or with dilute HCl to protonate the sulfonate groups also did not produce soluble polymers.

2.2.2. Optical Spectroscopy

Spectra (excitation, emission, and/or absorption) were collected for the fluorene-based polymers **PFF-SO₃ OE[1:x]** and **PFP-SO₃ Alkyl[1:3]** to understand how ionic functional groups affect the optical properties and solution aggregation of these materials. The shapes of the absorption, excitation and emission spectra were observed to be similar to that observed for the analogous non-ionic polymers that have been reported in the literature. Excitation spectra have been rarely reported in previous studies of IFCs. They are important because their overlap with

corresponding absorption spectra indicates that the species in solution doing the majority of the absorption is also doing the majority of emission. Such overlap was observed for all of the polymers studied. Both the absorption and excitation spectra are characterized by a single broad peak with λ_{max} in the UV (350-380nm range) and in certain cases a short wavelength shoulder.

Figure 2.12 shows a representative total luminescence spectrum for **PFF-SO₃_{OE[1:2]}**. Figure 2.13 is a two dimensional representation of the data in Figure 2.12. This two-dimensional plot is more convenient because it shows the emission spectrum as a function of the excitation wavelength, making it possible to see all of the data at the same time. As can be seen, the intensity of the emission changes with excitation wavelength, but the shape of the emission spectrum does not. This was also the case for the other polymers studied. More conventional excitation and emission spectra correspond to slices through the total luminescence spectrum at both a particular emission and excitation wavelength, respectively. Figures 2.14 and 2.15 show these spectra for **PFP-SO₃_{Alkyl[1:3]}** in methanol, and the family of **PFF-SO₃_{OE[1:x]}** polymers in DMSO, respectively. The **PFP-SO₃_{Alkyl[1:3]}** excitation spectrum was collected while observing at 390 nm, and the emission spectrum were recorded while the polymer was excited at 344 nm. The **PFF-SO₃_{OE[1:x]}** excitation spectra were collected while observing at 425 nm, and emission spectra were recorded while the polymer was excited at 380 nm. The emission spectra exhibit the vibronic structure typical of fluorene-based polymers. As with their non-ionic counterparts, the vibronic structure is clearer in the **PFF-SO₃_{OE[1:x]}** family relative to the **PFP-SO₃_{Alkyl[1:3]}**. In the **PFF-SO₃_{OE[1:x]}** series, the positions of the peaks are the same, but there is some difference in their relative strengths. The two polymers where the lowest energy peak of the vibronic progression is the most intense are also the

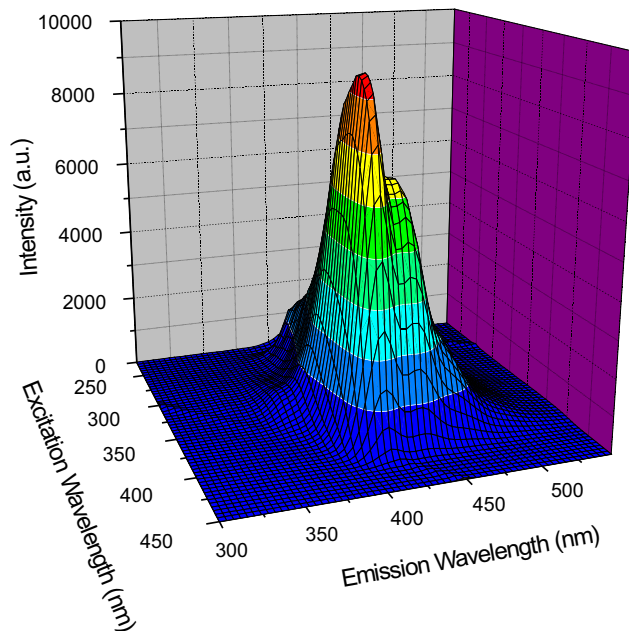


FIGURE 2.12. Three dimensional total luminescence plot for **PFF-SO₃ OE[1:2]**.

two polymers with the lowest molecular weights. A similar dependence on molecular weight has been previously observed by Gao *et al.*⁹² The relative strength of the red shifted vibronic structures changes, but the positions of the peaks are the same.

One of the goals in the polymer design was to make a family of soluble luminescent CPEs with similar backbone electronic structures. This was achieved with the **PFF-SO₃ OE[1:x]** series as evidenced by the very similar excitation and emission spectra across the family (see Figure 2.15). This is perhaps not surprising, because the bridging carbon on fluorene-based polymers tends to help lock in planarity. Further, the straight-chain oligoethers used in this family of polymers also minimize steric bulk close to the backbone, relative to often used branched side chains.

The **PFF-SO₃ Alkyl[1:3]**, **PFF-SO₃ Alkyl[1:2]**, and **PFF-SO₃ OE[1:x]** IFCPs exhibit solvatochromism as illustrated by comparing the polymers' emission in pure methanol to its binary mixtures with dichloromethane and water. Table 2.2 shows

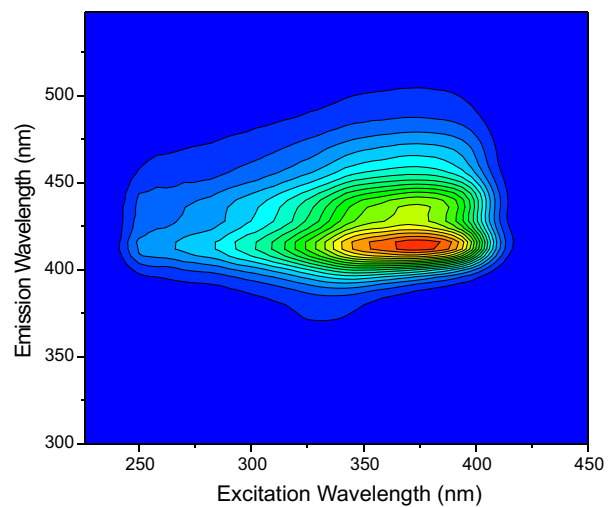


FIGURE 2.13. Two dimensional total luminescence plot for **PFF-SO₃ OE[1:2]**.

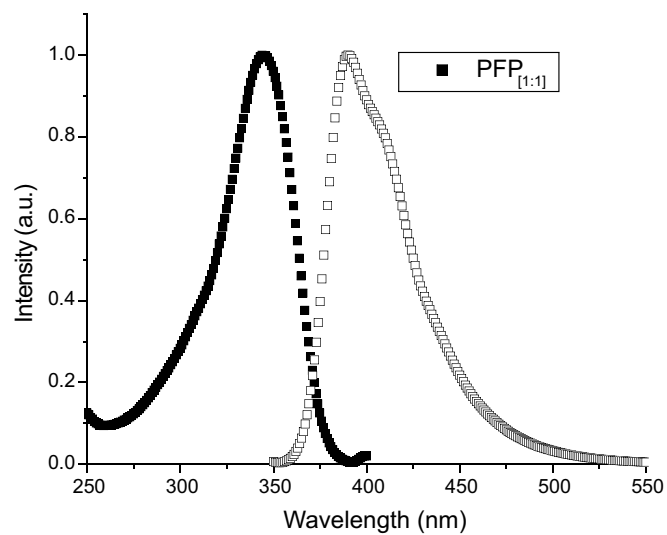


FIGURE 2.14. Normalized excitation (filled) and emission (open) spectra for the CP **PFP_[1:1]** (■)

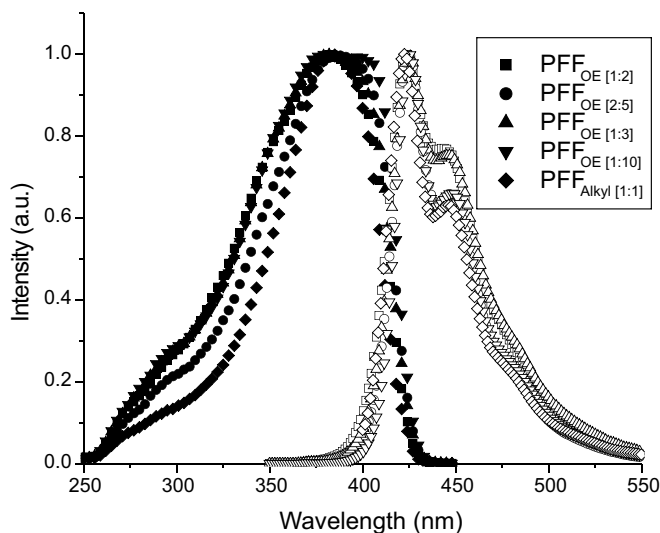


FIGURE 2.15. Normalized excitation (filled) and emission (open) spectra for the $\text{PFF}_{\text{OE}[1:2]}$ (■), $\text{PFF}_{\text{OE}[2:5]}$ (●), $\text{PFF}_{\text{OE}[1:3]}$ (▲), $\text{PFF}_{\text{OE}[1:10]}$ (▼) and $\text{PFF}_{\text{Alkyl}[1:1]}$ (◆) polymers

the wavelength of maximum emission for a given polymer and solvent mixture. A 6-12 nm bathochromic shift is observed for all of the polymers in going from methanol to a more polar methanol/water mixture, so-called positive solvatochromism. This bathochromic shift suggests increasing polymer aggregation as the non-solvent water is added. Interestingly, all but $\text{PFF-SO}_3 \text{OE}[1:2]$ show a bathochromic shift upon going from methanol to a less polar methanol/dichloromethane mixture, so-called negative solvatochromism. This shift is smaller ($\sim 4\text{nm}$), but it is again consistent with an increase in aggregation due to the addition of a non-solvent, in this case dichloromethane. It is somewhat puzzling that the polymer with the greatest ion content $\text{PFF}_{[1:2]}$ does not show any shift as the solvent polarity is decreased. Other than this observation, the data of Table 2.2 seem to suggest little dependence of the fluorescence and aggregation on ion density. These data, however, only reflect endpoints of solvent polarity.

Polymer	Solvent Mixture (v/v)	Emission λ_{max} (nm)
PFP-SO₃ Alkyl[1:3]	Methanol/Dichloromethane (1:1)	402
PFP-SO₃ Alkyl[1:3]	Methanol	398
PFP-SO₃ Alkyl[1:3]	Methanol/Water (1:1)	409
PFF-SO₃ Alkyl[1:2]	Methanol/Dichloromethane (1:1)	417
PFF-SO₃ Alkyl[1:2]	Methanol	414
PFF-SO₃ Alkyl[1:2]	Methanol/Water (1:2)	420
PFF-SO₃ OE[1:2]	Methanol/Dichloromethane (1:1)	414
PFF-SO₃ OE[1:2]	Methanol	414
PFF-SO₃ OE[1:2]	Methanol/Water (1:3)	425
PFF-SO₃ OE[1:4]	Methanol/Dichloromethane (1:1)	417
PFF-SO₃ OE[1:4]	Methanol	414
PFF-SO₃ OE[1:4]	Methanol/Water (1:2)	423
PFF-SO₃ OE[1:20]	Methanol/Dichloromethane (1:1)	418
PFF-SO₃ OE[1:20]	Methanol	414
PFF-SO₃ OE[1:20]	Methanol/Water (1:3)	426

TABLE 2.2. Table of emission λ_{max} of polyelectrolytes as a function of polymer type and solvent.

A more comprehensive study of solvatofluorochromism was conducted for **PFP-SO₃** Alkyl[1:3], **PFF-SO₃** Alkyl[1:2], and three compositions of the **PFF-SO₃** OE[1:x] family. In these studies, the polymers were dissolved in methanol and then either water or dichloromethane was added in small increments. Controls were run to ensure that any change in wavelength was not due to dilution. The polarity of the solvent mixture was calculated using the $E_T(30)$ -scale. The $E_T(30)$ is an empirical polarity scale for quantifying the polarity of a binary mixture, and it is defined by the following equation:

$$E_T(30) = E_D \cdot \ln\left(\frac{c_p}{c^*} + 1\right) + E_T^0(30) \quad (\text{Equation 2.1})$$

where $E_T^0(30)$ is the $E_T(30)$ value of the pure, less polar component, c_p is the molar concentration of the more polar component, and E_D and c^* are parameters determined experimentally when the equation was developed.⁹³ E_D is a measure of the sensitivity

of the $E_T(30)$ -scale to changes in c_p while c^* is used to divide the equation into a linear and logarithmic portion. The c^* term is the threshold value of c_p , at which the transition from a linear to a logarithmic relationship between the two solvents occurs.⁹³

Figure 2.16 shows the change in λ_{max} of emission as a function of $E_T(30)$. The endpoints of each curve in Figure 2.16 illustrate the same trends in solvatofluorochromism as the data in Table 2.2. With the exception of **PFF-SO₃ OE[1:2]** where there is little to no shift, the λ_{max} for the remaining polymers shift similarly and continuously upon lowering $E_T(30)$ from pure methanol (left side). However, the shift in λ_{max} upon increasing $E_T(30)$ from pure methanol (right side), occurs over a somewhat more narrow region of solvent polarity. Further, the region of this transition depends on the nature of the functionality and ion concentration. As the ion content increases within the **PFF-SO₃ OE[1:x]** series, so does the $E_T(30)$ at which the shift happens. **PFF-SO₃ OE[1:20]** has its shift centering around 58.25 kcal·nm·mol⁻¹, **PFF-SO₃ OE[1:4]** centers around 58.75 kcal·nm·mol⁻¹, while **PFF-SO₃ OE[1:2]** doesn't shift until 59.1 kcal·nm·mol⁻¹. Given the possibility for strong interactions between water and ions, it is perhaps not surprising that increasing the ionic functional group density causes the polymer to stay unaggregated up to a higher solvent polarity. Also significant is the nature of the non-ionic functionality on the polymer. When comparing **PFF-SO₃ OE[1:2]** with **PFF-SO₃ Alkyl[1:2]**, the solvent polarity at which aggregation occurs for **PFF-SO₃ Alkyl[1:2]** is much lower than solvent polarity at which **PFF-SO₃ OE[1:2]** aggregation occurs even though they have the same χ value of 0.5. This is consistent with the greater polarity of the oligoether side chains, which help promote solubility in more polar solvents.

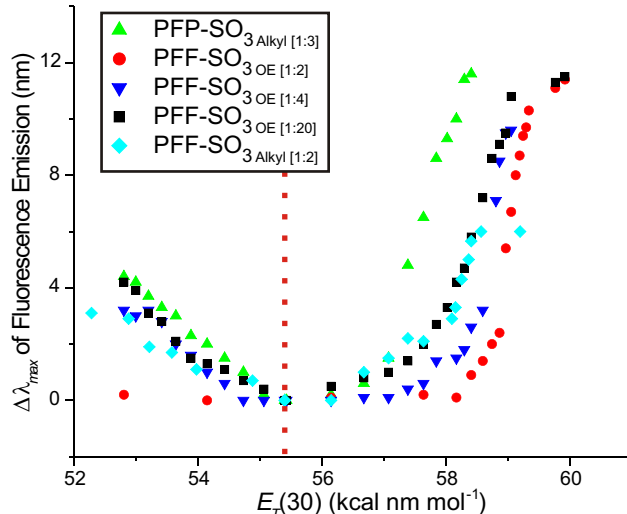


FIGURE 2.16. Change in λ_{max} of the fluorescence emission spectra from a change in the polarity of the solvent in which the polymer is found. The value of pure methanol is indicated by the vertical red dashed line and has an $E_T(30)$ value of $55.4 \text{ kcal}\cdot\text{nm}\cdot\text{mol}^{-1}$

The solvatofluorochromism of fluorene-based polymers somewhat complicates direct comparison of the IFCPs synthesized in this work with their non-ionic counterparts. Nevertheless, the excitation and emission of all of the IFCPs studied herein are comparable to other fluorene-based polymers. Excitation and emission spectra of **PFP-SO₃ Alkyl[1:3]** are each blue shifted by about 20 nm when compared to nonionically functionalized **PFP**s with no substituents on the phenylene ring.^{36;70} The monosubstituted **PFP-SO₃ Alkyl[1:3]** is red shifted by about 20 nm when compared to **PFP** with disubstituted phenylene rings.⁷⁰ The family of **PFF-SO₃ OE[1:x]** IFCPs and **PFF-SO₃ Alkyl[1:2]** all have very similar excitation and emission spectra, which correspond very well to the literature values for other ionically functionalized **PFF**s.³⁶ Note that in these comparisons, the data in methanol were used because of the most limited aggregation in this solvent.

PTPV excitation spectra were collected while observing at 417 nm, and emission spectra were recorded while the polymer was excited at 345 nm. The

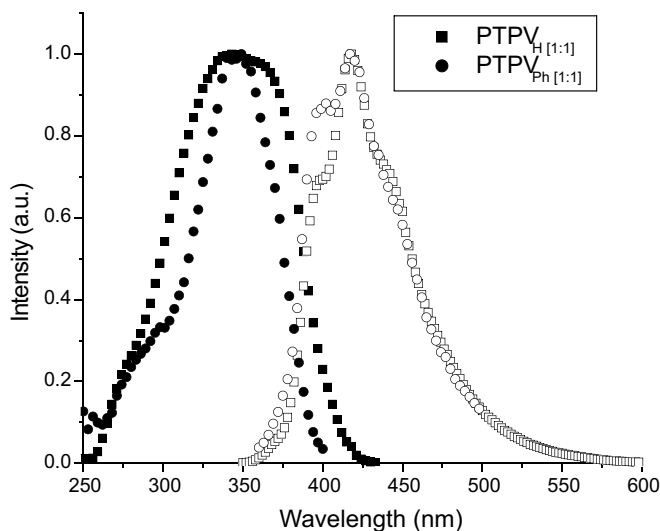


FIGURE 2.17. Normalized excitation (filled) and emission (open) spectra for **PTPV-SO₃ H[1:3]** (■), **PTPV-SO₃ Ph[1:3]** (●) polymers

excitation and absorption spectra for **PTPV-SO₃ H[1:3]** and **PTPV-SO₃ Ph[1:3]** are very similar to the nonionically functionalized poly(terphenylene vinylene)s reported in the literature.^{94–97} The emission spectra of both of these IFCPs are blue shifted by about 10nm from the nonionically functionalized polymers.

2.3. Summary

Chapter II presented the synthesis and characterization of phenylene-based anionically functionalized conjugated polymers with varying ionic density. This novel synthesis developed in the Lonergan lab utilizes direct polymerization, allows for easy control over ionic density, and elegantly avoids the two phase nature of other Suzuki polycondensation reactions. Challenges overcome were discussed. Namely by choosing amphiphilic monomers and carefully selected solvent systems, we were able to take advantage of the control afforded by direct polymerization of a three monomer reaction mixture, and synthesize a family of soluble, phenylene-based, anionically

functionalized, conjugated polymers with variable ionic density. The synthesis of monomers and polymers was given along with detailed reports of physical and optical characterization. Synthetic challenges associated with the synthesis of the anionically functionalized fluorene monomer **5** were detailed, and the successful synthesis using **5** as a phase transfer agent in its own synthesis was reported. I demonstrated the synthesis of the **PFF-SO₃ OE[1:x]** family, a series of anionically functionalized polyfluorene IFCPs with χ values varying between 0.5 and 0.05, a range not seen in any other luminescent anionic IFCPs. This was possible due to the inclusion of oligoether functionalized monomer and judicious choice of solvent mixture. The ability to directly synthesize a predetermined value of χ was shown. The family of **PFF-SO₃ OE[1:x]** was soluble in DMSO. **PFPs** and **PTPV** IFCPs were also studied. The solvatofluorochromic nature of the **PFF-SO₃ OE[1:x]** family along with **PFP-SO₃ Alkyl[1:3]** and **PFF-SO₃ Alkyl[1:2]** were studied. The nature of the backbone, ion density, and the choice of nonionic functional groups were shown to affect the onset of solvatofluorochromism.

2.4. Experimental

2.4.1. Monomer Synthesis

Sodium 2,5-dibromobenzyulsulfonate (2) α ,2,5-tribromotoluene (3.29g, 10 mmol) was added to a solution of Na_2SO_3 (1.26 g, 10 mmol) in 40 mL H_2O . The tribromotoluene did not dissolve in the water, but as the water heated, the tribromotoluene melted and formed a puddle on the bottom of the flask. This biphasic mixture was brought to reflux and refluxed for 60 hr. The starting material was not all reacted as evidenced by a small puddle of molten α ,2,5-tribromotoluene, but the reaction was removed from heat and from stirring and allowed to cool to room

temperature because it did not seem to be progressing anymore. Product crystallized from the water upon cooling and was separated by filtration while washing with ice cold water and ether. The recovered crystals were the monohydrate of the desired product and dehydrated by placing them under vacuum and heating to 100°C for 48 hours.

Yield=2.376g (67.5%) ^1H NMR (d_2 -H₂O, 300 MHz): δ (ppm) 4.24 (2H, s), 7.30 (1H, dd, $^4J_{HH} = 2.8$ Hz, $^3J_{HH} = 9.0$ Hz), 7.44 (1H, d, $^3J_{HH} = 9.0$ Hz), 7.56 (1H, d, $^4J_{HH} = 2.8$ Hz); ^{13}C NMR (d_2 -H₂O, 70 MHz): δ (ppm)

TOF-MS ES negative mode C₇H₅Br₂SO₃⁻=328.82

α ,2,5-Tribromotoluene (4) 3 (500 mg, 2.0 mmol), *N*-bromosuccinamide (534 mg, 3.0 mmol), benzoylperoxide (5 mg, 0.02 mmol) and CCl₄ (10 mL) were added to a round bottom flask and refluxed overnight. The reaction mixture was then washed with copious amounts of H₂O, and the organic layer was removed, dried over MgSO₄ and filtered. Silica gel (30 g) was added to the organic layer, and the solvent was removed *in vacuo*. The loaded silica was placed in filter and washed with hexanes until no more material came through. Solvent was removed leaving an off-white solid.

Yield=644 mg (98%) ^1H NMR (d_1 -CHCl₃, 300 MHz): δ (ppm) 4.52 (2H, s), 7.29 (1H, dd, $^4J_{HH} = 2.6$ Hz, $^3J_{HH} = 8.5$ Hz), 7.43 (1H, d, $^3J_{HH} = 8.5$ Hz), 7.80 (1H, d, $^4J_{HH} = 2.6$ Hz);

2,7-Dibromo-9,9-di-(6-sodium sulfonate-hexyl)fluorene (5) 6 (5.5 g, 8.46 mmol), Na₂SO₃ (10.6 g, 84 mmol), **5** (0.150 g, mmol) and cetyltrimethylammonium bromide (CTAB) (0.308 g, 0.84 mmol) were added to 100 mL H₂O and refluxed for 48 hours. The solvent was removed, and the solids were washed with CHCl₃ to remove leftover starting material and CTAB. The white solids were sonicated with 200 mL

methanol. The undissolved solids were filtered off and again sonicated with 200 mL methanol, and the solids were again filtered. Methanol was removed to give a white solid. Yield: 4.97 g (84%)(d_4 -CH₂OH, 300 MHz): δ (ppm)0.544 (4H, quint), 1.13 (8H, m), 1.59 (4H, quint), 2.03 (4H, m), 2.67 (4H, m), 7.48 (2H, dd, $^3J_{HH} = 8.0$ Hz, $^4J_{HH} = 1.6$ Hz), 7.56 (2H, d, $^4J_{HH} = 1.6$ Hz), 7.66 (2H, d, $^3J_{HH} = 8.0$ Hz). ¹³C NMR (d_2 -H₂O, 125 MHz): δ (ppm) 22.72, 24.44, 28.03, 29.15, 39.01, 51.24, 55.34, 121.12, 121.45, 126.52, 130.12, 138.67, 152.85.

2,7-Dibromo-9,9-di-(6-bromohexyl)fluorene (6) 50 g KOH in 100 mL of H₂O was heated to 75°C-80°C at which point 2,7-dibromofluorene (1.620 g, 5.0 mmol), dibromohexane (12.20 g, 50 mmol), and tetrabutylammonium bromide (0.161 g 0.5 mmol) were added and stirred vigorously for 45 minutes. The reaction was then extracted with CH₂Cl₂. The organic layer was washed with dilute HCl (100 mL), brine (100 mL), and H₂O (100 mL). The organic layer was dried over MgSO₄, and the solvent removed under vacuum resulting in yellow oil. Oil was distilled under vacuum to remove excess dibromohexane (about 100°C). The remaining yellow oil was run through a column of silica using chloroform/hexane (1/9) giving a white crystalline solid. Yield: 2.93 g (90%) ¹H NMR (d_1 -CHCl₃, 300 MHz): δ (ppm)0.578 (4H, m), 1.08 (4H, m), 1.20 (4H, m), 1.64 (4H, quin), 1.92 (4H, m), 3.29 (4H, t), 7.43 (2H, d, $^4J_{HH} 1.8$ Hz), 7.46 (2H, dd, $^3J_{HH} = 8.0$ Hz, $^4J_{HH} = 1.8$ Hz), 7.53 (2H, d, $^3J_{HH} = 8$ Hz). ¹³C NMR (d_1 -CHCl₃, 70 MHz): δ (ppm) 23.67, 27.52, 27.99, 29.18, 32.72, 32.82, 33.92, 40.27, 55.75, 121.47, 121.80, 126.31, 130.56, 139.27, 152.39.

2,7-Dibromo-9,9-di-(6-iodohexyl)fluorene (7) **6** was dissolved in acetone and NaI (10 equivalents) was added to the reaction flask. The reaction was brought to reflux and stirred for 12 hours. The acetone was removed under vacuum leaving a

white solid. The solids were extracted with chloroform. The organic layer was dried with MgSO_4 . The organic layer was removed leaving an off-white solid. Yield: 1.89 g (98%) ^1H NMR ($d_1\text{-CHCl}_3$, 300 MHz): δ (ppm) 0.575 (4H, quint), 1.11 (8H, m), 1.62 (4H, quint), 1.92 (4H, m), 3.06 (4H, t), 7.43 (2H, d, $^4J_{\text{HH}}$ 1.8 Hz), 7.47 (2H, dd, $^3J_{\text{HH}} = 8.0$ Hz, $^4J_{\text{HH}} = 1.8$ Hz), 7.52 (2H, d, $^3J_{\text{HH}} = 8$ Hz). ^{13}C NMR ($d_1\text{-CHCl}_3$, 70 MHz): δ (ppm) 7.46, 28.94, 30.20, 33.53, 40.21, 55.75, 121.51, 121.47, 121.85, 126.32, 130.54, 139.36, 152.46.

2,7-Dibromo-9,9-di-(6-thiolhexyl)fluorene (8) **6** (0.650 g, 1.0 mmol) and thiourea (0.166 g, 2.2 mmol) were dissolved in 50 mL refluxing ethanol and stirred for 16 hrs. NaOH (6 mL of 1.0 M) was added to the reaction causing it to become cloudy. The reaction mixture was refluxed for 3 hours during which time the solution cleared. The total reaction volume was reduced by half and 6M H_2SO_4 was added dropwise until precipitation of white solid stopped. The reaction volume was reduced to 20 mL and extracted with ether (3 x 100 mL). The organic extractions were combined and dried with MgSO_4 . Solvent was removed to give a sticky thick colorless oil. Yield: 0.550 g (98%)

2,7-Dibromo-9,9-di-(6-sulfonic acid-hexyl)fluorene (9) Concentrated nitric acid (15 mL) was added to **8** (0.55 g, 1.0 mmol) and refluxed during which time the **8** dissolved in the nitric acid. After 12 hours, water (50 mL) was added to the reaction mixture. Solvent was removed under vacuum to give a red oil, which was used without further purification.

2,7-Dibromo-9,9-di(1-(2-(2-methoxy ethoxy)ethoxy)ethyl)fluorene (11) A dry three-neck round bottom flask was charged with diisopropylamine (1.856 g, 18.35

mmol) and 15 mL freshly distilled THF. A magnetic stir bar was added and the solution was cooled to -78°C . After 10 minutes *n*-butyllithium (8.08 mL, 20.19 mmol) was added and stirred for 10 minutes. While LDA was stirring, 2,7-dibromofluorene was dissolved in 25 mL of freshly distilled THF and added dropwise to the now formed LDA solution and stirred at -78°C for 30 minutes. Upon addition, a dark orange solution formed. 1-(2-(2-methoxy ethoxy)ethoxy)ethyl bromide (5.0 g, 22 mmol) was added to the orange solution. The orange color lightened, and the reaction was stirred at -78°C for one and a half hours and allowed to come to room temperature overnight, during which time the solution turned green. Water was added to the solution and stirred for an hour. The organic layer was removed and washed with water (3 x 100 mL), then the aqueous layer was extracted with CHCl_3 (2 x 50 mL). The organic layers were combined and dried over MgSO_4 and concentrated to give an orange yellow oil. The oil was purified by column chromatography on silica with hexanes until all colored bands (3) moved off the column. After hexanes, 2:5 ethyl acetate:hexanes was used to give two bands. The second band is the product. ^1H NMR (d_1 - CHCl_3 , 300 MHz): δ (ppm) 2.33 (4H, t), 2.76 (4H, t), 3.20 (4H, m), 3.34 (6H, s), 3.39 (4H, m), 3.29 (4H, t), 3.45-3.55 (8H, m), 7.46 (2H, dd, $^3J_{HH} = 8.0$ Hz, $^4J_{HH} = 1.8$ Hz), 7.50 (2H, d, $^3J_{HH} = 8$ Hz), 7.53 (2H, d, $^4J_{HH} = 1.8$ Hz). ^{13}C NMR (d_1 - CHCl_3 , 125 MHz): δ (ppm) 39.51, 51.90, 59.01, 66.78, 70.07, 70.46, 70.49, 71.00, 121.22, 121.61, 126.72, 130.65, 138.45, 150.98.

2,7-Bis(4,4,5,5-tetramethyl-1,3,2-dioxaborolan-2-yl)-9,9-di(1-(2-(2-methoxy ethoxy)ethoxy)ethyl)fluorene (12) Monomer **11** (1.5 g, 2.4 mmol) was dissolved in 30 mL of freshly distilled THF and cooled to -78°C . *n*-butyllithium (2.44 mL, 6.11 mmol) was added dropwise to the cooled reaction and stirred at -78°C for 30 minutes resulting in an orange solution. 2-isopropoxy-4,4,5,5-tetramethyl-1,3,2-

dioxaborolane (1.59 g, 8.55 mmol) was added to the solution and stirred for 1.5 hr at -78°C and then allowed to warm to room temperature overnight, resulting in an opaque colorless solution. Water was added and stirred for 30 minutes. The organic layer was removed and washed with water (2 x 50 mL), and the aqueous layer was washed with ethyl acetate. The organic layers were combined, dried over MgSO_4 , and solvent removed under vacuum to give off white orange solid. The solids were washed with hexanes to give pure white solid. ^1H NMR ($d_1\text{-CHCl}_3$, 300 MHz): δ (ppm) 1.39 (24H, s), 2.44 (4H, t), 2.67 (4H, t), 3.18 (4H, m), 3.33 (6H, s), 3.39 (4H, m), 3.43-3.54 (8H, m), 7.70 (2H, d), 7.81 (2H, d), 7.84 (2H, d). ^{13}C NMR ($d_1\text{-CHCl}_3$, 125 MHz): δ (ppm) 24.97, 39.52, 51.02, 58.98, 66.94, 69.99, 70.45, 70.49, 71.86, 83.84, 119.53, 129.25, 134.07, 143.14, 148.59.

1,2-Di-(4,4'bis-(4,4,5,5-tetramethyl-1,3,2-dioxaborolan-2-yl)phenyl)-1-ethene (13) **15** (1.00 g, 2.95 mmol) was dissolved in dry THF (30 mL) and cooled to -78°C . $n\text{-BuLi}$ (2.48 mL, 6.21 mmol) was added via syringe, and the reaction was warmed to 0°C over 1 hour, during which time the reaction turned red. The reaction was cooled back to -78°C and 2-isopropoxy-4,4,5,5-tetramethyl-1,3,2-dioxaborolane (2.11 g, 6.21 mmol) was added dropwise and allowed to come to room temperature overnight.

Water was added until fizzing stopped, and the layers were separated. The organic layer was washed with saturated KCl brine, and twice with H_2O . The water layers were extracted with CHCl_3 . The organic layers were combined, dried over MgSO_4 , and evaporated *in vacuo*. Solids were recrystallized from hot hexanes to give white needles.

Yield=523 mg (41%) ^1H NMR ($d_1\text{-CHCl}_3$, 300 MHz): δ (ppm) 1.35 (24H, s), 7.18 (2H, s), 7.52 (4H, d, $^3J_{HH} = 8.3$ Hz), 7.80 (4H, d, $^3J_{HH} = 8.3$ Hz); ^{13}C NMR ($d_1\text{-CHCl}_3$, 70 MHz): δ (ppm) 24.8, 83.8, 125.9, 129.5, 135.1, 135.2, 135.3, 139.8.

***E*-4,4'-dibromostilbene (15)** The α ,4-dibromotoluene (500mg, 2.0 mmol) and PPh_3 (550mg, 2.1 mmol) were dissolved in 25 mL of toluene, and refluxed for 24 hours. A white precipitate came out of solution. NaH (120mg, 5.0 mmol) was added to the toluene and the reaction was refluxed for 4 hours. The reaction turned red orange. The reaction mixture was cooled to 0°C and 4-bromobenzaldehyde was added, causing the reaction to turn yellow. After 16 hours of reflux, the reaction had turned back to a red liquid with orange ppt. Water (30 mL) was added evolving gas. The organic layer was separated and dried over MgSO_4 . The organic layer was condensed *in vacuo* giving off-white crystals. The crystals were sonicated in ethanol to dissolve triphenylphosphine oxide. The ethanol liquor was exposed to UV light for 4 hours precipitating white crystals. The ethanol liquor was decanted, and the crystals were washed with cold ethanol. Decanting the ethanol liquor from the white crystals gave *E*-4,4'-dibromostilbene. The white crystals were then dried *in vacuo*. Yield = 0.437 g (64%) ^1H NMR ($d_1\text{-CHCl}_3$, 300 MHz): δ (ppm) 7.02 (2H, s), 7.36 (4H, d, $^3J_{HH} = 8.6$ Hz), 7.48 (4H, d, $^3J_{HH} = 8.6$ Hz); ^{13}C NMR ($d_1\text{-CHCl}_3$, 70 MHz): δ (ppm) 121.86, 128.22, 128.33, 132.07, 136.10.

1,2-di-(4-bromophenyl)-1-phenylethene (16) The α ,4-dibromotoluene (2.00 g, 8.0 mmol) and PPh_3 (2.11 g, 8.2 mmol) were dissolved in 100 mL of toluene and refluxed for 18 hours. Toluene was removed from white precipitate, and 100 mL of THF were added. NaH (120 mg, 5.0 mmol) was added to the THF solution and refluxed for 1 hour. The reaction turned red. The reaction mixture was cooled to

room temperature, at which point 4-bromobenzophenone was added and stirred for 18 hours. Water was added until the evolution of gas ended, at which point the reaction turned from red to yellow.

The THF was separated from the aqueous layer, and the aqueous layer was then extracted with CHCl_3 . The organic layers were combined, dried over MgSO_4 and filtered to remove the drying agent. The solvent was then removed *in vacuo* leaving behind an off-white solid. This solid was dissolved in CHCl_3 and precipitated by addition of heptane. These crystals were recrystallized by slow evaporation from benzene giving large single crystals of product.

Yield=1.42g (43%) ^1H NMR (d_1 - CHCl_3 , 300 MHz): δ (ppm) 7.06 (1H, d, $^3J_{HH} = 8.6$), 7.37 (1H, d, $^3J_{HH} = 8.7$ Hz), 7.48-7.53 (3H, m), 7.60-7.72 (6H, m), 7.78-7.81 (3H, m); ^{13}C NMR (d_1 - CHCl_3 , 70 MHz): δ (ppm)

2.4.2. Polymer Synthesis

PTPV-SO₃ H[1:3] Monomer **13** (432 mg, 1.00 mmol) was dissolved in 8.0 mL THF, and 3.0 mL of 2 M K_2CO_3 were added to a 14 mL centrifuge tube. Monomer **2** (352 mg, 1.00 mmol) was added to the tube, and the biphasic mixture was deoxygenated by bubbling N_2 through the mixture. After deoxygenating the solution, $\text{Pd}(\text{PPh}_3)_4$ was added, and the reaction was stirred for 18 hours. THF was removed and solids were washed 3 times with water (10 mL each). The solids were next washed 3 times with THF (10 mL each). The solids were dissolved in DMSO giving an orange solution and precipitated with chloroform. This washing and precipitating process was repeated 3 times. ^1H NMR (d_6 -dimethylsulfoxide, 300 MHz): δ (ppm) 4.0 (2H, s), 7.5-7.9 (11H, m).

PTPV-SO₃ Ph[1:3] Monomer **14** (432 mg, 1.00 mmol) was dissolved in 8.0 mL THF, and 3.0 mL of 2 M K₂CO₃ were added to a 14 mL centrifuge tube. **2** (352 mg, 1.00 mmol) was added to the tube, and the biphasic mixture was deoxygenated by bubbling N₂ through the mixture. After deoxygenating the solution, Pd(PPh₃)₄ was added, and the reaction was stirred for 18 hours. THF was removed, and the solids were washed 3 times with water (10 mL each). The solids were next washed 3 times with THF (10 mL each). The solids were dissolved in DMSO giving an orange solution and precipitated into chloroform. This washing and precipitating process was repeated 3 times. ¹H NMR (*d*₆-dimethylsulfoxide, 300 MHz): δ (ppm) 4.0 (2H, s), 7.5-7.9 (11H, m).

PFP-SO₃ Alkyl[1:3] Monomer **2** (352 mg, 1 mmol) and K₂CO₃ (1.382 g, 10 mmol) were dissolved in 5 mL H₂O. 9,9-Dihexylfluorene-2,7-diboronic acid bis(1,3-propanediol) ester (502 mg, 1 mmol) was dissolved in THF (20 mL). The organic and aqueous solutions were both placed in a 3 neck round bottom flask along with a magnetic stir bar and fitted with a water cooled condenser. The mixture of solutions was deoxygenated by bubbling N₂ through the solutions and heated to 85°C. After purging with N₂ for 10 minutes, the catalyst was added, and the reaction was stirred for 72 hours. The reaction was poured into water, and the solids were collected via centrifugation. The solids were washed with chloroform, dissolved in methanol and precipitated into water. This washing and precipitating process was repeated 3 times. ¹H NMR (*d*₄-methanol, 300 MHz): δ (ppm) 0.5-1.5 (22H, m), 2.1 (4H, m), 4.25 (2H, s), 7.4-8.2 (9H, m).

PFF-SO₃ OE[1:x] **General Polymerization Procedure** *n* equivalents **5**, *m* equivalents of **11**, and *n* + *m* equivalents of **12** were dissolved in 8 mL of

THF/methanol 50/50 (v/v). 1 mL of 2 M Na₂CO₃ and the organic solution were both placed in a round bottom flask fitted with a magnetic stir bar and condenser. The mixture of solutions was deoxygenated by bubbling N₂ through the solutions and heated to 85°C. After purging with N₂ for 10 minutes, the Pd(Ph₃)₄ (0.05 equivalents) catalyst was added, and the reaction was stirred for 48-72 hours. The reactions all proceeded with the formation of a yellow-orange precipitate that began forming around 18 hours. The resulting polymer was washed with CHCl₃, THF and water. The organic washes were found to contain both unreacted monomer and reaction byproducts but no polymer. Yields were in the 50-75% range.

PFF-SO₃ OE_[1:5] ¹H NMR (*d*₆-DMSO, 300 MHz): δ (ppm) .819 (8H, m), 1.21 (64H, m), 1.49 (16H, m), 1.97 (8H, m), 2.48 (64H, s), 2.79 (48H, m), 3.12-3.54 (289H, m), 7.55-8.07 (70H,m).

2.4.3. Characterization

NMR spectra were recorded with a Varian INOVA 300 MHz spectrometer with CP solutions in DMSO-*d*₆. Visible absorption spectroscopy was performed on either DMSO or methanol solutions using a Hewlett-Packard 8452A diode array spectrometer. Gel permeation chromatography was performed on a Waters chromatography system utilizing a Styragel HR4 size exclusion column, a 515 pump, and 2410 differential refractometer. The flow rate of the GPC was 0.1 mL/min.

CHAPTER III

CATIONICALLY FUNCTIONALIZED CONJUGATED POLYMERS

3.1. Introduction

In Chapter II, the successful synthesis of a family of processable, anionic IFCPs was demonstrated. A key aspect of this work was the wide range over which the anionic functional group density was varied. The control over ionic functional group density is important because it is the central materials parameter in IFCPs and controls properties such as solubility, doping chemistry, fluorescence quantum yield, surface adsorption, and ionic conductivity.³¹ For example, it has been shown in IFCPs with high ionic densities that ionic side chains and counter ions influence interactions between polymer strands, even in dilute solutions, inducing aggregation or even decomposition.^{88;98;99} These interactions were not seen in cationic IFCPs with low ionic density as reported by Hodgkiss *et al.*¹⁰⁰ Further, in many device applications involving ion-containing conjugated polymers, ion density can strongly affect device metrics.^{100;101}

In addition to their density, the sign of the ionic functional group is also a defining parameter of IFCPs. The sign of the mobile ion is important to many emerging applications of these materials. For instance, IFCPs are being studied as both active layers and injection layers in polymer light-emitting electrochemical cells (PLECs).^{101;102} In these structures, whether the mobile ion is positive or negative determines whether ions are accumulated or depleted at a given electrode. Therefore the counter ion can influence the efficiency with which electrons relative to holes are injected or transported.¹⁰³ In another example, the amplified quenching properties

of IFCPs are being explored in the development of biological sensors.²⁷ In this application, the charge attached to the polymer backbone determines the types of analytes that can be sensed.²⁹ Anionic IFCPs are being used to sense metal ions in solution⁷⁵ while cationic polymers are being used as fluorescent conjugates to DNA.^{26;89;104}

The defining nature of both the density and type (cationic or anionic) of ionic functionality in applications such as those described above motivates the synthesis of IFCPs where these structural features are controlled. The goal of the work in this chapter is to synthesize, as a complement to the anionically functionalized materials of Chapter II, a family of cationic IFCPs based on the same backbone and where the same level of control over ionic functional group density is achieved.

A wide range of cationic IFCPs have been synthesized in the literature, but as with anionic IFCPs, there has been limited control over ionic functional group density reported. The primary strategy used in the synthesis of cationic IFCPs is the coupling of two nonionic monomers A and B, followed by post-polymerization conversion involving the quaternization of an amine. Within this strategy, the control of ionic functional group density has been achieved in three primary ways. The first is through control over monomer structure. Variation in ionic functional group density has been achieved either by controlling the number of ionic functional groups on a given monomer or by varying the number of fundamental repeat units in the monomers (phenyl vs. biphenyl).¹⁰⁵ In this approach, a new monomer has to be synthesized for each ionic functional group density desired, and oligomeric monomers are required to achieve very low ionic functional group densities. The second approach has yielded families of polymers with the widest control over ionic functional group density. This approach involves the coupling of an amine functionalized monomer with

a nonionic monomer followed by non-exhaustive quaternization.^{50;74} This approach makes possible the synthesis of a range of polymers from a single precursor polymer, but it can be difficult to reproduce, and hence consistently achieve a predetermined ionic functional group density. Further, the incomplete quaternization leaves active amine functional groups. The third approach involves the incorporation of a third monomer C as a diluent. In the synthesis of more conventional polymers, this is the primary method that is used to control functional group density. It does not require the synthesis of many different monomers and enables deliberate control over polymer structure. The use of this strategy in the purposeful control of ionic density has been very limited. In most studies, the third monomer was introduced to alter the electronic properties of the polymers, and the change in ionic density was minimal and only incidental.¹⁰⁶⁻¹⁰⁸ The one exception is the work of Hodgkiss *et al.*, who in their study report a three monomer approach to expressly synthesize a cationic IFCP with low ionic functional group density in their study on the mechanism of fluorescence quenching by ionic centers. Specifically, they used post-polymerization quaternization of a polymer synthesized from three separate monomers to yield a cationic IFCP with $\chi = 0.046$.

It is the main goal of the work in this chapter to demonstrate the use of a three monomer, diluent strategy in the synthesis of cationic IFCPs with widely varying χ . A second goal is to achieve this in classes of polymers with varying solubility so as to provide processing flexibility. For direct processing, it is desirable to have soluble IFCPs. To this end, the synthesis of a family of oligoether derivatized polymers are prepared. It is also desirable to have materials whose solubility can be changed post deposition. One advantage of post-polymerization functionalization approaches to IFCPs is the possibility to do conversions in solid films. This approach allows one to

choose polymer backbone and side chain functionality in a precursor polymer without being restricted to systems which yield solution processable IFCPs. Developing polymers that can be processed from organic solvents and then quaternized in situ to become insoluble is advantageous in making multilayer structures because it allows multiple layers to be cast upon one another without layers penetrating into each other. For example, Elbing *et al.* used post-polymerization functionalization of thin films of $-Br$ functionalized derivatives of poly(2,5-bis(3-alkylthiophene-2-yl)thieno[3,2-b]thiophene). The IFCP of this thiophene was not sufficiently soluble to spin cast solid films and so they could only be made by post-polymerization quaternization of the films.¹⁰⁹ In an effort to provide polymers with very different solubilities pre- and post-quaternization, a family of alkyl functionalized **PFFs** are also synthesized.

The preparation of alkyl and oligoether functionalized **PFFs** also provides an opportunity to study the ability of the oligoether functional group to promote ionic conductivity, which is particularly relevant to many device applications of IFCPs. Polyethers are commonly used in solid polymer electrolytes, and oligoether functionalization is a common feature of other polymer electrolytes. The effect of such side chains on ionic conductivity has been indirectly explored in the study of PLECs based on IFCPs, but it has not been more directly characterized. The effect of oligoether side chains relative to alkyl side chains is explored through impedance spectroscopy on solid films.

Direct polymerization of IFCPs along with post-polymerization functionalization provide two approaches to the same target IFCP. Direct comparison of these two routes is rare in the literature. The families of polymers chosen herein allow me to investigate the IFCPs formed by these two separate avenues.

The abbreviations used in this dissertation to describe the polymers synthesized are broken into four parts. The first part is a bold abbreviation of the backbone of the polymer, in this chapter there will only be poly(flourene-co-alt-flourene) (**PFF**) polymers. The second part indicates the attached functionality along the backbone of the polymer, in this chapter they will include -NMe₃ and -Br, also in bold. The third part is a subscript indicating the type of nonionic functionality on the polymer, examples in this chapter are OE for oligoether, Alkyl for hexyl chains. The last part is subscripted in brackets and indicates the idealized density of functional groups from the second part of the abbreviation in units of functional group per aromatic ring shown in the $[y : z]$ where y is the number of functional groups and z is the number of aromatic rings. An example of this is the polymer **PFF-NMe₃**_{Alkyl}[1:2]. In this example we see that it has a poly(flourene-co-alt-flourene) backbone. A trimethylammonium ion (-NMe₃⁺) is the attached ionic group, while the nonionic functionality is a hexyl chain. The density of functionality is one -NMe₃⁺ per two aromatic rings.

3.2. Results and Discussion

Two separate families of cationic IFCPs were synthesized. The first had hexyl chains as the substituents in the 9 positions of the diluting and boronic ester monomers. The second family had triethylene glycol monomethyl ether (TEG) side chains in the 9 position. These two families of IFCPs were used to explore the effect of non-ionic functionality on the IFCPs' properties. The hexyl and TEG chains were chosen because they have very different polarities from one another. These differences result in two families of polymers with similar ion densities but very different solubilities.

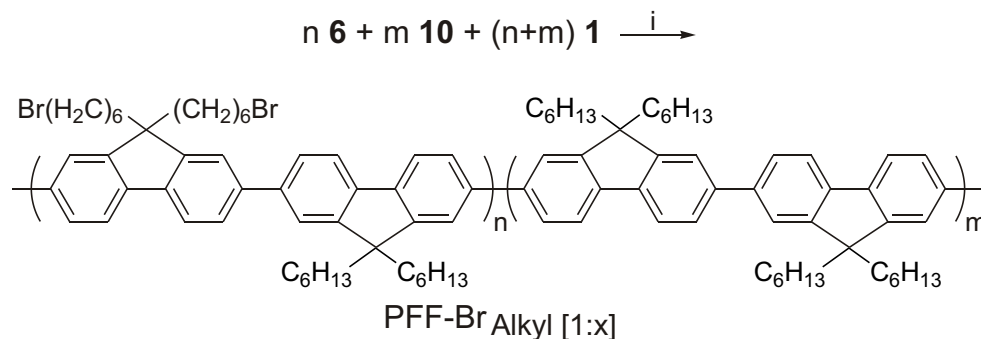


FIGURE 3.1. Synthetic conditions for **PFF-Br** Alkyl[1:x]:(i) Pd(PPh₃)₄, 2M K₂CO₃, THF and water.

The family of **PFF-Br** Alkyl[1:x] polymers were synthesized as shown in Figure 3.1 using the hexyl substituted monomers described above. Specifically, n equivalents of **6** (synthesized according to previously published procedure⁸⁹), m equivalents of commercially available 2,7-dibromo-9,9-dihexylfluorene (**10**), and $n + m$ equivalents of **1** were reacted together for eight hours to form polymers **PFF-Br** Alkyl[1:x]. Longer reaction times formed polymers which were not soluble in either chloroform or THF, and 8 hours produced polymers of high enough molecular weight to be cast as thin films. The family of **PFF-Br** OE[1:x] was synthesized in a similar manner, n equivalents of **6**, m equivalents of **11**, and $n + m$ equivalents of **12** were reacted together for 24 hours to form polymers **PFF**_{OEBR}, see Figure 3.2. Shorter reaction times were not necessary as the polymers remained soluble even after 24 hours of reacting.

It is useful here to note a few of the differences between the polymerizations in Chapter II and those in this chapter. The polymerizations in Chapter II were successful when the polymerization reaction was all one phase. In this chapter, the polymerizations were all two phase. Both the one- and two- phase polymerizations produce what are believed to be statistical copolymers of all three monomers in the

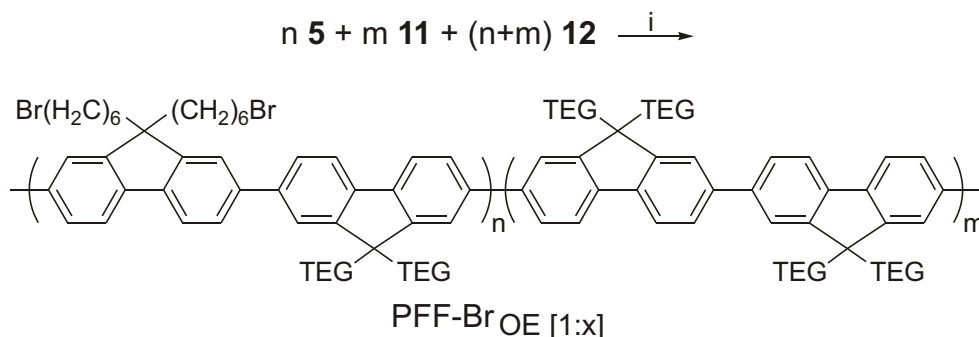


FIGURE 3.2. Synthetic conditions for **PFF-Br** $_{\text{OE}[1:x]}:(i)$ Pd(PPh₃)₄, 2M K₂CO₃, toluene and water.

reaction. The two-phase reaction works for the polymers in this chapter because all of the monomers partition into the organic phase. This was not the case with the monomers in Chapter II, as the anionic monomer partitions into the aqueous layer. Another difference between the two reaction conditions was the time the reactions were allowed to react. The reaction times for the direct polymerization of ionic monomers were 3-5 days. In contrast, the reaction times for the non-ionically functionalized monomers in this chapter were 8-24 hours. This difference in reaction times is consistent with the synthesis literature.¹⁸

The -Br functional group density in the **PFF-Br** $_{\text{Alkyl}[1:x]}$ series was determined by ¹H NMR of the purified polymers in chloroform-*d*₁ using the ratio of integrals from two sets of resonances. The first set is the triplet from four equivalent methylene protons on the 6-bromohexyl side chains (the number 6 carbon on the 6-bromohexyl chain). The second integral is the total number of aromatic protons. The -Br functional group density in the **PFF-Br** $_{\text{OE}[1:x]}$ series was also determined by ¹H NMR of the purified polymers in chloroform-*d*₁ using the ratio of integrals of two sets of resonances. The first set is from four equivalent methylene protons on the

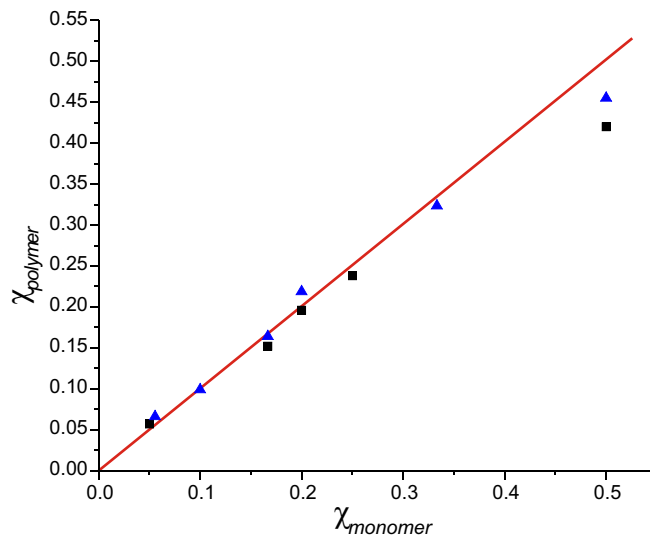


FIGURE 3.3. Correlation between $\chi_{monomer}$ and $\chi_{polymer}$ for the polymer families **PFF-Br**_{OE[1:x]} (black squares) and **PFF-Br**_{Alkyl[1:x]} (blue triangles).

6-bromohexyl side chains (the number two carbon on the 6-bromohexyl chain). The second integral is the total number of aromatic protons.

Figure 3.3 compares the polymer compositions from ¹H NMR to the idealized compositions based on the monomer feedstock. The polymer composition was successfully varied between $\chi = 0.05$ and $\chi = 0.5$. As can be seen, there is a good correlation between input monomer ratio and the ratio of monomers incorporated into the polymer. Table 3.1 summarizes the characterization data collected on the **PFF-Br**_{Alkyl[1:x]} and **PFF-Br**_{OE[1:x]} families.

CP	$\chi_{monomer}$	$\chi_{polymer}$	Molecular Weight (kDa)	Excitation λ_{max} (nm)	Emission λ_{max} (nm)
PFF-Br Alkyl[1:2]	0.5	0.45	43	376	416
PFF-Br Alkyl[1:3]	0.33	0.32	43	373	416
PFF-Br Alkyl[1:5]	0.20	0.22	65	387	416
PFF-Br Alkyl[1:6]	0.17	0.16	58	387	416
PFF-Br Alkyl[1:10]	0.10	0.099	24	371	416
PFF-Br Alkyl[1:18]	0.056	0.066	36	378	416
PFF-Br OE[1:2]	0.50	0.51	136	373	417
PFF-Br OE[1:4]	0.25	0.21	244	381	418
PFF-Br OE[1:5]	0.20	0.18	221	381	418
PFF-Br OE[1:6]	0.17	0.17	312	381	418
PFF-Br OE[1:20]	0.050	0.048	276	381	418

TABLE 3.1. $\chi_{monomer}$, $\chi_{polymer}$ found by ^1H NMR, molecular weight of polymers as determined by GPC running against polystyrene standards in THF, λ_{max} of the excitation spectrum in nanometers, λ_{max} of the emission spectrum in nanometers

Table 3.1 also shows the molecular weight data for the $-Br$ functionalized polymers. The molecular weights for the **PFF-Br**_{Alkyl[1:x]} family are in the 20-70 kDa molecular weight range with polydispersities in the 3-6 range. The **PFF-Br**_{OE[1:x]} family has higher molecular weights, 140-310 kDa, and is less polydisperse, 1.4-1.6, than the **PFF-Br**_{Alkyl[1:x]} family. These differences can be explained by the shorter reaction time of the **PFF-Br**_{Alkyl[1:x]} family. As was indicated in Section 1.1.3.1. on page 12, the Suzuki polycondensation reaction is a step growth polymerization, and so molecular weight and polydispersity have a high dependence on reaction time.

Excitation and emission spectra for the families of **PFF-Br**_{Alkyl[1:x]} and **PFF-Br**_{OE[1:x]} were collected and are shown in Figures 3.4 and 3.5. Note that the trends in excitation spectra and the relative intensity of the vibronic band at 440 nm follow the trends in molecular weight for the polymers. The highest molecular weight polymers have the longest excitation λ_{max} and the lowest relative intensity vibronic band in their emission spectrum. The emission λ_{max} of all of the **PFF-Br**_{Alkyl[1:x]} and **PFF-Br**_{OE[1:x]} polymers have less than a 2 nm difference in their λ_{max} values. This indicates that while the molecular weight variation among these polymers affects the relative intensities of the emission peaks in the polymers, the peak values do not depend upon the molecular weight. The fluorescence λ_{max} values reported here for these two families of $-Br$ functionalized PFFs, 416-418 nm, are very close to the literature reported value of 417 nm for poly(9,9-dihexylfluorene).¹¹⁰ Not surprisingly the addition of $-Br$ functionality in **PFF-Br**_{Alkyl[1:x]} did not greatly perturb the emission spectra when compared to poly(9,9-dihexylfluorene). Perhaps more surprising is that the addition of the more polar oligoether groups, along with the $-Br$ functionality did not change the emission either.

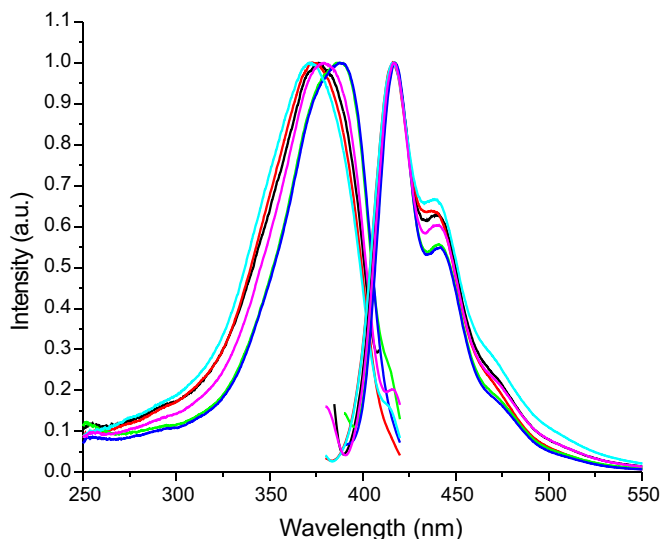


FIGURE 3.4. Excitation (left) and emission (right) spectra for **PFF-Br**_{Alkyl[1:2]} (black), **PFF-Br**_{Alkyl[1:3]} (red), **PFF-Br**_{Alkyl[1:5]} (green), **PFF-Br**_{Alkyl[1:6]} (blue), **PFF-Br**_{Alkyl[1:10]} (cyan), and **PFF-Br**_{Alkyl[1:18]} (magenta). Note that the trends in excitation spectra and relative intensity of the vibronic band at 440 nm follow the trends in molecular weight for the polymers.

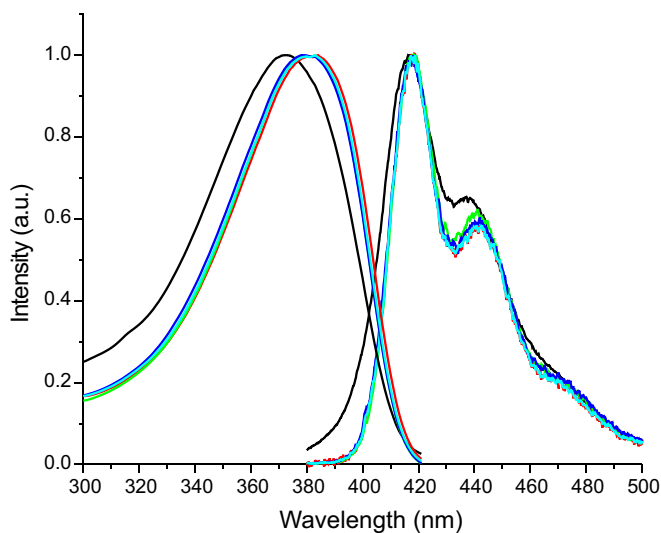


FIGURE 3.5. Excitation (left) and emission (right) spectra for **PFF-Br**_{OE[1:2]} (black), **PFF-Br**_{OE[1:4]} (red), **PFF-Br**_{OE[1:5]} (green), **PFF-Br**_{OE[1:6]} (blue), **PFF-Br**_{OE[1:20]} (cyan). Note that the trends in excitation spectra and relative intensity of the vibronic band at 440 nm follow the trends in molecular weight for the polymers.

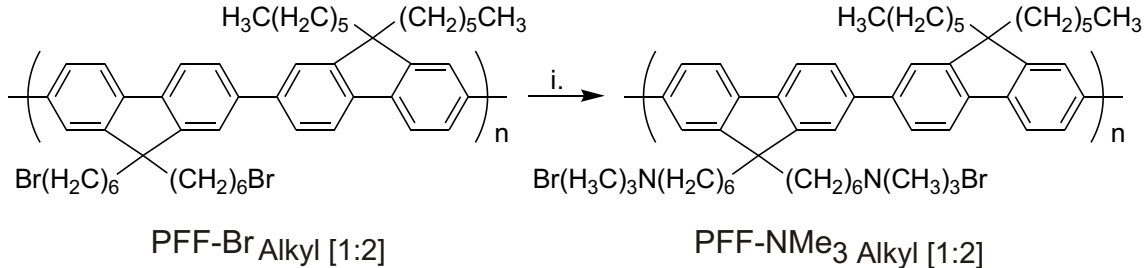


FIGURE 3.6. Synthetic conditions for **PFF-NMe₃ Alkyl[1:2]**:(i) N(CH₃)₃ in THF

3.2.1. Post-polymerization Functionalization

3.2.1.1. In Solution

In the introduction to this chapter, one intent of this work was to synthesize polymers with very different solubilities pre- and post-quaternization, and so both the oligoether functionalized **PFF-Br**_{OE[1:x]} and the family of alkyl functionalized **PFF-Br**_{Alkyl[1:x]} were prepared. If we achieved our goal, the two families should have very different solubility when quaternized with trimethylamine. To test this hypothesis, each of the polymers from the **PFF-Br**_{Alkyl[1:x]} and **PFF-Br**_{OE[1:x]} families were dissolved in chloroform and then were reacted with trimethylamine to form IFCPs **PFF-NMe₃ Alkyl[1:x]** and **PFF-NMe₃ OE[1:x]**. As an illustration, the reaction of **PFF-Br**_{Alkyl[1:2]} to form **PFF-NMe₃ Alkyl[1:2]** is shown in Figure 3.6.

Soon after the addition of trimethylamine to the solutions of the precursor polymers, the ionically functionalized **PFF-NMe₃ Alkyl[1:x]** or **PFF-NMe₃ OE[1:x]** precipitated from solution. In the case of the **PFF-NMe₃ OE[1:x]** IFCPs, they were dissolved in methanol and an additional portion of trimethylamine was added to ensure complete conversion. ¹H NMR was used to assess the completeness of reaction. **PFF-NMe₃ Alkyl[1:2]** was soluble in methanol, DMF, DMSO, and acetonitrile, but was

insoluble in chloroform, THF, water. All of the other **PFF-NMe₃** _{Alkyl[1:x]} polymers were insoluble in the aforementioned solvents and their mixtures.

The insolubility found in the **PFF-NMe₃** _{Alkyl[1:x]} family of IFCPs was not seen in the **PFF-NMe₃** _{OE[1:x]} IFCP family. All of these polymers were soluble in methanol to levels of >10 mg/mL, which further supports ion formation, because all of the polymers were insoluble in methanol prior to conversion. While IFCPs **PFF-NMe₃** _{OE[1:x]}, **PFF-NMe₃** _{OE[1:2]}, **PFF-NMe₃** _{OE[1:4]}, **PFF-NMe₃** _{OE[1:5]}, and **PFF-NMe₃** _{OE[1:6]} were insoluble in chloroform, **PFF-NMe₃** _{OE[1:20]} remained chloroform soluble even post-polymerization. This is similar to what Hodgkiss *et al.* saw with their low ionic density polymer.¹⁰⁰ It is interesting to note that each of these IFCPs had similar χ values of about 0.05.

The differences seen in solubility between **PFF-NMe₃** _{Alkyl[1:x]} and **PFF-NMe₃** _{OE[1:x]} are exactly as we predicted. The addition of ionic functional groups to the polymer with oligoether functionality was soluble in polar solvents while the addition of ionic functionality to the extremely nonpolar **PFF-Br** _{Alkyl[1:x]} polymers made the IFCP largely insoluble in most solvents.

The excitation and emission spectra of **PFF-Br** _{Alkyl[1:x]} in chloroform and **PFF-NMe₃** _{Alkyl[1:2]} in methanol are overlapped in Figure 3.7. Both polymers have an excitation λ_{max} of 373 nm while the emission λ_{max} for the precursor polymer is 416 nm, and 418 nm for the cationically substituted IFCP. Figure 3.8 shows excitation and emission spectra of the pre- (black) and post-polymerization (red) functionalization of the **PFF-Br** _{OE[1:x]} family. The λ_{max} of the precursor polymers is between 416 and 418 nm. This spread undergoes a hypsochromic shift of 2 nm to 414 to 416 nm. Adding ions and shifting the solvent from chloroform to methanol results in a hypsochromic shift of about 4 nm. These small shifts post-functionalization are

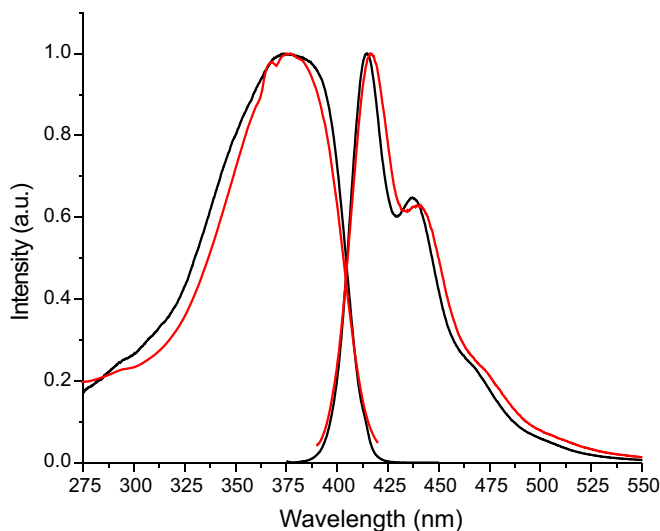


FIGURE 3.7. Excitation and emission spectra of $\mathbf{PFF}_{\text{AlkylBr}[1:2]}$ in chloroform (red) and $\mathbf{PFF}_{\text{Alkyl}[1:2]}$ in methanol (black).

probably not due to a change in the molecular weight of the polymer, but they can be attributed to the solvatofluorochromic properties of these IFCPs.¹¹¹

With the synthesis of the $\mathbf{PFF-NMe}_3_{\text{OE}[1:x]}$, the goal of making a family of soluble cationically functionalized IFCPs with varying ionic densities has been achieved. These IFCPs exhibit χ values between 0.05 and 0.5. All of the polymers were soluble in methanol with very similar electronic properties among the different ionic densities in the $\mathbf{PFF-NMe}_3_{\text{OE}[1:x]}$ family.

3.2.1.2. In Solid Film

In the introduction, I indicated a second goal of this work was to make polymers with varying solubility to provide processing flexibility. Polymers that can be functionalized in the solid state are desirable because this process can drastically change solubility. To show the possibilities of this technique, one example will illustrate. Using this approach allows for choice of a polymer backbone (\mathbf{PFF}) and side chain functionality (hexyl) in a precursor polymer, $\mathbf{PFF-Br}_{\text{Alkyl}[1:x]}$. the

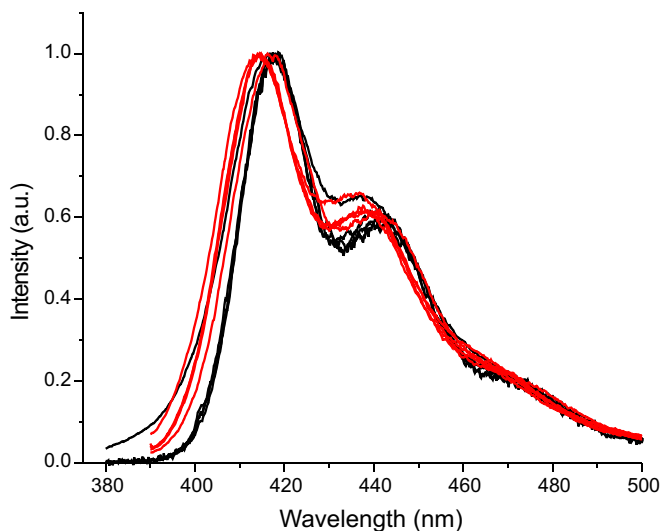


FIGURE 3.8. Excitation and emission spectra of the pre- (black, in chloroform) and post-polymerization (red, in methanol) functionalization of the **PFF-Br** $\text{Alkyl}[1:2]$ family

resulting IFCP is not solution processable and yet a film of the **PFF-NMe₃** $\text{Alkyl}[1:x]$ IFCP can still be made.

Post-polymerization functionalization of films was accomplished by exposing films to triethylamine liquid for 20 minutes. Figure 3.9 shows x-ray photon spectroscopy (XPS) data for films of **PFF-Br** $\text{Alkyl}[1:2]$ before (black line) and after (red) exposure to the triethylamine. For comparison a sample of **PFF-NMe₃** $\text{Alkyl}[1:2]$ is also shown (blue line). The synthesis of **PFF-NMe₃** $\text{Alkyl}[1:2]$ is given in the next section. Elbing *et al.* performed similar studies using a polythiophene derivative as precursor polymer and trimethylamine gas as the quaternizing amine.¹⁰⁹ The 3d electrons in neutral Br species have binding energies in the 70-72 eV range while the 3d electrons in Br⁻ ion species have binding energies in the 67-69 eV range. It is clear that the film of **PFF-Br** $\text{Alkyl}[1:2]$ contains only the neutral Br species while the **PFF-NMe₃** $\text{Alkyl}[1:2]$ film contains only Br⁻. The exposed film shows the presence of both neutral Br and Br⁻ in a ratio of about 3:1 for a χ of about 0.13. With a χ value

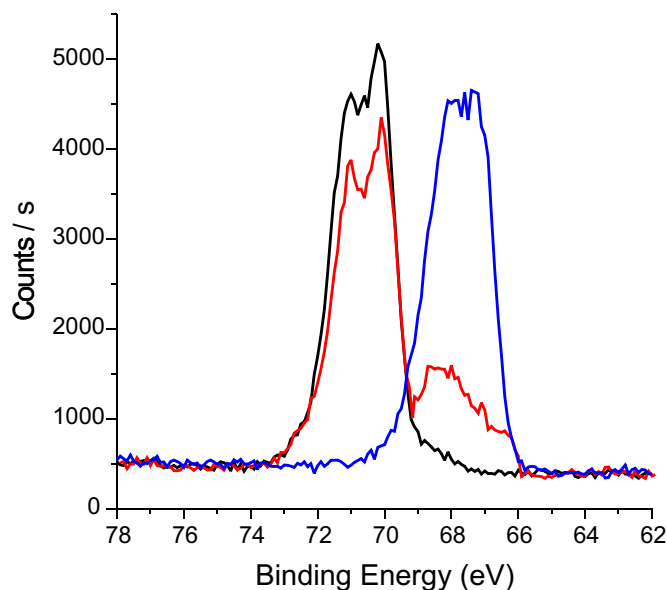


FIGURE 3.9. XPS data for films of **PFF-Br**_{Alkyl[1:2]} before (black line) and after (red line) exposure to triethylamine. **PFF-NMe₃**_{Alkyl[1:2]} (blue line) is given as a reference.

between 0.5 and 0.05, we would expect the IFCP film to be insoluble in both polar and nonpolar solvents. This is verified by washing the film with both methanol and THF and finding the film remaining afterwards. Studies looking at how the composition changed with depth were inconclusive.

3.2.2. **PFF-NMe₃**_{Alkyl[1:2]}

Post-polymerization functionalization is only one of two ways to synthesize IFCPs. The second common way to synthesize IFCP is direct polymerization of ionic monomers. There are very few reports comparing the products of post-polymerization functionalization and direct polymerization where the target IFCP is the same for both reactions. In this section, the synthesis of **PFF-NMe₃**_{Alkyl[1:2]} using both post-polymerization functionalization and direct polymerization will be reported. **PFF-NMe₃**_{Alkyl[1:2]} was directly synthesized

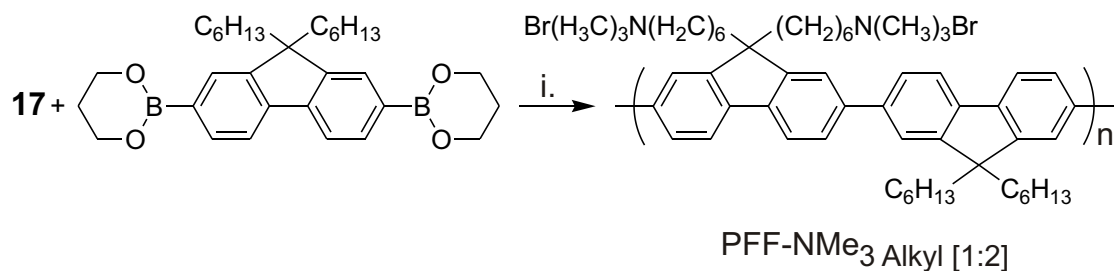


FIGURE 3.10. Synthetic conditions for **PFF-NMe₃ Alkyl[1:2]**:(i)Pd(PPh₃)₄, 2 M K₂CO₃, methanol/water

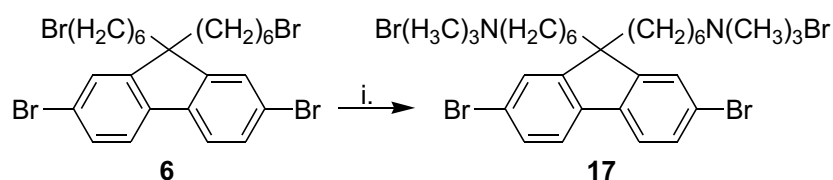


FIGURE 3.11. Synthetic conditions for **17**:(i) N(CH₃)₃

in a Suzuki polycondensation reaction between 2,7-dibromo-*N, N, N, N', N', N'*-hexamethyl-9,9-dihexanaminiumfluorene (**17**) and commercially available (**1**), see Figure 3.10. **17** was made from **6**, which was dissolved in ether. Trimethylamine was added, causing **17** to precipitate as a white solid; the reaction is shown in Figure 3.11. Attempts to dilute the cationic functionality by adding a third monomer, non-ionically functionalized 2,7-dibromo-9,9-dihexylfluorene, resulted in the formation of two homopolymers, **PFF-NMe₃ Alkyl[1:2]** and poly(9,9-dihexylfluorene). Explanations for why two polymers formed can be found in Chapter II. The synthesis of **PFF-NMe₃ Alkyl[1:2]** by post-polymerization functionalization was described above in 3.2.1.1.

Figure 3.12 compares the fluorescence properties of the post-polymerized **PFF-NMe₃ Alkyl[1:2]** and the directly polymerized **PFF-NMe₃ Alkyl[1:2]**. As can be seen, they show very similar characteristics. Both polymers have excitation λ_{max} values of 377 nm and emission λ_{max} values of 415 nm. The possibility that the two polymers

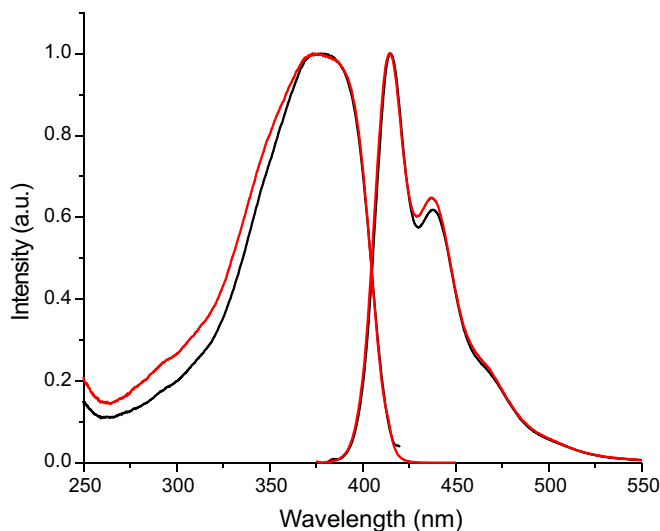


FIGURE 3.12. Excitation and emission spectra of directly synthesized **PFF-NMe₃ Alkyl[1:2]** (black) and **PFF-NMe₃ Alkyl[1:2]** synthesized through post-polymerization functionalization (red).

are very similar is a strong one, even though they were formed from two different pathways.

3.2.3. Impedance Spectroscopy

IFCPs are part of a broader class of materials called mixed ionic/electronic conductors. This class of materials includes multicomponent systems containing a semiconducting polymer mixed with a solid-state electrolyte, which is further made from a polar polymer like poly(ethylene oxide) and a salt. IFCPs are different from these multicomponent systems because they contain both the emissive polymer and the ions in the same material. Both the ionic and electronic transport characteristics play important roles in the electronic properties of this class of materials. These mixed ionic/electronic conducting materials are being studied for their potential in solid-state lighting,^{102;112} photovoltaics,^{113;114} and memory devices.¹¹⁵

IFCPs are not unique among conjugated polymers in that they contain ions. Conventionally doped conjugated polymers contain a substantial density of ionic carriers, but there is also present an equal concentration of the electronic carriers that dominate the electrical response due to their higher mobility. As a result, ion motion in conjugated polymers has largely been studied in the context of ion diffusion into or out of polymer thin films during doping.^{116;117} What is unique about IFCPs is that they contain ions in their undoped state where there are few, if any, electronic charge carriers, which usually swamp out the ionic carriers. Ionic conductivity measurements and nearly all device applications of IFCP use ion-blocking electrodes that prevent ions from directly contributing to the steady-state current. As a result, ionic conductivity measurements are usually performed using AC experiments with DC conductivity inferred by extrapolation to as close to zero frequency as the time scale for electrode polarization will allow.¹¹⁸ In an effort to minimize the injection of charges into the IFCP, which would complicate the analysis, small amplitude excitations (10-50 mV) are used.

The undoped IFCPs **PFF-NMe₃ _{OE[1:2]}** and **PFF-NMe₃ _{Alkyl[1:2]}** present an interesting pair of polymers for study by impedance spectroscopy. Except for the non-ionic functional group attached to the backbone of the polymer, they are structurally similar. The oligoether side chains in **PFF-NMe₃ _{OE[1:2]}** may act as an ion-solvating material, thus increasing the ionic conductivity of the material. It is also possible that the ion may be more stabilized in the oligoether side chains, and so have a higher activation energy.

Oh *et al.* studied the effect of oligoether side chains on ion mobility in light-emitting devices when the IFCP was used as an injection layer for an MEH-PPV device. The devices with IFCP injection layers containing oligoether side chains

reached their maximum brightness much faster than the devices made from IFCPs with no ether groups.¹¹⁹

In the following experiments, we are applying an AC voltage of 20mV at varying frequencies. The applied voltage creates an electric field, which switches direction as the voltage switches. At high frequencies, the voltage is switching so fast that the ions in the device do not have enough time to respond to the electric field. As the frequency decreases and the switching is occurring at a more moderate rate, the ions begin to migrate through the device. If we think of the electric field as a teeter-totter and the ions as marbles resting on it, we can better visualize the motion of the ions. The high side of the teeter-totter is the high energy side of the electric field. When the frequency is high, the ions do not have time to move towards the low energy side of the device, just as the marbles would not have time to roll down the teeter-totter if it were switching fast enough. As the frequency slows, the field is in one direction long enough for the ions to respond to the field, and so they move to the lower energy side of the field. At some point, the frequency is slow enough that the ions are able to move through the device and pile up on one electrode before the field switches, the piling up of ions is called ion polarization.

Dielectric spectra were collected for **PFF-NMe₃**_{OE[1:2]} and **PFF-NMe₃**_{Alkyl[1:2]} thin films between two gold electrodes. AC impedance spectra were collected by applying 20mV bias at frequencies ranging from 10⁶ to 10⁻³ Hz. The raw complex impedance ($Z' + Z''i$) can also be expressed in polar form as a magnitude, $|Z|$ (Ω) and an angle θ (radians). Z represents the ratio between the voltage and current amplitudes, and θ is the phase difference between them. Euler's formula lets us rewrite this as:

$$Z = Z' + Z''i = |Z|e^{i\theta} = |Z|\cos\theta + i|Z|\sin\theta \quad (\text{Equation 3.1})$$

Using Equation 3.1 we can calculate the real and imaginary portions of the apparent relative permittivity (Equation 3.2) and the apparent relative conductivity (Equation 3.3).

$$\epsilon_{\text{app}} = \epsilon'_{\text{app}} - \epsilon''_{\text{app}}i \quad (\text{Equation 3.2})$$

$$\sigma_{\text{app}} = \sigma'_{\text{app}} + \sigma''_{\text{app}}i \quad (\text{Equation 3.3})$$

ϵ_{app} is related to σ_{app} as shown in Equation 3.4

$$\epsilon_{\text{app}} = \frac{\sigma_{\text{app}}}{i\omega\epsilon_0} = \frac{L}{i\omega\epsilon_0AZ} \quad (\text{Equation 3.4})$$

where ω is the angular frequency (rad/s), ϵ_0 is the vacuum permittivity, A is the electrode area, L is the thickness, and Z is the complex impedance. By combining Equation 3.1 and Equation 3.4, the real and imaginary portions of the apparent relative conductivity can be calculated as shown in Equation 3.5 and Equation 3.6, respectively.

$$\sigma'_{\text{app}} = \frac{L\cos\theta}{AZ} \quad (\text{Equation 3.5}) \quad \sigma''_{\text{app}} = \frac{L\sin\theta}{AZ} \quad (\text{Equation 3.6})$$

Equation 3.5 and Equation 3.6 can be used to calculate the real (Equation 3.7) and imaginary (Equation 3.8) parts of the permittivity.

$$\epsilon'_{\text{app}} = \frac{L\sin\theta}{\omega\epsilon_0AZ} \quad (\text{Equation 3.7}) \quad \epsilon''_{\text{app}} = \frac{L\cos\theta}{\omega\epsilon_0AZ} \quad (\text{Equation 3.8})$$

The dielectric loss tangent can be calculated with ϵ'_{app} and ϵ''_{app} as shown in Equation 3.9, where θ is the measured phase angle.

$$\tan \delta = \frac{\epsilon''_{\text{app}}}{\epsilon'_{\text{app}}} = \tan \left(\theta + \frac{\pi}{2} \right) \quad (\text{Equation 3.9})$$

Figure 3.13 shows the raw data for a sample of **PFF-NMe₃**_{alkyl[1:2]} as it comes from the instrument. The magnitude of the complex impedance is plotted against the frequency of the oscillating current. The different lines for each color are at different temperatures. Two things to notice are first, that the impedance increases as the temperature decreases and second, that the data is reproducible over the temperature range studied, as the two experiments line up extremely well. The effect of ion motion due to the applied alternating bias can also be seen. At the lowest frequencies the electrode polarization process can be seen. The midrange frequencies show the dispersive ion transport regime, characterized by a slope close to 0. At the highest frequencies the response is governed by the test cell geometry.¹²⁰

After calculating ϵ'_{app} and σ'_{app} for **PFF**_{Alkyl[1:2]}, they were plotted against ω as shown in Figures 3.14 and 3.15. Figure 3.16 shows a representative set of impedance data collected from a 670 nm film of **PFF-NMe₃**_{Alkyl[1:2]} at 388 K.

Figure 3.16 shows how the dielectric function $\tan \delta$ changes as a function of angular frequency and temperature. The angular frequency at which the $\tan \delta$ function reaches its maximum value is given, denoted by the symbol ω_L . The value of ω_L increases with increasing temperature. For each ω_L value a corresponding σ'_{app} value can be found. An Arrhenius plot of $\sigma'_{\text{app}}(\omega_L)$ can be used to extract the activation energy needed to move the ions through the polymer film. Plotting the $\ln \sigma'_{\text{app}}(\omega_L)$ against $1000/T$ as seen in Figure 3.18 allows the activation energy for the ion motion to be extracted from the slope of the curve.

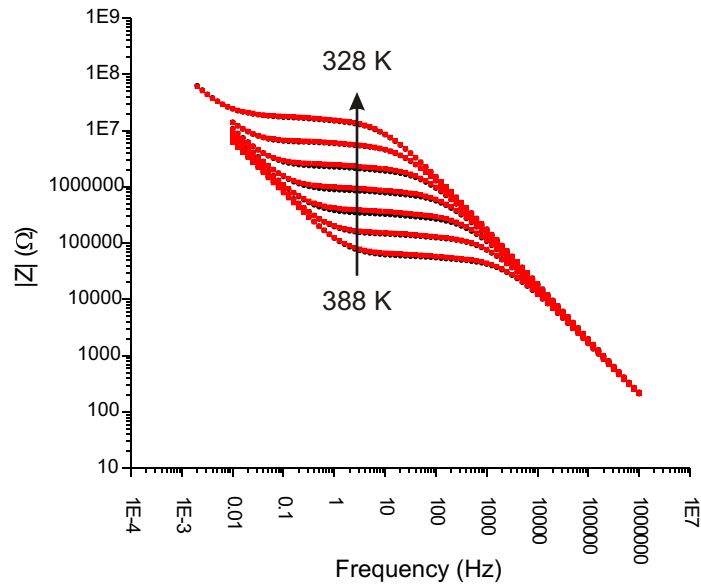


FIGURE 3.13. Plot of complex impedance magnitude as it varies with frequency and temperature for **PFF-NMe₃ Alkyl[1:2]**. Note the two separate experiments (red square and black circle) on the same sample showing that the device is not degraded during the measurements.

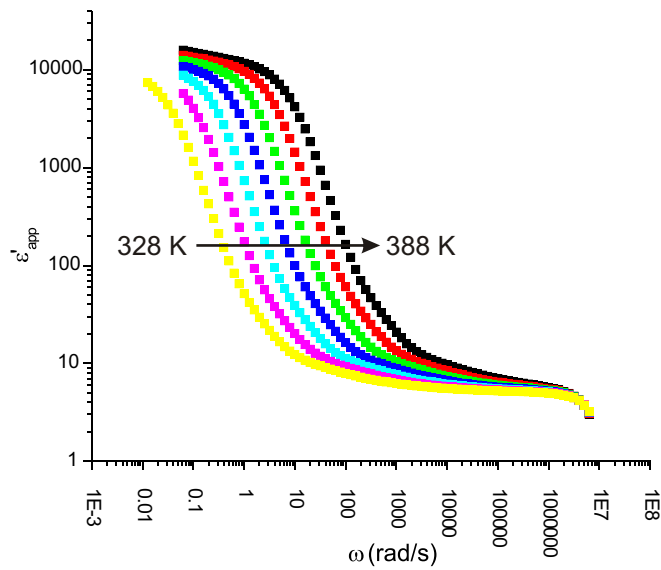


FIGURE 3.14. ϵ''_{app} for **PFF-NMe₃ Alkyl[1:2]** as a function of angular frequency and temperature.

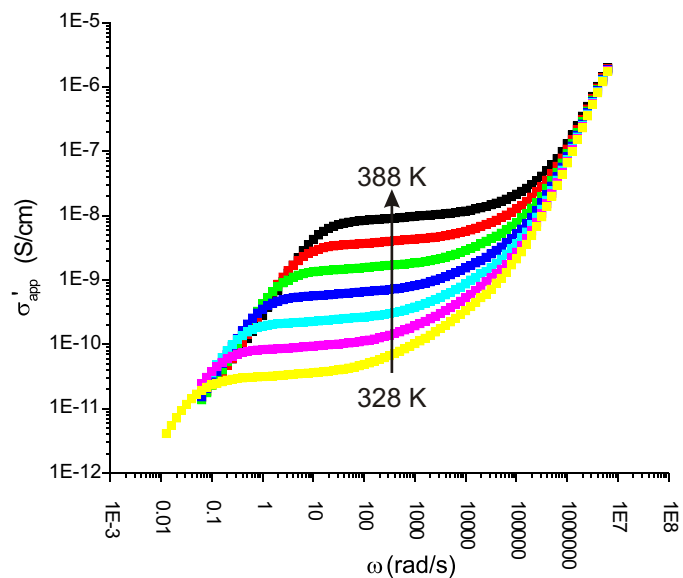


FIGURE 3.15. σ'_{app} for **PFF-NMe₃ Alkyl[1:2]** as a function of angular frequency and temperature.

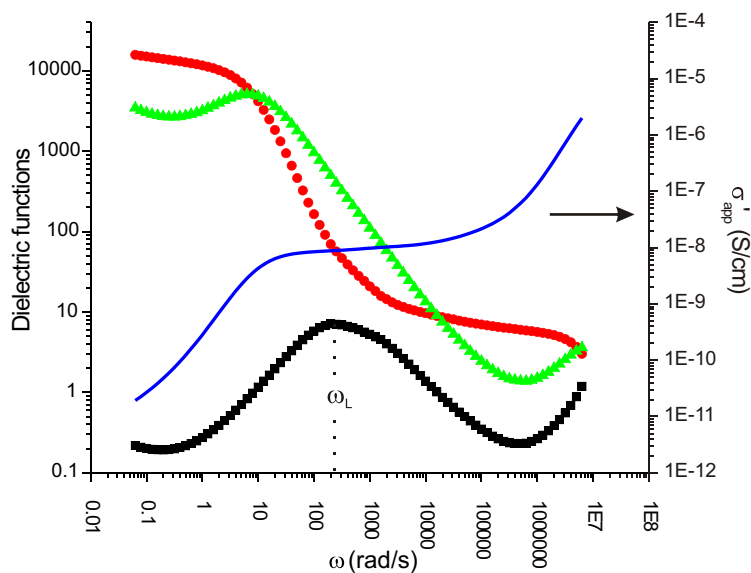


FIGURE 3.16. A representative set of impedance data collected from a 670 nm film of **PFF-NMe₃ Alkyl[1:2]** at 388K. Dielectric functions $\tan \delta$ (black square), ϵ'_{app} (red circle), and ϵ''_{app} (green triangle) are shown (left ordinate) along with σ'_{app} (solid blue line, right ordinate). ω_L is indicated on the $\tan \delta$ curve.

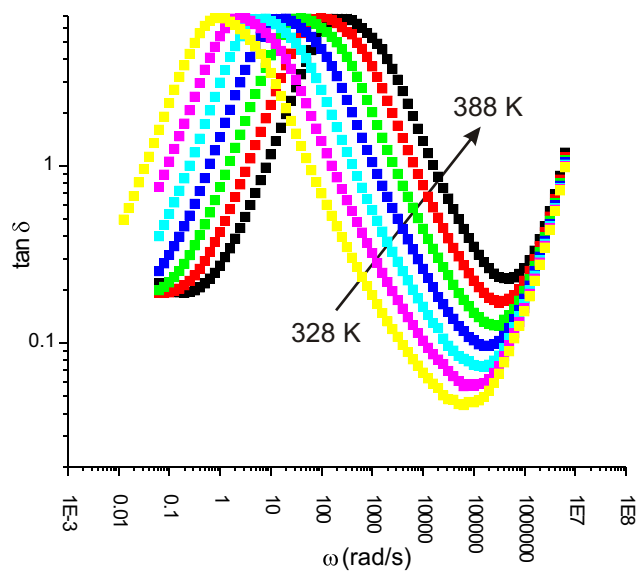


FIGURE 3.17. Changes in dielectric function $\tan \delta$ as a function of angular frequency and temperature in a sample of **PFF-NMe₃ Alkyl[1:2]**.

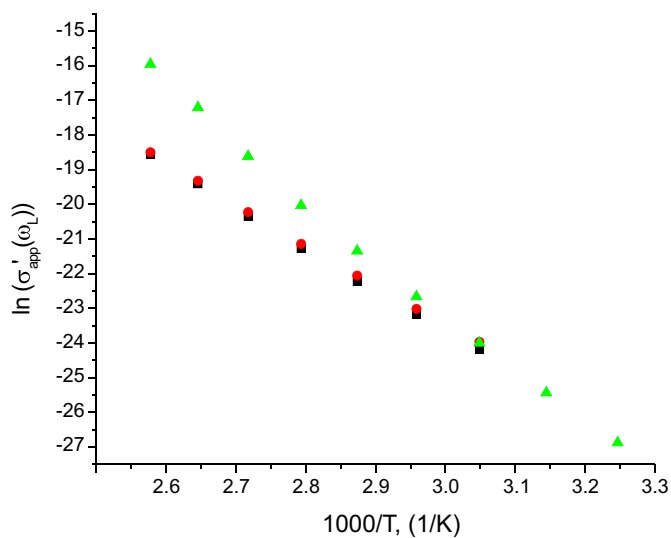


FIGURE 3.18. Arrhenius plot of $\ln \sigma'_{\text{app}}(\omega_L)$ vs. $1000/T$ for two samples of **PFF-NMe₃ Alkyl[1:2]** (black squares and red circles) with different thicknesses (670 nm and 250 nm respectively). The green triangles are for **PFF-NMe₃ OE[1:2]** with a thickness of 1900 nm.

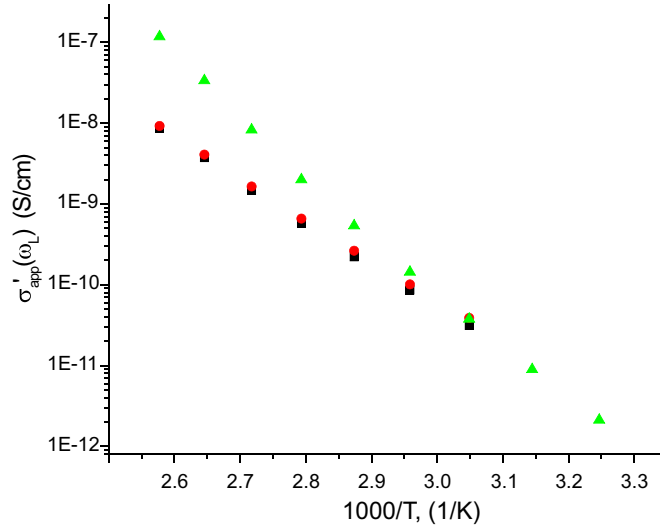


FIGURE 3.19. $\sigma'_{\text{app}}(\omega_L)$ plotted against $1000/T$ for two samples of **PFF-NMe₃ Alkyl[1:2]** (black squares and red circles) with different thicknesses (670 nm and 250 nm respectively). The green triangles are for **PFF-NMe₃ OE[1:2]** with a thickness of 1900 nm.

As can be seen from Figure 3.18, the activation energy for the two samples of **PFF-NMe₃ Alkyl[1:2]** overlap nicely. After extracting the slope for both thicknesses (670 nm, black squares and 250 nm, red circles), activation energies of 1.08 eV and 1.03 eV respectively, were found. The activation energy for **PFF-NMe₃ OE[1:2]** with a thickness of 1900 nm was found to be 1.40 eV. Figure 3.19 shows that while the activation energy for **PFF-NMe₃ OE[1:2]** is higher than that of **PFF-NMe₃ Alkyl[1:2]**, the total conductivity for **PFF-NMe₃ OE[1:2]** is also higher than the conductivity for **PFF-NMe₃ Alkyl[1:2]**. The DC ionic conductivity can be estimated by the σ'_{app} at (ω_L) .

At 388K the ion conductivities of **PFF-NMe₃ Alkyl[1:2]** and **PFF-NMe₃ OE[1:2]** are about 10^{-8} S/cm and 10^{-7} S/cm respectively. There have been few specific studies to which these data can be compared. Lin *et al.* studied ion transport in amorphous films of polyacetylene IFCPs and found activation energies of about 1 eV with ion

conductivities of $1 \times 10^{-9} - 6 \times 10^{-9}$ to near 388K.¹²⁰ Neher *et al.* studied the ionic conductivities of Na^+ and $\text{N}(\text{CH}_3)_3((\text{CH}_2)_{13}\text{CH}_3)^+$ in a **PPP** based IFCP and found at 0.1 Hz and room temperature, the ionic conductivities were 7×10^{-12} S/cm and 4×10^{-14} S/cm, respectively.¹²¹

3.3. Summary

It was the goal of this chapter to demonstrate the use of a three monomer, diluent strategy in the synthesis of cationic IFCPs with widely varying χ . A secondary goal was to achieve this in classes of polymers with varying solubility, so as to provide flexibility in processing the polymers. After coupling two or three different nonionic monomers to form prepolymers based on the same PFF backbone as in Chapter II, post-polymerization functionalization was used to convert the prepolymers to the cationic IFCP family **PFF-NMe₃_{OE[1:x]}** where x varies between 2 and 20, yielding χ values between 0.50 and 0.05. This was accomplished with both oligoether (**PFF-NMe₃_{OE[1:x]}**) and alkyl (**PFF-NMe₃_{Alkyl[1:x]}**) side chains. Quaternization of **PFF-Br_{Alkyl[1:x]}** with trimethylamine lead to insoluble products, except in the case where x=2 ($\chi = 0.50$). The quaternization of the **PFF-Br_{OE[1:x]}** family with trimethylamine stands in stark contrast to the previous example yielding solvent processable IFCPs in all cases.

Direct polymerization to form **PFF-NMe₃_{Alkyl[1:2]}** was explored and comparison to post-polymerized **PFF-NMe₃_{Alkyl[1:2]}** was made. Direct polymerization of IFCPs along with post-polymerization functionalization provide two approaches to the same target IFCP. Direct comparison of these two routes is rare in the literature. The families of polymers chosen herein allowed me to investigate the IFCPs formed by the two routes.

The preparation of **PFF-NMe₃ OE_[1:2]** and **PFF-NMe₃ Alkyl_[1:2]** provided an opportunity to study the ability of the oligoether functional group to promote ionic conductivity. Polyethers are commonly used in solid polymer electrolytes, and oligoether functionalization is a common feature of other polymer electrolytes. The effect of oligoether side chains relative to alkyl side chains was explored through impedance spectroscopy on solid films. It was found that at elevated temperatures the ionic conductivity of **PFF-NMe₃ OE_[1:2]** was close to an order of magnitude greater than, **PFF-NMe₃ Alkyl_[1:2]**, its alkyl substituted counterpart.

3.4. Experimental

3.4.1. XPS

All spectra were taken on a ThermoScientific ESCALAB 250 instrument with pass energy of 20 eV for “multiplex” (composition) scans, while using a 500 μm spot size and a monochromatized Al X-ray source. Binding energy scales were adjusted to C1s=284.8 eV.

3.4.2. Impedance

3.4.2.1. Device Fabrication

Gold Seal[®] Slides were cut to two inches by one inch and soaked in concentrated HCl overnight. The slides were then rinsed with DI water, dried with nitrogen, and dipped in 2-propanol and allowed to air dry. BJH-500 (Key High Vacuum Products, Inc.) thermal evaporator was used for evaporation of electrodes. The bottom electrodes were made by evaporating a Cr adhesion layer (20-30 Å) followed by an Au electrode (15-20 nm). The circular electrode area of $A = 0.12 \text{ cm}^2$ was

defined using a physical evaporation mask. Polymer films of **PFF-NMe₃**_{OE[1:2]} and **PFF-NMe₃**_{Alkyl[1:2]} were cast onto the bottom gold electrode via spin coating from 5 mg/mL methanol solutions. The thickness of the film was controlled by varying the spin speed and was measured using a Dektak6M profiler at 10 mg stylus force. After spin coating, films were dried under vacuum (20 mTorr) for at least 4 h. A 15-nm-thick Au layer was then thermally evaporated onto the polymer film to complete the sandwich structure. Devices were tested for shorts with a Fluke 111 RMS Multimeter.

3.4.2.2. Impedance Measurement

The sample in sandwich geometry was put into an evacuable stainless steel container fitted with electrical feedthroughs and a valve for evacuation. After contact wires were attached to the sample and a thermocouple was fixed to the surface of the glass substrate, the container was evacuated to less than 25 mTorr, and then kept under active vacuum during the annealing process and throughout the dielectric measurements. The temperature of the sample was controlled by a SUN EC10 environmental chamber. A Solartron SI-1296A dielectric interface in combination with a Solartron SI-1260 impedance analyzer was used for all dielectric measurements. The SMART software from Solartron analytical was used for interfacing both the SI-1296A and the SI-1260. The amplitude of the voltage signal was 20 mV.

3.4.3. Synthesis

3.4.3.1. Monomer Synthesis

2,7-Dibromo-*N, N, N', N', N'*-hexamethyl-9,9-dihexanaminiumfluorene

(17) Monomer **6** (2.925 g, 4.5 mmol) was dissolved in 100 mL ether in a round bottom flask with a stir bar fitted with rubber septum. Trimethylamine gas

was condensed into a cooled (-78°C) graduated cylinder until 5 mL of liquid trimethylamine had collected. The liquid trimethylamine was added to the round bottom flask via chilled canula and the reaction was stirred overnight. Soon after addition, a white precipitate started to form. After 18 hours the N₂ was bubbled through the reaction mixture and into a dilute HCl to trap excess trimethylamine. This continued until all solvent was removed. The solids were washed with chloroform to remove any starting material. The white solids were soluble in water and methanol. Yield: 3.40g (97%) ¹H NMR (*d*₄CH₃OH, 300 MHz): δ (ppm) 0.581 (4H, m), 1.18 (8H, m), 1.59 (4H, m), 2.09 (4H, m), 3.10 (18H, s), 3.26 (4H, m), 7.53 (2H, dd, ³*J*_{HH} = 7.7 Hz, ⁴*J*_{HH} = 1.8), 7.64 (2H, d, ⁴*J*_{HH} 1.7 Hz), 7.71 (2H, d, ³*J*_{HH} = 7.7 Hz) ¹³C NMR (*d*₄CH₃OH, 70 MHz): δ (ppm) 22.33, 22.54, 25.20, 28.69, 52.94 (²*J*_{CN} = 5Hz), 53.18, 55.76, 66.42, 121.7, 138.8, 153.33.

3.4.3.2. Polymer Synthesis

PFF-Br _{Alkyl[1..x]} **General Polymerization Procedure.** *n* equivalents **6**, *m* equivalents of 2,7-dibromo-9,9-dihexylfluorene, and *n* + *m* equivalents of **1** were dissolved in 15 mL of toluene. 5 mL of 2 M K₂CO₃ and the organic solution were placed together in a round bottom flask fitted with a magnetic stir bar and condenser. The mixture of solutions was deoxygenated by bubbling N₂ through the solutions and heated to 85°C. After purging with N₂ for 10 minutes, the Pd(Ph₃)₄ (0.05 equivalents) catalyst was added, and the reaction was stirred for 8 hours. The reaction mixture was poured into a 10/90 (v/v) water/methanol mixture. The yellow precipitate was collected and dissolved in chloroform and reprecipitated into methanol. The precipitated polymer was placed in a filter thimble and put into a Soxhlet extractor.

The polymers were extracted with acetone for 24 hours. Yields were in the 45-65% range.

PFF-Br _{OE[1:x]} **General Polymerization Procedure.** n equivalents **6**, m equivalents of **11**, and $n + m$ equivalents of **12** were dissolved in 15 mL of toluene. 5 mL of 2 M K₂CO₃ and the organic solution were both placed in round bottom flask fitted with magnetic stir bar and condenser. The mixture of solutions was deoxygenated by bubbling N₂ through the solutions and heated to 85°C. After purging with N₂ for 10 minutes, the Pd(Ph₃)₄ (0.05 equivalents) catalyst was added, and the reaction was stirred for 8 hours. The reaction mixture was poured into a 10/90 (v/v) water/methanol mixture. The yellow precipitate was collected and dissolved in chloroform and precipitated a second time into methanol. Yields were in the 60-80% range.

CHAPTER IV

SUMMARY

Synthetic polymer chemistry has come a long way since Baekeland first synthesized Bakelite. Polymer scientists have explored the nature of polymer bonds, methods for controlling the monomer arrangement, models for how polymers behave in solution, and techniques for instilling polymers with desired properties based on the monomers chosen. Notwithstanding the enormous amount of work done by Staudinger, Natta, Ziegler, Flory, MacDiarmid, Heeger, Shirikawa, and others who have influenced the last century of polymer research, there is significant work yet to be done.

My part in this vast body of polymer research has focused on synthesizing and characterizing linear, alternating copolymers, of ionically functionalized conjugated polymers, synthesized using the Suzuki polycondensation reaction. I have specifically looked at methods for varying the type and density of ionic functionality. The control over ionic functional group density is desirable because it is an integral materials parameter of IFCPs and influences properties such as polymer solubility, doping chemistry, optical properties, surface adsorption, and ionic conductivity.³¹ In addition to their density, the sign of the ionic functional group is also a defining parameter of IFCPs. The sign of the bound ion has been shown, for instance, to affect stability of conjugated polymers exposed to the atmosphere. Additionally, the sign of the mobile ion in IFCPs is important to many devices made from these materials. The effect of the mobile counter ion has been extensively studied and yet, most of these polymers lie in a very narrow range of ionic density.

Up until now, most polymers reported in the literature have ionic densities of $\chi > 0.5$, with one IFCP having a $\chi < 0.05$. Between these two values there are very few examples. There are a few possible reasons why this range of IFCPs has yet to be explored. First, many scientists have thought of the bound ions solely as a way to make traditional conjugated polymers soluble in polar organic or aqueous solvents, and so try to place as many ions on the chain as possible. That is to say, they have been exploring only the upper ranges of the ionic functional group density space. A second possible reason the mid- to low-range of ionic functional group densities has not been explored is synthetic in nature. The most common method for synthesizing IFCPs is through the Suzuki polycondensation reaction, typically a two phase reaction. As was experimentally demonstrated in both Chapter II and III, this two-phase approach does not work in the direct polymerization of an ionic monomer with two different non-ionic monomers because it leads to the formation of two different homopolymers instead of one copolymer with diluted ionic functionality. A third reason IFCPs with χ values between 0.5 and 0.05 have been overlooked is that even if they were to be made, they lie in a range where there are not enough ions to make the nonpolar backbone soluble in polar solvents, and where there are too many polar ions for the nonpolar backbone to solubilize in nonpolar solvents.

The central goal of the work in this dissertation was to synthesize solution processable anionic and cationic IFCPs based on the same luminescent backbones, with similar electronic structures, and spanning a much wider range of ionic density than has been previously reported. This goal was successfully achieved with the synthesis of the family of oligoether functionalized IFCPs: **PFF-SO₃**_{OE[1:x]} and **PFF-NMe₃**_{OE[1:x]}. These anionic and cationic polymers, respectively, were synthesized with χ values between 0.05 and 0.5, thereby spanning the largely

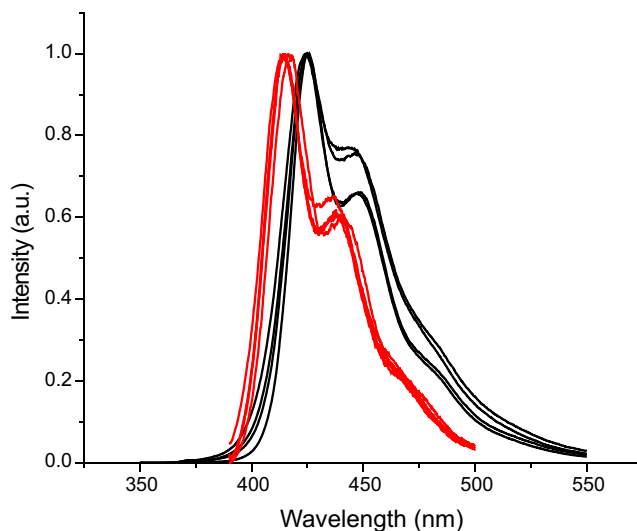


FIGURE 4.1. Fluorescence emission spectra for **PFF-NMe₃ OE[1:x]** (red) and **PFF-SO₃ OE[1:x]** (black).

unrealized range described above. The anionic polymers are solution processable from DMSO, and the cationic from methanol. Finally, the electronic structures of the polymers is very similar as evidenced by strong overlap of their emission spectra as shown in Figure 4.1, which collects together the fluorescence data shown separately in Chapters II and III.

In the course of synthesizing the oligoether functionalized IFCPs **PFF-SO₃ OE[1:x]** and **PFF-NMe₃ OE[1:x]**, several approaches to processable IFCPs with controlled ionic functional group density were developed. A number of synthetic challenges were overcome in developing these approaches. Most of these challenges had their root in the fact that ionic and nonionic compounds tend to have very different solubilities. For instance, the synthesis of the monomer **5** was hindered by differential solubility and required the development of **5** as a phase transfer agent in its own synthesis. Solubility also critically informed the design of the polymer targets, both as it affected the final product and the application of Suzuki polycondensation. Most notably, the synthesis of the IFCPs required overcoming

the preferential partitioning between phases. To this end, a one-phase Suzuki polycondensation was developed through careful solvent choice and the incorporation of oligoether functional groups. This approach was used in the direct synthesis of **PFF-SO₃ OE[1:x]** which precisely controls ionic density and elegantly avoids the two-phase nature of other Suzuki polycondensation reactions. In the synthesis of **PFF-NMe₃ OE[1:x]**, a post-polymerization approach was developed so that during polymerization all of the monomers partitioned into the same phase. The choice of oligoether functional groups was not only an important part of the polymerization strategy, but it also proved a key design element in achieving solution processable polymers. The insolubility of the **PFF-NMe₃ Alkyl[1:x]** family clearly illustrates this point.

The interplay of the ionic functional groups and the nonionic functionality was demonstrated to have a number of effects. Take for instance, the **PFF-NMe₃ Alkyl[1:x]** polymer where the nonpolar hexyl and polar ionic groups confound together to yield an insoluble polymer. The interplay of the ionic and nonionic groups is also presumably responsible for the observed solvatochromism with polymer aggregation in many of the polymer solutions increasing when solvent polarity was either increased or decreased from an intermediate value. Such control over polymer aggregation in solution is important because it has been reported to directly translate into the morphology of cast films for device application. Finally, the specific combination of ionic and nonionic functional groups also affected the ionic conductivity of the IFCPs as illustrated by the comparison made between the ionic conductivity of **PFF-NMe₃ Alkyl[1:2]** and **PFF-NMe₃ OE[1:2]**. The ability to promote ionic conductivity is important because of the many applications of IFCPs that rely on ion transport.

The syntheses developed in this dissertation open the door to comprehensive studies of ionic functional group density on the properties of luminescent IFCPs. Future work using these polymers could touch on a number of different areas. For instance, IFCPs are being explored as injection layers in light-emitting devices but the relative roles of ion polarization and ion modulated frontier orbital offsets has been controversial. A systematic study as a function of ion density would be helpful in separating out these two effects. As another example, ion functional groups have been shown to strongly interact with charges on the polymer backbone, and in doing so influence exciton separation into charge transfer states or the stability of charge transfer complexes implicated in the photochemical degradation of conjugated polymers. It is not known at this point, however, the range over which ionic functional groups have an effect. Studies of photochemical degradation in IFCPs as a function of ion density will help elucidate this issue. Finally, the polymer design and synthetic approaches developed herein are widely applicable to the many classes of conjugated polymers synthesized by metal-catalyzed cross coupling reactions. As such, this study should help pave the way for the development of other families of IFCPs with widely varying ionic functional group density.

REFERENCES CITED

- [1] Staudinger, H. *Berichte der deutschen chemischen Gesellschaft* **1920**, *53*, 1073–1085.
- [2] Nobelprize.org, The Nobel Prize in Chemistry 1953.
http://www.nobelprize.org/nobel_prizes/chemistry/laureates/1953/.
- [3] Carothers, W. H. *Journal of the American Chemical Society* **1929**, *51*, 2548–2559.
- [4] Carothers, W. H.; Mark, H. F.; Whitby, G. S. *Collected papers of Wallace Hume Carothers on high polymeric substances*; Interscience Publishers, inc.: New York, 1940.
- [5] Wilke, G. *Angewandte Chemie-International Edition* **2003**, *42*, 5000–5008.
- [6] Nobelprize.org, The Nobel Prize in Chemistry 1963.
http://www.nobelprize.org/nobel_prizes/chemistry/laureates/1963/.
- [7] Flory, P. J. *The Journal of Chemical Physics* **1949**, *17*, 1347–1348.
- [8] Flory, P. J.; Krigbaum, W. R. *The Journal of Chemical Physics* **1950**, *18*, 1086–1094.
- [9] Nobelprize.org, The Nobel Prize in Chemistry 1974.
http://www.nobelprize.org/nobel_prizes/chemistry/laureates/1974/.
- [10] Natta, G.; Mazzanti, G.; Corradini, P.; Giannini, U.; Cesca, S. *Atti accad. nazl. Lincei. Rend. Classe sci. fis., mat. e nat.* **1959**, *26*, 150–154.
- [11] Shirakawa, H.; Ikeda, S. *Polymer Journal* **1971**, *2*, 231.
- [12] Shirakawa, H.; Louis, E. J.; Macdiarmid, A. G.; Chiang, C. K.; Heeger, A. J. *Journal of the Chemical Society-Chemical Communications* **1977**, *16*, 578–580.
- [13] Nobelprize.org, The Nobel Prize in Chemistry 2000.
http://www.nobelprize.org/nobel_prizes/chemistry/laureates/2000/.
- [14] Nobelprize.org, The Nobel Prize in Chemistry 2005.
http://www.nobelprize.org/nobel_prizes/chemistry/laureates/2005/.
- [15] Nobelprize.org, The Nobel Prize in Chemistry 2010.
http://www.nobelprize.org/nobel_prizes/chemistry/laureates/2010/.

- [16] McNaught, A. D.; Wilkinson, A. In *IUPAC Compendium of Chemical Terminology*; Nic, M., Jirt, J., Koata, B., Jenkins, A., McNaught, A., Eds.; IUPAC, 1997; Vol. 2nd; pp 2007–2007.
- [17] Miyaura, N.; Suzuki, A. *Chemical Reviews* **1995**, *95*, 2457–2483.
- [18] Schluter, A. D. *Journal of Polymer Science Part a-Polymer Chemistry* **2001**, *39*, 1533–1556.
- [19] Burroughes, J. H.; Bradley, D. D. C.; Brown, A. R.; Marks, R. N.; Mackay, K.; Friend, R. H.; Burns, P. L.; Holmes, A. B. *Nature* **1990**, *347*, 539–541.
- [20] Carey, F. A. *Organic chemistry*, 4th ed.; McGraw-Hill: Boston, Mass. [u.a.], 2000.
- [21] Eisenberg, A.; Kim, J. *Introduction to Ionomers*; Wiley: New York, 1998.
- [22] Kudaibergenov, S. E. *Polyampholytes: synthesis, characterization, and application*; Kluwer Academic/Plenum Publishers, 2002.
- [23] Farinato, R. S. *Polyelectrolytes and Polyzwitterions: Synthesis, Properties, and Applications* **2006**, *937*, 153–168.
- [24] Hoven, C. V.; Garcia, A.; Bazan, G. C.; Nguyen, T. Q. *Advanced Materials* **2008**, *20*, 3793–3810.
- [25] Pinto, M. R.; Schanze, K. S. *Synthesis-Stuttgart* **2002**, 1293–1309.
- [26] Liu, B.; Bazan, G. C. *Chemistry of Materials* **2004**, *16*, 4467–4476.
- [27] Thomas, S. W.; Joly, G. D.; Swager, T. M. *Chemical Reviews* **2007**, *107*, 1339–1386.
- [28] Huang, F.; Wu, H. B.; Peng, J. B.; Yang, W.; Cao, Y. *Current Organic Chemistry* **2007**, *11*, 1207–1219.
- [29] Feng, F. D.; He, F.; An, L. L.; Wang, S.; Li, Y. H.; Zhu, D. B. *Advanced Materials* **2008**, *20*, 2959–2964.
- [30] Jiang, H.; Taranekar, P.; Reynolds, J. R.; Schanze, K. S. *Angewandte Chemie-International Edition* **2009**, *48*, 4300–4316.
- [31] Stay, D. P.; Robinson, S. G.; Lonergan, M. C. In *Iontronics : Ionic carriers in organic electronic materials and devices*; Leger, J., Berggren, M., Carter, S., Eds.; CRC Press, 2011; Chapter Development and applications of ionfunctionalized conjugated polymers, pp 43–83.
- [32] Shi, S. Q.; Wudl, F. *Macromolecules* **1990**, *23*, 2119–2124.

- [33] Patil, A.; Ikenoue, Y.; Wudl, F.; Heeger, A. *J. Am. Chem. Soc.* **1987**, *109*, 1858–1859.
- [34] Ewbank, P.; Loewe, R.; Zhai, L.; Reddinger, J.; Sauve, G.; McCullough, R. *Tetrahedron* **2004**, *60*, 11269–11275.
- [35] Wallow, T. I.; Novak, B. M. *Journal of the American Chemical Society* **1991**, *113*, 7411–7412.
- [36] Huang, F.; Wu, H. B.; Wang, D.; Yang, W.; Cao, Y. *Chemistry of Materials* **2004**, *16*, 708–716.
- [37] Pinto, M. R.; Kristal, B. M.; Schanze, K. S. *Langmuir* **2003**, *19*, 6523–6533.
- [38] Brodowski, G.; Horvath, A.; Ballauff, M.; Rehahn, M. *Macromolecules* **1996**, *29*, 6962–6965.
- [39] Viinikanoja, A.; Lukkari, J.; Aaritalo, T.; Laiho, T.; Kankare, J. *Langmuir* **2003**, *19*, 2768–2775.
- [40] Durben, S.; Dienes, Y.; Baumgartner, T. *Org. Lett.* **2006**, *8*, 5893–5896.
- [41] de Boer, B.; Facchetti, A. *Polymer Reviews* **2008**, *48*, 423–431.
- [42] Forrest, S. R. *Nature* **2004**, *428*, 911–918.
- [43] Zotti, G.; Zecchin, S.; Schiavon, G.; Berlin, A.; Pagani, G.; Canavesi, A. *Chemistry of Materials* **1997**, *9*, 2940–2944.
- [44] Havinga, E.; Hoeve, W.; Meijer, E.; Wynberg, H. *Chem. Mater.* **1989**, *1*, 650–659.
- [45] Havinga, E. E.; Vanhorssen, L. W.; Tenhoeve, W.; Wynberg, H.; Meijer, E. W. *Polymer Bulletin* **1987**, *18*, 277–281.
- [46] Sonmez, G.; Schwendeman, I.; Schottland, P.; Zong, K. W.; Reynolds, J. R. *Macromolecules* **2003**, *36*, 639–647.
- [47] Langsdorf, B. L.; Zhou, X.; Adler, D. H.; Lonergan, M. C. *Macromolecules* **1999**, *32*, 2796–2798.
- [48] Langsdorf, B. L.; Zhou, X.; Lonergan, M. C. *Macromolecules* **2001**, *34*, 2450–2458.
- [49] Gao, L.; Johnston, D.; Lonergan, M. C. *Macromolecules* **2008**, *41*, 4071–4080.
- [50] Liu, B.; Yu, W. L.; Lai, Y. H.; Huang, W. *Macromolecules* **2002**, *35*, 4975–4982.

- [51] Ho, H.; Boissinot, M.; Bergeron, M.; Corbeil, G.; Dore, K.; Boudreau, D.; Leclerc, M. *Angew. Chem. Int. Ed.* **2002**, *41*, 1548–1551.
- [52] Peng, Z. H.; Xu, B. B.; Zhang, J. H.; Pan, Y. C. *Chemical Communications* **1999**, 1855–1856.
- [53] Fan, Q. L.; Zhou, Y.; Lu, X. M.; Hou, X. Y.; Huang, W. *Macromolecules* **2005**, *38*, 2927–2936.
- [54] Child, A. D.; Reynolds, J. R. *Macromolecules* **1994**, *27*, 1975–1977.
- [55] Qin, C. J.; Cheng, Y. X.; Wang, L. X.; Jing, X. B.; Wang, F. S. *Macromolecules* **2008**, *41*, 7798–7804.
- [56] Qin, C. J.; Wu, X. F.; Gao, B. X.; Tong, H.; Wang, L. X. *Macromolecules* **2009**, *42*, 5427–5429.
- [57] Huang, F.; Hou, L. T.; Shen, H. L.; Jiang, J. X.; Wang, F.; Zhen, H. Y.; Cao, Y. *Journal of Materials Chemistry* **2005**, *15*, 2499–2507.
- [58] Slaven, W. T.; Li, C. J.; Chen, Y. P.; John, V. T.; Rachakonda, S. H. *Journal of Macromolecular Science-Pure and Applied Chemistry* **1999**, *A36*, 971–980.
- [59] McQuade, D. T.; Hegedus, A. H.; Swager, T. M. *Journal of the American Chemical Society* **2000**, *122*, 12389–12390.
- [60] Ding, L.; Jonforsen, M.; Roman, L. S.; Andersson, M. R.; Inganäs, O. *Synthetic Metals* **2000**, *110*, 133–140.
- [61] Tan, C. Y.; Pinto, M. R.; Schanze, K. S. *Chemical Communications* **2002**, *5*, 446–447.
- [62] Tan, C. Y.; Pinto, M. R.; Kose, M. E.; Ghiviriga, I.; Schanze, K. S. *Advanced Materials* **2004**, *16*, 1208–+.
- [63] Shi, W.; Fan, S. Q.; Huang, F.; Yang, W.; Liu, R. S.; Cao, Y. *Journal of Materials Chemistry* **2006**, *16*, 2387–2394.
- [64] Ramey, M. B.; Hiller, J. A.; Rubner, M. F.; Tan, C. Y.; Schanze, K. S.; Reynolds, J. R. *Macromolecules* **2005**, *38*, 234–243.
- [65] Rau, I. U.; Rehahn, M. *Acta Polymerica* **1994**, *45*, 3–13.
- [66] Balanda, P. B.; Ramey, M. B.; Reynolds, J. R. *Macromolecules* **1999**, *32*, 3970–3978.
- [67] Zhai, L.; McCullough, R. D. *Advanced Materials* **2002**, *14*, 901–905.

- [68] Herland, A.; Nilsson, K. P. R.; Olsson, J. D. M.; Hammarstrom, P.; Konradsson, P.; Inganas, O. *Journal of the American Chemical Society* **2005**, *127*, 2317–2323.
- [69] Huang, F.; Wu, H. B.; Wang, D.; Yang, W.; Cao, Y. *Chemistry of Materials* **2004**, *16*, 708–716.
- [70] Yang, G. Z.; Chen, P.; Liu, T. X.; Wang, M.; Huang, W. *Polymers for Advanced Technologies* **2006**, *17*, 544–551.
- [71] Huang, F.; Hou, L. T.; Shen, H. L.; Yang, R. Q.; Hou, Q.; Cao, Y. *Journal of Polymer Science Part a-Polymer Chemistry* **2006**, *44*, 2521–2532.
- [72] Gao, Y.; Wang, C. C.; Wang, L.; Wang, H. L. *Langmuir* **2007**, *23*, 7760–7767.
- [73] Peng, H.; Soeller, C.; Travas-Sejdic, J. *Chemical Communications* **2006**, 3735–3737.
- [74] Mikroyannidis, J. A.; Barberis, V. P.; Cimrova, V. *Journal of Polymer Science Part a-Polymer Chemistry* **2007**, *45*, 1016–1027.
- [75] Dwivedi, A. K.; Saikia, G.; Iyer, P. K. *Journal of Materials Chemistry* **2011**, *21*, 2502–2507.
- [76] Qin, C. J.; Tong, H.; Wang, L. X. *Science in China Series B-Chemistry* **2009**, *52*, 833–839.
- [77] Garcia, A.; Bakus, R. C.; Zalar, P.; Hoven, C. V.; Brzezinski, J. Z.; Nguyen, T. Q. *Journal of the American Chemical Society* **2011**, *133*, 2492–2498.
- [78] Rau, I. U.; Rehahn, M. *Polymer* **1993**, *34*, 2889–2893.
- [79] Chaturvedi, V.; Tanaka, S.; Kaeriyama, K. *Macromolecules* **1993**, *26*, 2607–2611.
- [80] Rulkens, R.; Schulze, M.; Wegner, G. *Macromolecular Rapid Communications* **1994**, *15*, 669–676.
- [81] Xu, Q. L.; An, L. L.; Yu, M. H.; Wang, S. *Macromolecular Rapid Communications* **2008**, *29*, 390–395.
- [82] Wang, F. K.; Bazan, G. C. *Journal of the American Chemical Society* **2006**, *128*, 15786–15792.
- [83] Hager, H.; Heitz, W. *Macromolecular Chemistry and Physics* **1998**, *199*, 1821–1826.

- [84] Jiang, H.; Zhao, X. Y.; Schanze, K. S. *Langmuir* **2006**, *22*, 5541–5543.
- [85] Yu, D. Y.; Zhang, Y.; Liu, B. *Macromolecules* **2008**, *41*, 4003–4011.
- [86] Fujii, A.; Sonoda, T.; Fujisawa, T.; Ootake, R.; Yoshino, K. *Synthetic Metals* **2001**, *119*, 189–190.
- [87] Zhao, X. Y.; Pinto, M. R.; Hardison, L. M.; Mwaura, J.; Muller, J.; Jiang, H.; Witker, D.; Kleiman, V. D.; Reynolds, J. R.; Schanze, K. S. *Macromolecules* **2006**, *39*, 6355–6366.
- [88] Wang, D. L.; Moses, D.; Bazan, G. C.; Heeger, A. J.; Lal, J. *Journal of Macromolecular Science-Pure and Applied Chemistry* **2001**, *38*, 1175–1189.
- [89] Liu, B.; Bazan, G. C. *Nature Protocols* **2006**, *1*, 1698–1702.
- [90] Kim, S.; Jackiw, J.; Robinson, E.; Schanze, K. S.; Reynolds, J. R.; Baur, J.; Rubner, M. F.; Boils, D. *Macromolecules* **1998**, *31*, 964–974.
- [91] Tapia, M. J.; Burrows, H. D.; Valente, A. J. M.; Pradhan, S.; Scherf, U.; Lobo, V. M. M.; Pina, J.; de Melo, J. S. *Journal of Physical Chemistry B* **2005**, *109*, 19108–19115.
- [92] Gao, J.; Loi, M. A.; de Carvalho, E. J. F.; dos Santos, M. C. *ACS Nano* **2011**, *5*, 3993–3999.
- [93] Dimroth, K.; Reichardt, C.; Siepmann, T.; Bohlmann, F. *Justus Liebigs Annalen der Chemie* **1963**, *661*, 1–37.
- [94] Kim, Y. H.; Ahn, J. H.; Shin, D. C.; Kim, J. H.; Park, Y. W.; Choi, D. S.; Kim, Y. K.; Kwon, S. K. *Bulletin of the Korean Chemical Society* **2001**, *22*, 1181–1182.
- [95] Kim, Y.-H.; Shin, D.-C.; Ahn, J.-H.; Kim, H.-S.; Kwon, S.-K. *Molecular Crystals and Liquid Crystals* **2002**, *377*, 109–112.
- [96] Krebs, F. C.; Jorgensen, M. *Macromolecules* **2002**, *35*, 7200–7206.
- [97] Kim, Y. H.; Ahn, J. H.; Shin, D. C.; Kwon, S. K. *Polymer* **2004**, *45*, 2525–2532.
- [98] Nguyen, T. Q.; Schwartz, B. J. *Journal of Chemical Physics* **2002**, *116*, 8198–8208.
- [99] Al Attar, H. A.; Monkman, A. P. *Journal of Physical Chemistry B* **2007**, *111*, 12418–12426.
- [100] Hodgkiss, J. M.; Tu, G. L.; Albert-Seifried, S.; Huck, W. T. S.; Friend, R. H. *Journal of the American Chemical Society* **2009**, *131*, 8913–8921.

- [101] van Reenen, S.; Matyba, P.; Dzwilewski, A.; Janssen, R. A. J.; Edman, L.; Kemerink, M. *Advanced Functional Materials* **2011**, *21*, 1795–1802.
- [102] Edman, L. *Electrochimica Acta* **2005**, *50*, 3878–3885.
- [103] Mills, T. J.; Lonergan, M. C. *Phys. Rev. B* **2012**, *85*, 035203.
- [104] Gaylord, B. S.; Heeger, A. J.; Bazan, G. C. *Proceedings of the National Academy of Sciences of the United States of America* **2002**, *99*, 10954–10957.
- [105] Bohrisch, J.; Eisenbach, C. D.; Jaeger, W.; Mori, H.; Muller, A. H. E.; Rehahn, M.; Schaller, C.; Traser, S.; Wittmeyer, P. *Polyelectrolytes with Defined Molecular Architecture I* **2004**, *165*, 1–41.
- [106] Pu, K. Y.; Liu, B. *Macromolecules* **2008**, *41*, 6636–6640.
- [107] Huang, F.; Hou, L. T.; Wu, H. B.; Wang, X. H.; Shen, H. L.; Cao, W.; Yang, W.; Cao, Y. *Journal of the American Chemical Society* **2004**, *126*, 9845–9853.
- [108] Hou, L. T.; Huang, F.; Zeng, W. J.; Peng, J. B.; Cao, Y. *Applied Physics Letters* **2005**, *87*, 153509.
- [109] Elbing, M.; Garcia, A.; Urban, S.; Nguyen, T. Q.; Bazan, G. C. *Macromolecules* **2008**, *41*, 9146–9155.
- [110] Monkman, A.; Rothe, C.; King, S.; Dias, F. *Polyfluorenes* **2008**, *212*, 187–225.
- [111] Blondin, P.; Bouchard, J.; Beaupre, S.; Belletete, M.; Durocher, G.; Leclerc, M. *Macromolecules* **2000**, *33*, 5874–5879.
- [112] Pei, Q. B.; Yu, G.; Zhang, C.; Yang, Y.; Heeger, A. J. *Science* **1995**, *269*, 1086–1088.
- [113] Lin, F. D.; Walker, E. M.; Lonergan, M. C. *Journal of Physical Chemistry Letters* **2010**, *1*, 720–723.
- [114] Thackeray, J. W.; White, H. S.; Wrighton, M. S. *Journal of Physical Chemistry* **1985**, *89*, 5133–5140.
- [115] Gao, J.; Yu, G.; Heeger, A. J. *Advanced Materials* **1998**, *10*, 692–695.
- [116] Pickup, P. G. *Journal of Materials Chemistry* **1999**, *9*, 1641–1653.
- [117] Doblhofer, K.; Rajeshwar, K. In *Handbook of Conducting Polymers 2nd ed.*; Skotheim, T., Elsenbaumer, R., Reynolds, J. R., Eds.; Dekker: New York, 1998; p 1097.

- [118] Barsoukov, E.; MacDonald, J. *Impedance spectroscopy: theory, experiment, and applications*; Wiley-Interscience: Hoboken, N.J., 2005.
- [119] Oh, S. H.; Na, S. I.; Nah, Y. C.; Vak, D.; Kim, S. S.; Kim, D. Y. *Organic Electronics* **2007**, *8*, 773–783.
- [120] Lin, F. D.; Wang, Y. J.; Lonergan, M. *Journal of Applied Physics* **2008**, *104*.
- [121] Neher, D.; Gruner, J.; Cimrova, V.; Schmidt, W.; Rulkens, R.; Lauter, U. *Polymers for Advanced Technologies* **1998**, *9*, 461–475.